7-14-2010

Cancer Therapy Combining Modalities of Hyperthermia and Chemotherapy: in vitro Cellular Response after Rapid Heat Accumulation in the Cancer Cell

Yuan Tang
Florida International University, ytang001@fiu.edu

FLORIDA INTERNATIONAL UNIVERSITY

Miami, Florida

CANCER THERAPY COMBINING THE MODALITIES OF HYPERTHERMIA AND CHEMOTHERAPY: *IN VITRO* CELLULAR RESPONSE AFTER RAPID HEAT ACCUMULATION IN THE CANCER CELL

A dissertation submitted in partial fulfillment of the

requirements for the degree of

DOCTOR OF PHILOSOPHY

in

BIOMEDICAL ENGINEERING

by

Yuan Tang

2010

To: Dean Amir Mirmiran
College of Engineering and Computing

This dissertation, written by Yuan Tang, and entitled Cancer Therapy Combining Modalities of Hyperthermia and Chemotherapy: *in vitro* Cellular Response after Rapid Heat Accumulation in the Cancer Cell, having been approved in respect to style and intellectual content, is referred to you for judgment.

We have read this dissertation and recommend that it be approved.

_____
Anuradha Godavarty

_____
Yen-Chih Huang

_____
Fenfei Leng

_____
Wei-Chiang Lin

_____
Anthony J. McGoron, Major Professor

Date of Defense: July 14, 2010

This dissertation of Yuan Tang is approved.

_____
Dean Amir Mirmiran
College of Engineering and Computing

_____
Interim Dean Kevin O'Shea
University Graduate School

Florida International University, 2010

DEDICATION

To My Parents and Xiaowen Zhang.

ACKNOWLEDGMENTS

I want to thank the members of my dissertation committee for their consistent support.

I would like to give my deepest thanks to my advisor Dr. Anthony J. McGoron for his patience and support. Without his constant guidance and encouragement, the completion of this work would not have been possible.

I also want to thank all my lab mates, Dr. Romila Manchanda, Denny Carvajal, Alicia Fernandez-Fernandez, Abhignyan Nagesetti, Supriya Srinivasan and Tingjun Lei for their inspiration and friendship. My appreciation also goes to Chang Liu, Jiali Wang, Qiang Wang, Lu Wang, and Zhiqi Zhang for their kind support.

Lastly, and most importantly, I would like to thank my parents and Xiaowen Zhang. They make me live a wonderful life.

ABSTRACT OF THE DISSERTATION

CANCER THERAPY COMBINING THE MODALITIES OF HYPERTHERMIA AND CHEMOTHERAPY: *IN VITRO* CELLULAR RESPONSE AFTER RAPID HEAT ACCUMULATION IN THE CANCER CELL

by

Yuan Tang

Florida International University, 2010

Miami, Florida

Professor Anthony J. McGoron, Major Professor

Hyperthermia is usually used at a sub-lethal level in cancer treatment to potentiate the effects of chemotherapy. The purpose of this study is to investigate the role of heating rate in achieving synergistic cell killing by chemotherapy and hyperthermia. For this purpose, *in vitro* cell culture experiments with a uterine cancer cell line (MES-SA) and its multidrug resistant (MDR) variant MES-SA/Dx5 were conducted. The cytotoxicitiy, mode of cell death, induction of thermal tolerance and P-gp mediated MDR following the two different modes of heating were studied. Doxorubicin (DOX) was used as the chemotherapy drug. Indocyanine green (ICG), which absorbs near infrared light at 808nm (ideal for tissue penetration), was chosen for achieving rapid rate hyperthermia. A slow rate hyperthermia was provided by a cell culture incubator. The results show that the potentiating effect of hyperthermia to chemotherapy can be maximized by increasing the rate of heating as evident by the results from the cytotoxicity assay. When delivered at the same thermal dose, a rapid increase in temperature from 37 °C to 43 °C caused more cell membrane damage than gradually heating the cells from 37 °C to 43 °C and

thus allowed for more intracellular accumulation of the chemotherapeutic agents. Different modes of cell death are observed by the two hyperthermia delivery methods. The rapid rate laser-ICG hyperthermia @ 43 °C caused cell necrosis whereas the slow rate incubator hyperthermia @ 43 °C induced very mild apoptosis. At 43 °C a positive correlation between thermal tolerance and the length of hyperthermia exposure is identified. This study shows that by increasing the rate of heating, less thermal dose is needed in order to overcome P-gp mediated MDR.

TABLE OF CONTENTS

LIST OF FIGURES

FIGURE PAGE

I. INTRODUCTION

Hyperthermia (thermal therapy or thermotherapy) could be used for cancer treatment where high temperature (up to 45°C) is applied to body tissue. Research has shown that hyperthermia can kill cancer cells by exerting protein or structure damage within cells [1]. An advantage of using hyperthermia to kill cancer cells is that usually normal tissues or cells are not as susceptible to high temperature as are cancerous tissues [2]. Thus, hyperthermia may shrink tumors with minimum injury to the surrounding healthy tissues. Although hyperthermia's encouraging potential on cancer treatment has been shown in a large number of clinical trials, its exact mechanism of action is still somewhat unclear [3, 4]. In pre-clinical investigations such as in vitro cell culture experiments and animal studies, the cell killing effect of hyperthermia was found to be highly thermal dose dependent, although a correlation between temperature and response rate was achieved within a broad range of temperatures from 41°C to 47°C [5-7]. On the one hand, treatment outcome varied greatly among cancer types and among different cancer cell lines even in the same hyperthermia settings while on the other hand, small changes in hyperthermia settings could lead to huge difference in the treatment outcome, such as the rate of temperature change, exposure duration, and means of heat delivery. Since all these uncertainties and variations in the hyperthermia treatment, recent research interests have been shifted to the molecular and cellular targets of hyperthermia as well as the action mechanism of hyperthermia in the cellular and molecular level.

In this study, a chemotherapy-hyperthermia combinational cancer treatment regime was studied; various parameters that could influence the final treatment outcome were studied by *in vitro* cell culture experiments. The cell killing/growth inhibition effect was assessed

with two different hyperthermia delivery approaches in two cancer cell lines. Through this comparative study, we try to understand the cellular and molecular basis of hyperthermia in this combinational treatment regime, therefore giving a plausible explanation to those effects we have observed, such as thermal chemosensitization. In this respect, the study focuses on the distinct cellular and molecular events following hyperthermia, particularly those that participated in protein expression and cell death pathways induced by hyperthermia chemotherapy interaction.

1. Biological Response Following Hyperthermia

The cancer cell killing/growth inhibition ability of hyperthermia has been reported in numerous *in vivo* and *in vitro* studies [8-10]. Some research showed moderate hyperthermia (41-43 °C) did not affect normal cells while significantly inhibiting tumor cell growth [11]. In clinical applications, therapeutic hyperthermia ranges from 39-60 °C. Usually lower temperatures (39-43 °C) are used as an adjuvant treatment modality to radiotherapy or chemotherapy in whole-body and regional therapy. Higher temperature itself could be applied to kill deep seated tumors by focal lesions through laser or microwave produced hyperthermia.

1.1 Intracellular Changes after Heat Application

A variety of changes have been observed in cells after hyperthermia treatment including changes in cell membrane, metabolism, nuclear and cytoskeletal structures, macromolecular synthesis, expression of the heat shock genes and intracellular signal transduction [4]. However, it is generally believed that protein denaturing and cell membrane damage is the most direct effect of hyperthermia toxicity [3, 12, 13]. Protein starts to denature when the temperature is greater 40 °C, which leads to alterations in

multimolecular structures (e.g. cytoskeleton and membrane) and enzyme activity [14]. When the function of the enzyme complexes for DNA synthesis and repair is impaired, irreversible damage could occur.

Nucleic acid damage is more likely to happen during the S phase of the cell cycle when the DNA is being synthesized. The newly synthesized DNA is vulnerable to heat stress. The double strand DNA might be joined incorrectly or contain aberrant base pairs under heat stress. At the same time, mutations can occur due to damaged DNA repair mechanisms under hyperthermia. Hyperthermia can also inhibit the DNA replication process itself through inactivation of some key enzymes [15]. Nucleic acid damage could also occur in the M phase of the cell cycle when chromosomes are dividing. As a result, cells die when they undergo mitosis.

Cell membranes could be affected during hyperthermia, which is a key feature in thermal chemosensitization as altered membrane properties may facilitate drug uptake. Fluidity and permeability of the cell membrane may be modified upon heat exposure [16]. Generally, during hyperthermia permeability is increased especially to some small molecules. The efflux of proteins and enzymes from within the cell might trigger an immune response against tumor cells *in vivo*. If chemotherapy drug is applied together with hyperthermia, more drugs can accumulate at the tumor site due to the increased membrane permeability.

Hyperthermia affects several key functions of the cytoskeleton. Cytoplasmic streaming processes can be halted. Heat stress can also lead to the depolymerization and inactivation of microtubule proteins, and fragmentation of the mitotic spindle, which will result in cytokinesis disruption. Actin filaments can become insoluble under heat stress

and loose their function with increased temperature [17-19]. Cells undergoing division are most vulnerable to hyperthermia related cytoskeletal damage leading to cell death. Since Nucleic acids and cytoskeleton damages are most likely to happen during mitosis, cancer cells are more susceptible to hyperthermia as cancer cells undergo much faster cell division events than normal cells do.

1.2 Thermotolerance and Heat Shock Protein Expression

Cancer cells may confer thermotolerance as a result of continuous heat exposure or after pre-hyperthermia treatment. Cells that have developed thermotolerance are less susceptible to heat induced cytotoxicity. The induction of thermotolerance seems to be temperature dependant. Moderate hyperthermia is more likely to induce thermotolerance, where 43°C seems to be a critical temperature [20]. After exposure to temperatures higher than that, cells undergo extensive protein denaturing and die passively (necrosis). After exposure to lower temperature hypertehrmia, thermotolerance develops rapidly after 8 – 10 hours [20]. In one report, it was found to be developed after 30 minutes under continuous 43 °C hyperthermia exposure [16]. Also thermotolerance can develop rapidly by cooling down to 37 °C between two heat shock treatments [16]. Thermotolerance is reversible if the cells are returned to normal temperature. However, thermotolerance decay takes much slower than its induction, usually in 3 to 5 days in most cells [21, 22].

The development of thermotolerance is mainly due to heat shock protein (HSP) expression [23]. HSP has been discovered in human as well as various other animals. *In vitro* cell culture experiments have demonstrated that hyperthermia below a certain temperature could induced HSP expression, which subsequently induces thermotolerance.

This has been confirmed by other means such as HSP transfection into cultured cells resulting in significant decrease of thermosensitivity [1].

HSP are molecular chaperones [24]. The function of chaperone is to correctly assembly other macromolecules such as proteins and nucleosomes. When proteins and nucleosomes are synthesized, chaperones attach to them and help them fold to correct 3D conformation and perform their normal biological function. Chaperones themselves are not components of these macromolecules. When folding is complete, they disassociate. Hyperthermia can severely affect protein folding. Under heat stress, newly formed protein polypeptide chains and subunits tend to aggregate and lose their biological function. Thus, HSP as a molecular chaperone, its overexpression is a normal cellular protective mechanism to encounter heat stress because they can repair misfolded proteins. HSP are classified by their molecular weight. To date, HSP are usually divided into 5 groups: small HSP (MW<40 kDa), HSP60, HSP70, HSP90 and HSP100. Elevated HSP expression is not restricted to hyperthermia, other stresses such as infection or hypoxia could also trigger their upregulation. HSP are actively involved in the protection of cells against heat damage. They localize to the cytoskeleton and help reinforce structural proteins and enhance their tertiary configuration following treatment with heat [23, 25]. HSP also helps resist DNA fragmentation upon heating and decreases cell apoptosis [26]. The expression of HSP is also temperature dependant. Moderate hyperthermia stimulates HSP synthesis. With further elevation of temperature to a distinct threshold, inhibition of HSP expression occurs. In general, it is widely accepted that HSP inhibits hyperthermic cell death, especially apoptosis [27-30].

1.3 Hyperthermia Induced Apoptosis and Necrosis

Generally, cells are committed to death through two distinct pathways: apoptosis and necrosis. Necrotic cell death is passive and involves lysis formation from the damaged cell and the release of its cellular content to the surrounding environment [31]. Necrosis is a traumatic cell death and occurs when the injury to the cell is acute. As a result, inflammatory response always follows.

Apoptosis, in contrast, is an active and programmed cell death which involves condensation of nuclear chromatin, cytoplasmic shrinkage, membrane blebbing and externalization of phosphatidylserine, nuclear fragmentation and, finally, formation of apoptotic bodies [32]. Apoptosis plays an important role for cell death in development (e.g., apoptosis of the cells between the fingers lead to the differentiation of fingers and toes at embryo stage), maintaining homeostasis, and removing both the ineffective and immature cells of the body by the immune system. It could also be initiated by external stresses such as viral infection, DNA damage from excessive heat, radiation or toxic chemicals, which are routine strategies used by many cancer therapeutic agents. Apoptosis process malfunction is a major reason for cancer development as it permits the survival of cells after mutagenic DNA damage and uncontrolled growth. Studies have demonstrated that p53 gene is required for the efficient activation of apoptosis after irradiation or chemotherapy [33, 34]. Therefore, mutations on p53 can lead to increased resistance to chemotherapeutic agents on cancer cells [35].

Hyperthermia is capable of inducing both necrosis and apoptosis *in vitro* depending on the temperature [36]. In a malignant fibrous histiocytoma cell line, Yonezawa and coworkers proved that apoptosis could only be induced by heating up to 43 °C for 1 hour,

a temperature lower than that was not able to induce apoptosis no matter how long the exposure duration is [37]. They also observed that, with increased temperature (46°C for 1 hour), necrotic cell death seems to be dominant where cells are seriously injured and die before the initiation of apoptosis.

HSP expression is also involved in the transition from apoptosis to necrosis. HSP expression initiates with temperatures beyond 37 °C, they refold damaged intracellular proteins and helps resist DNA fragmentation thus protecting cells from stress injury. When the critical temperature for triggering apoptosis is reached (around 43 °C), the sustained thermal stress degenerates the regulation process. Nuclear chromatin condensates with HSP overexpression; meanwhile, the cytoplasma starts to shrink, and apoptotic tissue forms. If the temperature continues to increase, the critical temperature for triggering necrosis is reached (around 46 °C), the cellular proteins are denatured at that high temperature and the cell dies passively, which is necrotic cell death.

The induction of apoptosis by hyperthermia in cancer cells is cell line dependant. The reason might be that cancer cells usually have an impaired apoptotic regulation system. The apoptotic pathway is missing in at least some types of cancer cells. Yonezawa and coworkers observed a direct transition to necrosis in osteosarcoma with increasing temperature [37]. Those cells survived in 43 °C but directly underwent necrosis when they increased the temperature to 44 °C.

1.4 Thermal Dosimetry

1.4.1 Thermal dose dependent cell death

Treatment outcome of hyperthermia is highly thermal dose dependant. The temperature of the hyperthermia treatment and the exposure duration at that temperature could make a

great difference in tumor growth. After examining numerous survival curves of different cell lines upon heat treatment, the threshold temperature for thermal damage was found. This threshold temperature is also called a “breakpoint”. For example, Roizin-Towle [38] studied the cell death of Chinese hamster ovary (CHO) cells from 42-45 °C for up to 5 hours. He observed that a 42 °C hyperthermia treatment for 5 hours showed very little cytotoxicity. However, after increasing the temperature to 42.5 °C, almost all cells were killed during the same period of heat exposure. Other research groups observed similar phenomena using different cell lines. Dewhirst et al. [39] concluded that once the hyperthermia treatment starts to show cytotoxicity, the rate of cell death, which is exponential with exposure time, is dependent on temperature. The change in the rate of cell killing below and beyond the breakpoint is generally believed to be related to the cells acquiring resistance to hyperthermia treatment during heating [39]. Heating above the breakpoint would not induce thermotolerance during the heating period; however cells could acquire thermotolerance after that heating period no matter whether the temperature is above or below the breakpoint.

From the survival curve, researchers tried to build mathematical models to connect cell killing with the temperature of exposure and the duration of exposure. Some of the first attempts involved using Arrhenius analysis to study the cell survival curve mentioned above. The Arrhenius plot, which is produced by Arrhenius analysis to those curves, could be used to estimate the energy (heat) needed to inactivate the cells. Here, I will not go into the details of this analysis since it is not the focus of this study. Detailed procedure could be found in a number of publications [6, 38]. The Arrhenius plot is typically biphasic which also suggests the existence of a “breakpoint”. The plot is steeper

below the breakpoint than above it. The calculated inactivation energy is usually around 120–150 kcal/mole, which is consistent with the heat energy required to inactivate proteins and enzymes [40].

1.4.2 Cumulative equivalent minutes @43 °C model (CEM_{43})

Although the Arrhenius analysis could be used to calculate the inactivation energy, it is hard to compare two different time-temperature combinations in the Arrhenius plot. Therefore, in order to normalize different treatment regimes (time-temperature combination) to a common unit, several methods have been developed.

Sapareto and Dewey [41] proposed the term "thermal isoeffective dose" (meaning two different time-temperature combinations produced the same cell killing effect) for comparing different time-temperature combinations. This simple method is based on the fact that cell death under hyperthermia treatment is exponential; therefore, this relationship can be expressed mathematically by the following isoeffect equation:

$$t_1 = t_2 * R^{(T_1 - T_2)}, \textbf{\textit{(Equation 1)}}$$

where T_1 & T_2 are two different treatment temperatures and t_1 & t_2 are the duration of treatment at temperature T_1 & T_2 respectively. R is an empirical value which defines the shape of the dose-response curve. Usually, R is termed as a compensation constant and is assumed to be 0.5 above 43 °C and 0.25 below 43 °C by Sapareto and Dewey [41]. It has been shown in a number of rodent and human cell lines that cytotoxicity start to occur around 43 °C after continuous heat exposure; therefore, it was considered as the breakpoint temperature in this model [39]. Sapareto and Dewey [41] also found out that, when the temperature is above 43°C, with each 1 °C increase, the time needed to produce the same cell killing effect is cut in half; while below 43 °C, with each 1 °C temperature

drop, treatment time has to be extended by 4 times to compensate for that 1 °C difference. Therefore, for any hyperthermia treatment, its thermal dose can be described as the cumulative equivalent minutes at 43°C. From equation (1), if we set T_1 = 43 °C and allow T_2 to be vary during heat treatment, we get

$$CEM_{43} = \int R^{(43-T(t))} dt \text{ , } \textbf{\textit{(Equation 2)}}$$

which is the widely used cumulative equivalent minutes @43 °C model.

2. Hyperthermia as an Adjuvant Treatment Modality to Chemotherapy or Radiotherapy

The efficacy of current hyperthermia treatment modalities alone is not sufficient enough to substitute for already established methods such as chemotherapy or radiation therapy, but, they could be applied adjuvant to those modalities to enhance the cancer cell killing/growth inhibition effect. More recent researches have been focusing on magnifying the synergistic effects of combining hyperthermia and chemotherapy or radiotherapy in order to achieve better therapeutic effects [42]. Thermal chemosensitization and thermal radiosensitization effects have been observed both *in vivo* and in *in vitro* cell culture experiments [1].

Clinically, several phase-III studies have been carried out to study the effect of the hyperthermia radiotherapy combinational treatment modality. Patients within the combinational treatment group achieved better response rate and survival rate over the radiotherapy alone group. Compared to hyperthermia radiotherapy, there are many trials to date regarding the application of hyperthermia as an adjuvant to chemotherapy. Most

of the reports were focusing on the effect of hyperthermia-chemoperfusion following surgery compared to surgery alone [43-46].

2.1 Chemotherapy in Cancer Treatment and Multidrug Resistant

In cancer treatment, chemotherapy involves using any type of chemicals to kill cancer cell. Most chemotherapy agents target at fast dividing cells and impair cell mitosis. Since cancer cells divide much faster than most normal cells, they are more sensitive to chemotherapy agents because cell division events are more likely to happen at any time. The downside of this cancer targeting strategy is that other healthy fast dividing cells can also be affected, such as those functioning in hair growth and those responsible for the replacement of the intestinal epithelium.

Cancer cells can become resistant to chemicals over time. Research has shown that if an anticancer drug (e.g. doxorubicin (DOX)) can not kill the entire tumor when they are first introduced, then the survived cancer cells can become insensitive to not only DOX but also a variety of other chemotherapy agents. This effect is called multidrug resistant (MDR). The therapeutic effect of chemotherapy is greatly hindered by multidrug resistant, which is the major cause of treatment failure in metastatic cancers. Cancer cells which respond initially can acquire resistant by spontaneous mutation or DNA transfer to acquire multidrug resistant [47].

Cancer cells achieve multidrug resistant by altered membrane transporter activity, which is mediated by an energy dependent drug efflux pump. A decreased net cellular accumulation of the chemotherapy agent is always observed in MDR cells. Research has shown that a plasma membrane P-glycoprotein (P-gp), which belongs to a large ATP-binding cassette protein family with a molecular weight of 170,000, is consistently found

to be over-expressed in a variety of multidrug-resistant cell lines [48]. To date, P-gp overexpression is still the best-understood mechanism of MDR. Cancer cells achieve drug resistant by P-gp actively exporting many functionally and structurally unrelated hydrophobic anticancer drugs using the energy of ATP hydrolysis [49]. Therefore, P-glycoprotein is believed to be the primary mediator in multidrug resistance.

2.2 Hyperthermia-Chemotherapy Interaction

Various Pre-clinical reports have suggested the role of hyperthermia in overcoming P-gp regulated MDR. Using ultrasound induced moderate hyperthermia (20 min @41°C), Liu and his research group [49] observed a 2-6 fold increase in DOX uptake in MDR cells compared to control cells. In Moriyama-Gonda's data [50], membrane permeability as well as reduced P-gp expression was achieved by 44 °C heating for 60 min. The exact mechanism of hyperthermia overcoming MDR is still under investigation. Some research groups consider the mechanism exemplary, which means its causes are multifactorial: transmembrane conductivity, sodium/potassium-ATPase activity, and glutathione metabolism could all be affected [1]. Whereas in other observations, only increased drug uptake was found due to enhanced membrane permeability under hyperthermia [49].

On the other hand, MDR has been observed to be associated with the occurrence of thermotolerance induced by hyperthermia. It is not clear whether there is a causation relationship between MDR and thermotolearnce, however, the simultaneous induction of MDR and thermotolerance under hyperthermia has been reported extensively in various trials [23, 30, 51-53]. Again, it seems that the induction and overcoming of MDR using hyperthermia is temperature dependant. Below a critical temperature (around 42°C), hyperthermia is more likely to induce MDR and thermotolerance (through HSP

expression). Beyond that temperature, hyperthermia has shown great potential in inducing thermal chemosensitization and overcoming MDR which may result in the accumulation of chemotherapy agents within the target cells [1].

3. Overview of the Specific Intracellular Events Following Hyperthermia Supporting the Hypothesis for This Study

So far, the cancer cell killing/growth inhibition capability of hyperthermia has been established both by itself and as an adjuvant treatment modality. However, its exact mechanism of action is still not very clear. The only thing that is widely accepted is that the temperature and the duration of the heat treatment play a very important role. The specific cellular events following hyperthermia, such as HSP expression, development/reversal of thermotolerance and MDR, hyperthermia-chemotherapy interaction, apoptosis/necrosis cell death, are all temperature dependant.

Figure 1 gives a schematic roadmap of the intracellular events following hyperthermia (with increasing temperature). Unfortunately, since each research group has their own specific interest and experimental setup (e.g. different cell lines, hyperthermia delivery), it is hard to compare the results between different research groups. Therefore, the diagram is an approximation and may be incomplete since there are other parameters that can influence the effect of hyperthermia, such as the rate of heating which are not included in this diagram. The reason is that reports regarding the influence of heating rate are very rare. This dissertation attempts to address the influence of heating rate.

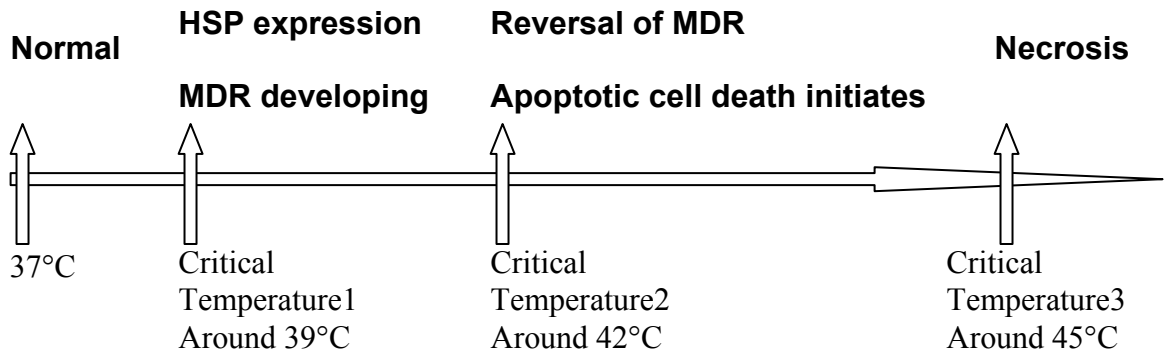

Figure 1 Hypothesized time course of intracellular events following hyperthermia based on current literature.

Practically, temperatures ranging from 41-47 °C are usually used for inducing hyperthermia. Hyperthermia lower than 41 °C may have adverse effects as cells can protect themselves through cellular HSP expression in that temperature range. Moreover, mild hyperthermia may help cells develop MDR. Temperatures higher than 47 °C could effectively induce necrosis in almost any type of cells through protein denaturing; however, those temperatures are hard to apply in practice, as healthy tissue will also be affected. Thus, hyperthermia treatment to tumor tissue at around 43 °C seems to be optimal for achieving a successful final treatment outcome; this temperature is easier to reach clinically compared to 47 °C so it could reverse MDR and initiate apoptotic cell death.

Another issue that needs to be pointed out is the initiation of these intracellular events (HSP overexpression, induction/reversal of MDR, apoptotic cell death, etc.) requires extended exposure, usually in tens of minutes at least. Therefore, it is reasonable to **hypothesize that the rate of temperature increase will affect the development of HSP expression, induction/reversal of MDR, and apoptotic cell death. A rapid rate of**

hyperthermia to 43 °C can circumvent extensive HSP expression and induce thermal chemosensitization thus killing cancer cells synergistically.

4. Current Hyperthermia Delivery Methods: Pros and Cons

4.1 The Treatment of Cancer by Hyperthermia – Rationale

From *in vivo* experiments, it has been observed that normal tissue and tumor tissue behave differently during hyperthermia treatment. This difference is because of the characteristic difference between normal and tumor tissue physiology but not the hyperthermia sensitivity of normal and tumor cells [2]. Compared to normal tissue, tumor vascular architecture is usually more chaotic. As a result, hypoxia and low pH (2-4) is usually found in tumor tissues, which makes tumor cells more sensitive to hyperthermia than normal cells [2]. Most normal tissues, except for in the nervous system, can maintain their function under up to 44 °C hyperthermia within 1 hour [54]. Irreversible damage in the central nervous system was observed after 40-60 min hyperthermia at a temperature of 42-42.5 °C [55]. The peripheral nervous system appears to be more resistant to heat stress than the central nervous system; Wondergem et al [56] reported a full recovery within four weeks from temporary functional loss of the peripheral nervous system after a 44 °C hyperthermia treatment for longer than 30 minutes.

4.2 Types of Hyperthermia

In clinical applications, hyperthermia can be divided into three types: local, regional and whole-body hyperthermia.

4.2.1 Local hyperthermia

Local hyperthermia is usually applied to a tumor while the surrounding normal tissue is not heated. Local hyperthermia treatment is a well-established cancer treatment modality

with a basic principle, that is, if a 42 ºC hyperthermia can be maintained in a tumor for one hour, the tumor cells will be destroyed [57]. Local hyperthermia can be applied by external or interstitial methods.

External local hyperthermia: External local hyperthermia is usually performed with superficial applicators, such as RF, microwave or ultrasound. Although the penetration depth can be tuned by the size or the frequency of the applicator, the therapeutic depth of this type of hyperthermia is usually no more than 3-4 cm [57]. In regions with an irregular surface (head, neck, etc.), the treatment depth is further limited.

Intraluminal local hyperthermia: Intraluminal or endocavitary methods can be used to treat tumors within or near body cavities. These cavities include gastrointestinal (esophagus, rectum), gynecological (vagina, cervix, and uterus), genitourinary (prostate, bladder), and pulmonary (trachea, bronchus) [58]. During the procedure, endocavitary antennas will be inserted into these lumens for delivering heat.

Interstitial local hyperthermia: In order to treat deep seated tumors where external local hyperthermia is unreachable, such as brain tumors, interstitial local hyperthermia can be applied [59]. There are several types of applicators for delivering energy interstitially, including local current field techniques utilizing RF energy at a frequency of 0.5 MHz; small microwave antennas delivered by hollow tubing at 300-2450 MHz; ferromagnetic seed implants, hot water tubes and laser fibers [57]. However, due to its invasive nature, it is difficult to perform this procedure repeatedly, also, the applicable sites are limited.

4.2.2 Regional hyperthermia

When a tumor is locally advanced or deep seated, such as those in the abdomen or pelvis, regional hyperthermia can be used. Unlike local hyperthermia, in regional hyperthermia it

is hard to avoid a temperature increase in normal tissues; therefore, it requires that heat dissipation in normal tissue is faster than in the tumor, usually due to blood flow. Most clinical trials have used regional hyperthermia as an adjuvant to chemotherapy or radiotherapy, mostly in the pelvis when locally advanced or recurrent tumors are present, including rectal carcinoma, cervical carcinoma, bladder carcinoma, prostate carcinoma or soft tissue sarcoma.

Deep regional hyperthermia by external applicators: Treatments of deep seated tumors are difficult with electro-magnetic (EM) energy since it can be absorbed by human tissue very quickly [60]. Therefore, in order to deliver energy to the tumor while avoiding overheating adjacent normal tissue, applicator arrays are usually used [61]. Typical systems include the Sigma-60 and Sigma-Eye.

Regional perfusion hyperthermia: Regional perfusion is a technique where heated fluids (usually carrying chemotherapeutic agents) are used to perfuse cancerous tissue. It is usually used to treat cancers in the arms and legs like melanoma or soft tissue sarcoma, where the cancer is in advanced stage and nonresectable. When regional hyperthermia is applied to limbs and without a cytotoxic agent, the temperature can be increased to around 43 °C for as long as 2 hours [2]. However, if a cytotoxic drug is applied simultaneously, the temperature must be lower to avoid unacceptable toxicities. It can also be applied in an organ such as the liver and lung, or in a body cavity, such as the peritoneal cavity, where the temperature can reach 41-42 °C with heated anticancer drug [57]. Clinically, regional perfusion hyperthermia combined with chemotherapy has shown much higher response rate than treating the caner with systemic chemotherapy. However, compared to externally applied hyperthermia, the procedure is more risky.

Adverse effects can be more sever and persistent, such as neuropathy which can lead to amputation of limbs in the worst cases.

4.2.3 Whole body hyperthermia (WBH)

WBH has been investigated since he 1970s as an adjuvant modality to chemotherapy or radiotherapy [62], where metastatic cancer has spread throughout the body. The temperature of WBH is usually limited to 42 °C because temperature higher than that can cause irreversible damage to brain and liver tissue. But this temperature can be maintained for several hours.

The application of WBH can be divided into three major types: thermal conduction, extracorporeal induction and radiant or EM induction [57]. Thermal conduction can be achieved by immersion in heated fluids [63], heated air [57], heated blanket [64] or using thermal chambers (similar to incubator). In extracorporeal induction, blood is first pumped out of the patient's body, heated to 42 °C, and then put back into the body [65].

Since the whole body temperature will be elevated, WBH can be applied only to patients in a good health condition, otherwise, significant adverse effects may occur given that the basal metabolic rate of a patient will be doubled at 42 °C compared to 37 °C [66].

4.3. Hyperthermia Heating Systems

Recently, localized hyperthermia has been achieved by external energy sources. Especially diathermic heating devices have became a new research focus in the treatment of cancer due to their targeting capability, which eventually leads to accurate hyperthermia delivery to the tumor and small side effects to the healthy tissues [16]. Most clinically used hyperthermia systems are diathermic, which means the heating of body tissues due to their resistance to the passage of high-frequency electromagnetic radiation,

electric current or ultrasonic waves. These systems can be interfaced with magnetic resonance image (MRI) systems for noninvasive monitoring of tumor temperature. With the advance in nanotechnology, nanotechnology-based sources have become a new research focus [67].

4.3.1 Ultrasound

The ultrasound induced hyperthermia effect is caused by tissue absorption of ultrasound waves at the frequency of 2-20 MHz. Theoretically, ultrasound has the best combination of short wavelengths among all diathermic devices and therefore has low attenuation coefficient, which allows for deep penetration the in human body with the ability to focus power into small regions [57]. With the technique advance, newly designed ultrasound hyperthermia delivery systems equipped with multiple applicators have achieved improved heating uniformity and controlled depth of penetration [68, 69]. However, in application, the use of ultrasound is limited by the fact that it is incapable of penetrating air and bone.

4.3.2 EM fields

EM field can cause temperature increase in biological tissues. According to the frequency, EM field can be in the radiofrequency (RF) or microwave range. Frequency between 300 MHz and 300 GHz are assigned to microwave. The most commonly used frequencies for microwave hyperthermia are 433, 915, and 2450 MHz [58]. Frequencies higher than 2450 MHz have no practical value due to their limited penetrations. RF by definition occupies the band between 3 kHz and 300 GHz. In hyperthermia application, it generally means frequencies below microwave range, usually between 10-120 MHz [57]. The RF frequencies of 13.56 and 27.12 MHz have been widely used in hyperthermia [58].

4.3.3 Radiofrequency

Exposure of living organisms to radio frequency electromagnetic radiations (RF-EMFs) produces heat within tissues primarily from molecular rotation [70]. There are three major types of RF hyperthermia, according to the mode of generating RF field.

Resistive: Resistive heating is achieved by an EM field produced by alternating RF currents through needle or plate electrodes. The operating frequency should be higher than 100 kHz to prevent excitation of nerve action potentials.

Capacitive: Capacitive heating operates by putting patients inside a capacitor. More specifically, by displacement currents generated between two capacitor plates. It is simple to apply, but a major problem associated with it is that the subcutaneous fat tissue is often overheated.

Inductive: Inductive heating is achieved by a time varying magnetic field passing through the body and generating eddy currents which subsequently produces Joule's heat. The magnetic field is usually generated by solenoidal loops. Since the induced electric fields are parallel to the tissue interface, heating is maximized in muscle rather than in fat and therefore can penetrate tissues > 5 cm. The disadvantage with inductive heating is that the temperature distribution is not homogenous [71]. The pattern is usually toroidal shape with very small temperature elevation at the center.

4.3.4 Microwave

When treating patients with an EM device within the microwave frequency range, energy is coupled into tissues through waveguides, dipoles, or other radiating devices [57]. Due to its high frequency, a microwave hyperthermia device is capable of directing and focusing the energy into tissues by direct radiation from a small applicator [72]. However,

also due to its high frequency, its penetration depth is shallow compared to RF; besides, most microwave equipment requires cooling (usually water) of the device-patient interface.

Early diathermic devices use a single applicator which is unable to steer or focus energy. Therefore, single applicator devices can only treat relatively small superficial tumors. In order to apply heat into deep seated tumors without overheating skin or superficial normal tissue, multichannel coherent phased-array systems have been developed. An array of applicators with variations in phase, frequency, amplitude, and orientation can theoretically deliver heat more precisely with deeper penetration compared to a single applicator.

The major problem with diathermic heating is to achieve an elevated temperature in the cancerous tissue, meanwhile, avoid excessive heating of the surrounding healthy tissue in the presence of electrical inhomogeneitites. This problem could be solved by nanotechnology based sources.

4.4 Nanotechnology Based Sources

One major obstacle that prevents hyperthermia from achieving therapeutic effect is the lack of direct targeting techniques. Superficial malignances could be treated with hyperthermia effectively; however, other treatment modalities are also superior in treating exposed malignances. Deep body tumors are hard to reach by noninvasive external energy sources, where direct heating methods like whole body hyperthermia aiming to deliver hyperthermia from outside the body to the tumor will inevitably cause damage to healthy tissue before the deep tumor region temperature can reach the therapeutic temperature. This problem could be solved by invasive methods such as

regional perfusion or interstitial hyperthermia through probes; the disadvantage, of course, is that those methods are invasive and require complex procedures.

The currently available modalities of hyperthermia are often limited by their inability to selectively target tumor tissue and therefore carry the risk of collateral organ damage. Nanotechnology-based thermal therapy is a special form of interstitial hyperthermia which can selectively delivery heat to the tumor by depositing energy-absorbing agents within tumor tissues to facilitate localized heating. The localization of nanoparticle into the tumor tissue can be achieved by passive targeting of nanoparticles due to the leaky vasculature of tumor, or by active targeting through tagging it with appropriate ligands that selectively interact with tumor cell membrane receptors. To date, many nanoscale agents have been tested with different activation techniques.

4.4.1 Near-infrared (NIR) photothermal therapy with nanoparticles

Agents that absorb within the near infrared (NIR) region can be an ideal candidate for delivering hyperthermia. Light activation of dyes result in heat production. Normal tissue absorption of light is minimal within the NIR region, between 700 nm and 900 nm, which is above the hemoglobin absorption band and below water absorption peak, the two major light absorbers of light in the human body. Therefore, compared to other wavelengths, NIR light can penetrate deeper with little energy loss. Under certain thresholds of irradiation, tissue will not sustain irreversible damage [73]. Currently, gold nanospheres, gold nanorods, gold nanoshells, gold nanocages, and carbon nanotubes are the chief nanostructures that have been demonstrated in photothermal therapy due to their strongly enhanced absorption in the visible and NIR regions [74]. Of these, the first three

nanostructures are studied extensively because of their ease of preparation, ready multi-functionalization, and tunable optical properties.

Carbon nanotube: The mechanism of carbon nanotube producing heat involves excitation of optical transitions with relaxation resulting in enhanced vibrational modes in the carbon lattice that cause solution heating. Various *in vitro* and *in vivo* studies have been conducted to test their photothermal effect on cancer therapy. For most *in vitro* studies, a typical system includes a laser emitting around 800 nm, with a power flux of 1-3 $W/cm^{2.}$ The treatment time is usually 3 minutes. The concentration of the nanotubes used is around 2.5-5 mg/L [75-77]. Recently, more and more *in vivo* trials have been reported. In a study conducted by Moon et al [78], single walled carbon nanotubes (SWCNs) were coated with PEG to increase their retention time in the circulation. Using an 808 nm laser with an output at 5.3 W, they managed to eliminate a 70 mm^3 tumor by 3 minutes laser exposure in mice. The concentration they used was 120 mg/L, which is much higher than the *in vitro* cases reported. Burke et al [79] examined the long term survival of mice treated with multi-walled carbon nanotubes (MWCNs) after NIR radiation, however, even higher concentration (1000 mg/L) has to be used to achieve complete tumor recession.

Gold (Au) nanoparticles: Another important candidate for NIR photothermal therapy is Au nanoparticles, including Au nanoshells, nanoclusters and nanorods. Research has shown that the interaction of Au nanoparticles with excitation light corresponding to their surface plasmon resonance (SPR) could generate heat [80]. Therefore, by tuning the SPR of Au nanoparticles, which is controlled by the aspect ratio of the nanoparticle [74], Au nanoparticels with different absorption peak could be synthesized easily. Phase I human

clinical trials are ongoing to test their clinical potential [12]. Au nanoparticles can be much stronger NIR absorbers than conventional NIR dyes and therefore a more effective photothermal coupling agent. For example, the calculated absorption cross sections of Au nanoshell are 6 orders of magnitude of indocyanine green (ICG) [81, 82].

In a mouse model, O'Neal et al [81] treated tumors with Au nanoshell by tail vein injection and achieved complete tumor regression. The 808 nm NIR illumination was applied with an 800 mW laser for 3 minutes at 4 W/cm^2. In the tumor region, the recorded temperature was around 50 °C after 30 seconds laser exposure [81]. In an early study conducted by Hirsch et al [82], PEG coated Au nanoshells were injected interstitially into the tumor region and excited with a 800 mW laser emitting at 820 nm. The power density was also 4 W/cm^2 and the treatment time was less than 6 minutes [82]. Both studies showed that laser application to nearby healthy tissue or to tumor without nanoshell treatment did not induce a significant temperature increase probably because of the preferential accumulation of the Au nanoshells into the tumor region which minimized the damage to surrounding tissues.

In a more recent study, Li et al [83] compared passive targeting and active targeting in a mouse tumor model. They used arginine-glycine-aspartic acid (RGD) conjugated dendrimer-modified gold nanorods (RGD-dGNRs), where RGD is used to achieve tumor targeting, dendrimer coating was used to conjugate RGD with Au nanorods. In their study, the NIR laser was emitting at 808 nm at a power density of 24 W/cm^2 and a spot size of 5 mm diameter. Therefore, the calculated power output of the laser was around 4.7 W. The treatment time was 5 minutes. When the tumors reached 5 mm in diameter, they were irradiated four times per month, once every week. Prior to NIR irradiation, mice

were injected with either 200 μg of RGD-dGNRs to study active targeting or 200 μg of dGNRs to study passive targeting. Their results showed a much higher tumor growth inhibition capability of RGD-dGNRs than pure dGNRs 28 days post treatment.

The biodistribution of Au nanoshell studies have been carried out by several research groups using tumor bearing mice [83, 84]. Results showed that PEG coated Au nanoshell were mainly concentrated in the spleen, liver, and tumor.

Dye encapsulated nanoparticles: Encapsulating NIR dye into a nanoparticle can increase its availability at the tumor site as well as decrease its presence in the healthy tissue. In our lab, indocynine green (ICG) encapsulated within PLGA nanoparticle at a concentration of 5.5 mg/L (~7μM ICG) has been shown capable of producing a 43 ºC hyperthermia within 3 min of laser exposure at a power density of 1 W/cm^2.

4.4.2 Nanoparticles excited with RF field

Carbon nanotubes and Au nanoparticles can also be excited by RF field. Recently, some research groups have explored the possibility of using the conductivity properties of gold nanoparticles (GNPs) and single-walled carbon nanotubes (SWNTs) to potentiate heating efficiency of an RF field. Traditional RF field induced hyperthermia is usually invasive and can cause collateral organ overheating. GNPs and SWNTs can be absorbers of RF energy and thus can improve heating specificity and produce noninvasive heating.

The heating capacity of GNPs is determined by the concentration of the GNPs and the power of the RF field [85, 86]. From Gannon's study [85], the rate of heating increased with increasing concentration of GNPs. Using a 200 W RF field working at 13.56 MHz, their data showed that 67 μM GNPs can raise the temperature to 90 °C (from a baseline of around 25 °C) after 5 minutes whereas 1.1 μM barely had any heating effect. If the

power is increased to 800 W, 67 μM GNPs can raise the temperature to 90°C within 90 seconds. Cardinal et al. [86] exposed tumor-bearing rats to a RF field following the injection of GNPs and achieved total tumor ablation. In their study, they used a 35 W RF field generator working at 13.56 MHz. However, in the control groups which were injected with water, 4 °C temperature increase was recorded after applying the RF for 7 minutes, but they claimed that thermal injury was not seen in control samples.

SWNTs can also be excited by an RF field due to their resistive conductivity [87]. Similar to gold nanoparticles, the rate of heating is dependent on the concentration of the SWNTs and the power of the RF field. Gannon et al. [87] treated tumor-bearing rabbits with RF field following intratumor injection of SWNTs and achieved complete thermal tumor necrosis.

When comparing GNPs with SWNTs, GNPS exhibit a higher heat production capacity. From Gannon's data, using 600 W RF field, 67 μM GNPs (11.19 mg/L) was able to increase the temperature 80 °C (from 25 °C) within 2 minutes of exposure, whereas 250 mg/L SWNTs can only increase temperature by 33°C within 5 minutes exposure [85, 87].

4.4.3 Magnetic fluid hyperthermia (MFH) by magnetic nanoparticles

Magnetic fields can induce heat when a local inductive material is implanted into the body. The problem with this type of heating is that overheating of superficial normal tissue could occur due to the occurrence of eddy currents near the surface of the human body. For this reason, eddy-current absorbers have to be applied during the application of magnetic field [57]. The absorbers are usually made of silicon rubber encapsulated with carbon powder.

Magnetic nanoparticles can be used to replace the local inductive implant to achieve more precise and noninvasive heating, which is called magnetic fluid hyperthermia (MFH). The magnetic nanoparticles are delivered to a tumor either intravenously or through direct injection. The heating mechanism of MFH is due to the rotation of the magnetic moment within a nanoparticle or of the entire nanoparticle within its surroundings [88, 89]. This magnetic moment of a particle changes orientation to align with the magnetic field. As the particle moment returns to its equilibrium position, the magnetic energy dissipates as thermal energy [88]. Meanwhile, the movement of particles in low-viscosity fluids causes frictional losses of their energy, which is released as heat.

Currently the most commonly used particle formulation in MFH is iron oxide particles. They demonstrated no adverse effects on tissue when delivered into the lymph nodes of dogs [12]. Furthermore, it presents a high Curie temperature (minimum temperature at which the particle becomes paramagnetic) and high saturation magnetic moment [57].

The problem with MFH is that the thermal enhancement capability of iron oxide is low, which leads to a high quantity of iron particles required to induce heating; tumors were injected with up to 10% total weight of iron oxide [82, 90].

4.4.4 Advantages and disadvantages of different nanoparticle-based hyperthermia

As has been discussed before, there are three major types of nanoparticle-based hyperthermia, NIR photothermal therapy, nanoparticle enhanced RF field hyperthermia, and MFH.

For MFH, the advantage is that if low Curie temperature nanoparticles can be synthesized, the temperature of hyperthermia can be controlled fairly easily as the particles will stop responding to the magnetic field and thus stop producing heat when the Curie

temperature is reached. However, the disadvantage of MFH is also obvious. First of all, the application of a magnetic field would cause overheating of superficial normal tissue. Secondly, the heating capacity of iron particles is low which means a high quantity of particles is needed.

Nanoparticle enhanced RF field hyperthermia could be a promising strategy for hyperthermia delivery. Compared to traditional RF field hyperthermia, it is noninvasive and more targetable. Furthermore, RF energy has been shown to penetrate tissue more deeply than NIR light. At 220 MHz, RF can penetrate 7 cm and this number increases to 17 cm when the frequency is 85 MHz [12], whereas NIR light only penetrates ~1 cm into the tissue. The disadvantage of RF field is that it can cause temperature increase in healthy tissues. In one report [86], a 4 ºC increase was observed in tumor injected with water. Although no thermal damage was observed, this slight temperature increase could cause HSP overexpression and subsequently compromise the treatment outcome.

When comparing GNPs and SWNTs in the application of RF field hyperthermia, GNPs might be a better choice since GNPs are better conductors of RF energy than SWNTs and fewer GNPs are need to achieve a target temperature.

NIR photothermal therapy has shown the highest safety among all the three types of hyperthermia. When no absorber is present, the application of NIR laser would cause little if any temperature increase in the tissue because the tissue absorbs little light in the NIR and because the power of the laser used in this type of treatment is low (usually around 1-3 W, whereas power of the RF field is at least 100 W).

When comparing organic and non-organic absorbers, non-organic absorbers, such as Au nanoparticles, carbon nanorubes, usually have a higher heating capability. But the issue

with those non-organic absorbers is their biocompatibility. Whether they are accumulated or removed from the body after finishing their role as heat inducers is not clear. In Li's report [83], gold nanoparticles were still present 28 days after injection. With biodegradable organic absorbers, this issue would not exist. They will be cleared fairly quickly, usually in days. Another advantage with the organic dyes is that they can be more easily encapsulated, or incorporated into nano-scale drug carriers such as polymers or liposome and therefore can be more easily combined with drugs or imaging tracers.

5. Hyperthermia-Chemotherapy Combinational Treatment Modality Used in This Study

The application of heat by itself as a cancer treatment modality has not yielded general success and its efficacy is still controversial. Compared to radiation which induces direct cellular DNA damage via breaking DNA double-strand, heat is not able to cause severe DNA-damage by itself. Compared to chemotherapy which mostly target fast dividing cells, hyperthermia lacks a specific feature which makes it targetable. This situation leads to a dilemma in hyperthermia application: on the one hand, extreme temperature (>47°C) is preferred in order to achieve ideal cancer cell killing and avoid adverse effect (HSP expression, MDR induction, etc) while on the other hand, extreme temperature will inevitably induce healthy tissue injury due to the lack of targeting capability. Therefore, in most clinical settings, lethal hyperthermia (>47°C) is rarely used although it is superior in inducing tumor necrosis; instead, hyperthermia is often used at sub-lethal level (<43°C) as an adjuvant treatment modality to magnify the therapeutic effect of radiation or chemotherapy. **For this purpose, an ideal hyperthermia should be: 1) targetable; 2) able to avoid adverse effect such as HSP overexpression when delivered at sub-lethal**

temperature; 3) able to achieve thermo-chemo sensitization when combined with chemotherapy (synergistic effect), especially when treating MDR cancer cells.

In this study, a synergistic effect means hyperthermia aided the functionality of the chemotherapy drug, which could happen through facilitated drug uptake in cancer cells due to increased cell membrane permeability under hyperthermia conditions, or through inhibition of MDR thus allowing the drug to have a greater impact in MDR positive cells. The interaction between hyperthermia and chemotherapy could also be "additive" or "sub-additive". An additive effect occurs when hyperthermia and chemotherapy act on the cancer cells on their own and do not affect each other; if the addition of hyperthermia compromises the effect of chemotherapy, the resulting total effect will be considered "subadditive". An additive effect is calculated by summation of the cytotoxicity of each individual cancer treatment. Therefore, a synergistic effect can be determined by comparing the cytotoxicity of the actual combinational treatment to the calculated additive effect. If the cytotoxicity from the combinational treatment group is greater than the calculated additive effect, the combinational effect is defined as "synergistic".

In this work, a novel dye enhanced hyperthermia cancer treatment modality with future targeting capability was studied. This new approach employs a rapid temperature increase of localized heating to the cancer cell. The concept of combining chemotherapy and hyperthermia for treating cancer is not new. Many research groups have investigated the effect of hyperthermia on different cancer cell lines with and without chemotherapy. However, most of them employed an external heating apparatus which heats up cells gradually; none of them investigate the effect of rapid heat accumulation to the cancer cell. **In this respect, this research is novel and therefore, it is important to first test**

the cancer cell killing/growth inhibition effect of rapid rate localized heating *in vitro* and understand its mode of action.

This new treatment approach was comprised of an ICG-NIR laser hyperthermia delivery system and a chemotherapy drug, DOX. NIR laser is chosen because of its tissue penetration property and its safety.

5.1 DOX as the Chemotherapy Agent

DOX was chosen as the chemotherapy agent in this combinational approach and was added with ICG simultaneously to a MDR positive cancer cell to study hyperthermia-chemotherapy interaction through laser excited ICG.

DOX is one of the most widely used chemotherapy agent in cancer treatment [91]. It is an anthracycline antibiotic that has the ability to stabilize DNA - topoisomerase II complex thus leading to the breakdown of DNA double strand and trigger p53-mediated apoptosis [92, 93]. Pegylated Liposomal DOX is recommended by the National Institute of Clinical Excellence, as the drug of choice for many patients with advanced ovarian cancer for whom first line chemotherapy has failed [94].

5.2 NIR Laser-ICG Hyperthermia Delivery System

In this study, ICG was used as the heating agent. It absorbs laser energy in the near infrared range and converts the energy to heat. ICG is a dye with a tricarbon structure. Its absorption peak is about 800 nm. Upon exposure, ICG absorbs NIR energy and emits fluorescence light as well as heat upon returning to the ground state. The whole process takes place almost instantaneously. The final temperature that can be reached and the time it takes to reach that temperature depend on the power density of the laser and the concentration of ICG.

ICG has been approved by the FDA since 1956 for various clinical uses such as determining cardiac output and blood plasma volume, hepatic function assessment, capillary patency measurement, and localization of tumors in tissues [95, 96]. The application of ICG as a hyperthermia agent has not been reported extensively. Some use it to achieve high temperatures (beyond 60°C) for tissue welding. For example, Joie and coworkers used ICG as a hyperthermal agent in sutureless laser tissue welding, where pieces of tissue are fused using NIR irradiation [97].

So far, there are few reports in using ICG as a hyperthermia agent for cancer treatment. Most researches are focusing on its photodynamic effect [98, 99] which involves the generation of reactive oxygen free radicals (mostly singlet oxygen) to kill cancer cell by photooxidation. ICG is capable of producing both a photodynamic and photothermal effect using a NIR laser, depending on the laser's power density. Usually, a low power density laser (< 0.1 W/cm^2) [98] and a high concentration of ICG (>50 μM) were used to induce a photodynamic effect. In comparison, in photothermal applications, a higher energy laser is used (up to 20 W/cm^2) [98] with a lower concentration of ICG, depending on the target temperature (usually <10 μM).

II. STATEMENT OF PURPOSE

The purpose of this study, therefore, was to explore the efficacy and effectiveness of rapid rate localized heating and lay the foundations for future development of a DOX/ICG loaded nanocarrier for targeted drug delivery and therapy. Its cytotoxicity and mechanism of action on cancer cell killing/growth inhibition was studied. These basic understandings will serve as a foundation for the ultimate achievement of targeted chemotherapy-hyperthermia treatment.

For this purpose, cell culture experiments *in vitro* have been conducted on a MDR human uterine sarcoma cell line MES-SA/Dx5 and its non-MDR parent cell line MES-SA. Since the purpose was to establish the efficacy of the proposed treatment modality on cancer cells, normal cell lines were not included. A standard cell culture incubator targeting at 43 °C was used as the energy source to mimic a slow rate hyperthermia. All the experiments were carried out with both hyperthermia delivery modalities.

It is hypothesized that, if applied at moderate temperature (43 °C), this highly localized and rapid heat accumulation will induce necrotic rather than apoptotic cell death without triggering cellular protective mechanisms, such as the simultaneous induction of MDR and HSP expression, usually associated with slow rate hyperthermia targeting at the same temperature. Also, if applied together with chemotherapy, a synergistic cell killing is expected through thermal chemosensitization, especially in MDR cell lines.

We expect to see greater and synergistic cell killing/growth inhibition when combining chemotherapy with NIR laser-ICG hyperthermia, while HSP expression will maintain at the basal level. During this mode of therapy, necrosis will be the major cause of cell death; when combining chemotherapy with slow rate incubator hyperthermia, most cells will die through the apoptotic pathway.

III. SPECIFIC AIMS

Specific Aim 1: Conduct cell culture experiments in vitro to study the level of HSP expression in the slow rate (incubator) hyperthermia and rapid rate (NIR laser-ICG) hyperthermia to both non-MDR human uterine sarcoma cell line and its MDR variant.

Cancer cells acquire thermal tolerance through HSP overexpression. The purpose of specific aim 1 is to find out how HSP overexpression is related to the temperature of heating, duration of heating and rate of heating.

In most thermo dosimetry models, such as the widely used CEM 43 °C model, temperature and duration of heating are the two parameters that define thermal damage. In other words, if two treatments have the same CEM_{43} value, they should have the same cell killing/growth inhibition effect. However, in our preliminary study, we observed different hyperthermia chemotherapy interaction with two types of hyperthermia delivered at similar thermal dose but at different heating rate [100]. The rapid rate photothermal treatment showed synergy to chemotherapy whereas a sub-additive effect was found using the slow rate incubator hyperthermia. It is highly possible that the HSP was overexpressed in the latter mode of heating and thus protected the cells from being damaged by heat stress. Based on this observation, we hypothesize that 1) the rate of heating is a determinant factor in causing HSP overexpression; 2) the proposed rapid rate NIR laser-ICG hyperthermia could avoid HSP overexpression because the duration of treatment is short; 3) the slow rate incubator hyperthermia will cause extensive HSP overexpression.

For this purpose, experiments have been conducted to identify HSP level in different hyperthermia treatment regimes. The comparison was between the treatments that have similar thermal dose but different heating rate, using the CEM 43°C model.

Specific Aim 2: Conduct cell culture experiments in vitro to assess the cancer cell killing/growth inhibition capability of hyperthermia delivered by incubator and NIR laser-ICG system to both non-MDR human uterine sarcoma cell line and its MDR

variant. Monitor the initiation and propagation of cell death induced by the two different hyperthermia delivery modalities.

As described before, ICG absorbs laser energy and converts it to heat; therefore, it is reasonable to hypothesize that the intracellular binding site of ICG would be the direct target in the proposed hyperthermia. The transport kinetics and subcellular localization of ICG has been studied extensively by various research groups [98, 101]. Both groups showed that ICG is taken up by the cells through a carrier-mediated transport process against a concentration gradient. Once the ICG enters the cell, it binds to cytoplasmic proteins such as gluthathione *S*-transferase and ligandin. These proteins will be the direct target during the ICG excitation process. Therefore, during the application of NIR laser-ICG hyperthermia, the temperature at these cellular organelles could be much higher than measured at the thermocouple which is placed in the surrounding supernatant.

We hypothesize that the cancer cell killing/growth inhibition effect induced by incubator hyperthermia and NIR laser-ICG hyperthermia are through two different pathways. Moderate hyperthermia at 43 °C induced by the incubator is not enough to exert necrosis; indirect cellular damage is most likely and apoptotic cell death result from this process; while in the NIR laser-ICG hyperthermia, extensive necrotic cell death is expected through protein denaturing induced by rapid heat accumulation at the ICG bound cellular proteins. Therefore, the purpose of this specific aim is 1) measure the cytotoxicity of both hyperthermia delivery methods; then 2) determine the necrotic/apoptotic cell death associated with them.

To fulfill this aim, cytotoxicity assay and apoptotic/necrotic cell death assay to a human uterine sarcoma cell line MES-SA and its MDR variant MSE-DA/Dx5 has be carried out.

The purpose of incorporating a MDR cell line is to set up a baseline measurement of the cytotoxicity of hyperthermia alone for further comparing the cytotoxicity of hyperthermia plus chemotherapy in specific aim 3.

Assays were carried out in the following groups:

Incubator hyperthermia;

NIR laser-ICG hyperthermia:

- ICG alone

- Laser alone

- NIR laser-ICG

The cell proliferation after each treatment was compared to the control group by SRB assay, which evaluates the total protein content of the living cells. Apoptotic and necrotic cell death was first distinguished by a method using fluorescence microscopy with Hoechst 33342 (Invitrogen Corporation, Carlsbad, California) and propidium iodide (PI) (Invitrogen Corporation, Carlsbad, California) [102, 103]. Caspase 3 activity was monitored as an indicator of cell apoptosis.

Specific Aim 3: Conduct cell culture experiments to study hyperthermia chemotherapy (DOX) interaction with hyperthermia delivered by NIR laser-ICG system to both non-MDR human sarcoma cell line and its MDR variant. A synergistic cell killing/growth inhibition effect is expected. The cytotoxicity of DOX alone was also accessed.

Different from ICG which is a hydrophilic molecule and taken by the cells through carrier-mediated active transport, DOX is lipophilic and transport into the cell is by simple diffusion [104]. The membrane permeability is therefore the most important parameter in determining DOX intracellular concentration. At elevated temperatures, the

cell membrane is found to be more fluidic and unstable. Therefore, it is hypothesized that hyperthermia could magnify the cytotoxic effect of DOX through facilitated DOX uptake. Generally, a synergistic cell killing/growth inhibition effect is expected in both DOX sensitive and MDR cell lines when hyperthermia is applied in combination with DOX. However, the situation in MDR cells is more complicated due to the presence of the drug efflux pump P-gp. Although hyperthermia could increase DOX uptake in MDR cells, it is still unclear whether the increased uptake can last after the temperature returns to 37 °C. One group claims that they observed both reduced P-gp and increased membrane permeability [1] whereas in other observations, only increased drug uptake by enhanced membrane permeability was found during hyperthermia [49]. In this study, the activity of P-gp drug efflux pump under heat stress was measured.

For this purpose, Specific aim 3 has three sub-aims:

1). Investigate the synergistic cell killing/growth inhibition effect when combining DOX with NIR laser-ICG hyperthermia; To fulfill this aim, the SRB assay was used to measure cytotoxicity; Synergistic/additive effect was determined by statistical analysis. All these tests have been carried out on both DOX sensitive MES-SA cell and its MDR variant MES-SA/Dx5.

Assays were carried out in following groups:

DOX alone;

DOX with incubator hyperthermia;

DOX with NIR laser-ICG

2) Compare the cellular uptake and intracellular distribution of DOX at normal temperature (37 °C) and elevated temperature achieved by either incubator or

photothermally activated ICG. DOX uptake by the two cells was determined using a fluorescence microscope. This test was performed in the above mentioned groups.

3) Measure P-gp drug efflux pump activity during and after heat stress delivered by NIR laser-ICG hyperthermia

The calcein-AM test was used to monitor the function of P-gp drug efflux pump during and after hyperthermia treatment. Similar with DOX, calcein-AM is a lipophilic non-fluorescent dye and can penetrate cell membrane by free diffusion. After entering the cell, the ester bonds of calcein-AM will be cleaved. This transforms lipophilic non-fluorescent calcein-AM to hydrophilic fluorescent calcein, which can no longer diffuse out. P-gp can actively transport calcein-AM outside the cell membrane. Therefore, P-gp activity can be quantified by calcein fluorescence intensity: non-MDR cells will show strong fluorescence while MDR cells will show little fluorescence.

In order to examine whether hyperthermia down-regulates P-gp activity, the calcein-AM assay was performed immediately after NIR radiation. The calcein-AM assay was also performed in non-heated drug sensitive cells to serve as a positive control and in non-heated MDR cells to serve as a negative control.

IV. METHODOLOGY

In this section, general cell culture procedures and hyperthermia delivery systems will be described as they were used throughout the whole study; then different assays and data analysis methods for fulfill each specific aim will be introduced accordingly.

1. Cell Culture

All the experiments were carried out by *in vitro* cell culture studies. A DOX sensitive human uterine cancer cell line MES-SA and its MDR variant MSE-SA/Dx5 was

purchased from ATCC together with appropriate cell culture medium and serum. Cells were grown according to ATCC instructions; detailed cell culture protocols are presented in the Appendix, including the preparing of culture medium, cell splitting and cell seeding. A Hera Cell incubator which was set at 37°C and supplied with 5% CO_2 provides a standard environment for cell growth. All cell culture experiments were carried out in a class 2 biological safety cabinet in sterile treated 96-well plates.

2. Incubator Hyperthermia Delivery System

In order to mimic a conventional whole body hyperthermia, a cell culture incubator was used as the energy source. The temperature of the incubator was set at 43°C. 96-well plates that were originally incubated in the 37°C incubator were transferred to the 43°C incubator. Temperature calibration studies were carried out to find out the temperature profile of the transferred 96-well plates.

3. NIR Laser-ICG Hyperthermia Delivery System

3.1 System Establishment

For delivering rapid hyperthermia from within the cell, ICG (Cardiogreen, Sigma-Aldrich) has to be first delivered into a cell and then activated by a NIR laser. For this purpose, a laser heating system was assembled (shown in the following figure). The system was comprised of a laser module (RLDH808-1200-5, Roithner Laserthchnik Gmbh), a laser holder, a heated stage insert (WPI Heated Stage Insert, World Precision Instruments Inc) and a mobile stage with an extension arm. The external cover of the system was also designed for safety consideration; power supplies for the laser and the heated stage insert are also placed outside the box for the same reason. The system is shown in Figure 2.

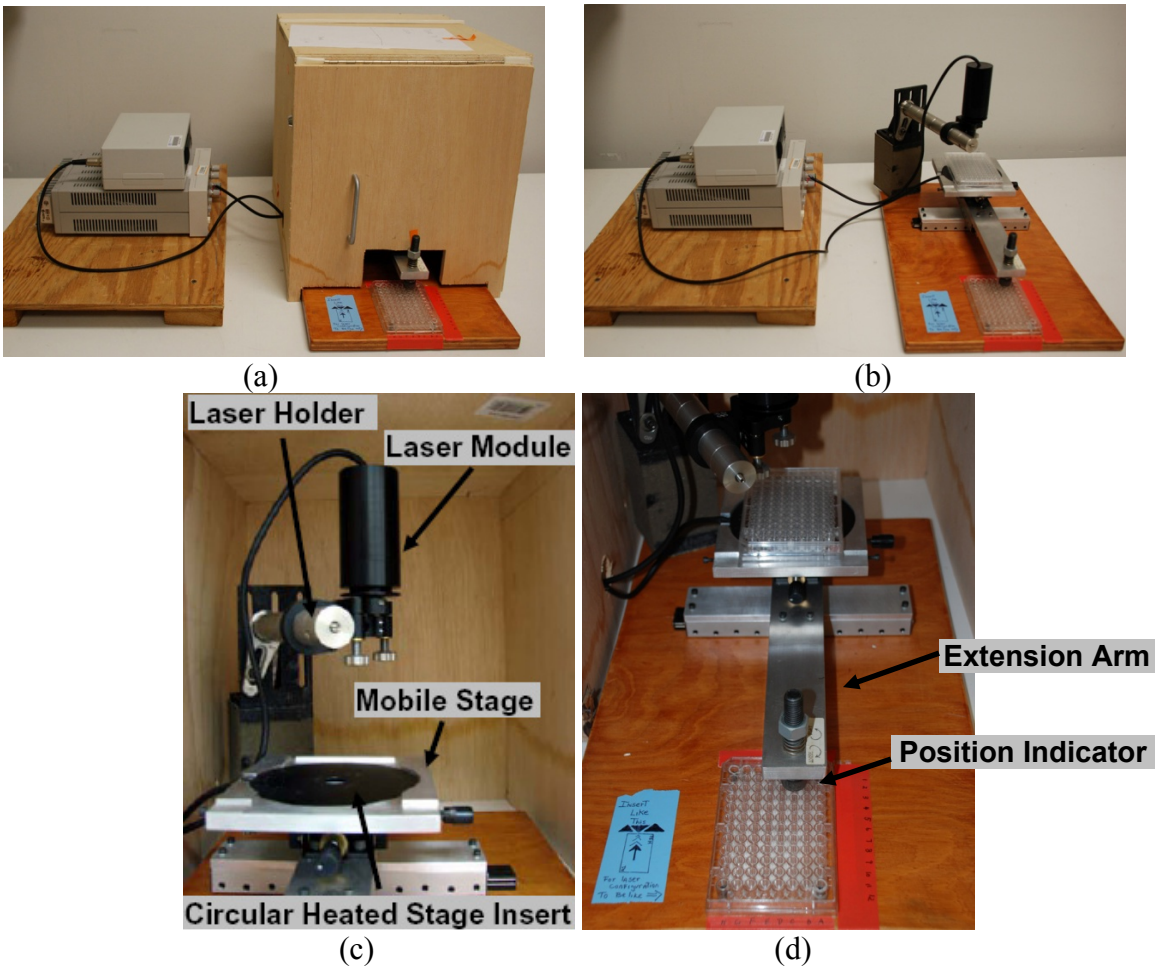

Figure 2 NIR laser system for laser-induced hyperthermia. (a) system overview with box cover; (b) without cover; power supplies for the laser and the heated stage insert are placed outside the box; (c) & (d) different parts of laser system.

During operation, the whole system was covered in a wooden box to eliminate air currents and also to prevent the laser light from exiting. The laser module was fixed to a holder so that its beam is perpendicular to the 96-well plate which was placed on the heated stage insert. The heated stage insert, placed on a mobile stage positioned directly below the laser was powered by an external source to ensure that the plate is at 37°C prior to the laser application.

The NIR laser source emits light at 808 nm with an output power of 1 Watt. Given its 15 mm^2 spot size, the calculated power density is 6.7 W/cm^2. This small spot size also guaranteed only one well being excited at a time. The exact positioning of a well with the laser beam was achieved by moving the stage using the extension arm outside of the box as shown in the right side of Figure 2. The arm was used to move the location of the well plates thereby allowing different wells to be exposed to the NIR energy one at a time without opening the box.

To verify the positioning of the laser relative to the wells, an infrared beam finder card (IRC-42R, Sofradir EC) was used to visualize the NIR laser beam. At the same time, the specific well under exposure and its relative position outside the box was indicated by a position indicator (another 96-well plate). Laser protection goggles that block NIR light were worn by the user during laser operation. Other necessary safety measures were also taken, especially appropriate engineering and administrative controls.

3.2 System Calibration

A temperature calibration procedure was carried out after the system in Figure 2 was built. The purpose was to find out the optimal settings for the heated stage insert controller so that a well filled with 230uL of media could be maintained 37°C. The temperature in each cell across the entire 96-well plate when using the heated stage insert was measured using a thermocouple and recorded. During this calibration process, a 96-well plate filled with 230uL of media was placed on the heated stage insert and the settings on the heated stage controller adjusted so that the temperature in the well as at 37°C. A 20 minutes time interval was allowed for steady temperature to be achieved. Finally, the temperature of

each well was recorded to generate a temperature distribution profile of the culture plate. The temperature distribution of the 96-well plate is shown in Table 1.

	1	2	3	4	5	6	7	8	9	10	11	12
A	29	33	35.8	36.1	**36.7**	35.9	**36.9**	**36.9**	**36.8**	35.7	33.2	29.8
B	31.6	34.4	**36.8**	**36.7**	**37.1**	**36.6**	**36.7**	**36.9**	**36.5**	**36.6**	34.8	32.7
C	32.9	35	**37.1**	**37.2**	**37.3**	**36.9**	**37.4**	**37.3**	**37.3**	**37.2**	35.7	33.8
D	33.8	35.6	**37.3**	**37.3**	**37.1**	35.7	**36.9**	**37.4**	**37.3**	**37.2**	35.7	34.1
E	33.8	35.5	**37.3**	**37.4**	**37.2**	35.7	**37.1**	**37.3**	**37.3**	**37.2**	35.9	33.9
F	33.4	35.4	**37**	**37.1**	**37.3**	**36.9**	**37.3**	**37.3**	**37.2**	**37.1**	35.8	33.7
G	31.1	34.1	**36.6**	**36.7**	**36.8**	**36.8**	**37.6**	**37.4**	**37.3**	**36.6**	35.1	31.3
H	29.1	33.2	35.7	35.9	36.5	36.4	**37.1**	**36.9**	**36.7**	35.8	34.7	29.6

Table 1Temperature distribution of 96-well plate in the heated stage insert.

Note that the temperature distribution is not homogenous across the whole plate with the peripheral regions lower and central higher. This is because the heated stage is round with a hole in the center and the multi-well plate is rectangular. The temperature at wells 6D and 6E was lower because the heated stage has a whole at that position. Wells with temperature ranging from 36.5°C – 37.5°C (bold) were be used for laser studies.

3.3 Thermal Dose Calculation

In order to be able to compare the effect of rapid rate hyperthermia with slow rate hyperthermia, an isoeffect dose of the two different types need to be calculated. As the first step the temperature profile of the two heating modality needed to be obtained.

3.3.1 Temperature profile of incubator hyperthermia

The temperature increase during incubator hyperthermia was measured in a 96-well plate that was filled with 230 μL of media in a well. The plate was initially kept in a 37 °C

incubator and then transferred into the hyperthermia incubator so that the baseline of the heating is 37 °C. During the measurement, a thermal couple was placed in the media of a well for temperature recording. The incubator was set at 43 °C and 50 °C and the temperature profile obtained from both cases.

3.3.2 Temperature profile of laser-ICG hyperthermia

This procedure was carried out with the liquid in the wells initially at 37 °C to find out an optimal concentration at which ICG is not cytotoxic when it is not excited while it is able to produce a peak temperature of 43 °C or 50 °C.

30 μL of ICG at concentrations of 7.7 μM, 38.5 μM, and 77 μM was added to the wells that were originally loaded with 200 μL media to achieve final concentrations of 1 μM, 5 μM, and 10 μM, respectively. Wells were then excited by the NIR laser and their temperature profiles obtained using a thermal couple placed inside the well.

After obtaining the temperature profile during both incubator and laser-ICG hyperthermia, the CEM_{43} model was applied to calculate the thermal doses in each treatment.

4. The Fulfillment of Specific Aim 1

Specific Aim 1: Conduct cell culture experiments in vitro to study the level of HSP expression in the slow rate (incubator) hyperthermia and rapid rate (NIR laser-ICG) hyperthermia to both non-MDR human uterine sarcoma cell line and its MDR variant.

Heat-caused damage may be weakened by HSP overexpression. HSP could protect cells from heat induced damage by stabilizing unfolded or misfolded peptides and giving cells time to repair or re-synthesize damaged proteins. This specific aim will test HSP expression in both incubator hyperthermia and NIR laser-ICG hyperthermia.

The 70 kilodalton heat shock proteins (HSP70s) are the focus in this part of the research because they provide thermotolerance to cells exposed to heat stress. An Enzyme-Linked Immuno Sorbent Assay (ELISA) was used to detect the expression of HSP using an antigen that can specifically detect HSP. Basal level HSP expression was identified in the cells incubated at normal temperature (37 °C). At 43 °C, the level of HSP in NIR laser-ICG hyperthermia treated cells is expected to be the same as in cells incubated in 37 °C; while elevated HSP expression is expected in cells incubated in a 43 °C incubator. At 50 °C, both slow rate incubator hyperthermia and rapid rate laser-ICG hyperthermia should have similar HSP levels compared to cells maintained at 37 °C.

4.1 HSP Expression in 43 °C & 50 °C

The procedure for this experiment is as follows: at the first day, cells were seeded, and allowed 24 hours to attach and stabilize. At the second day, cells were divided into 2 groups. Group1: no treatment was given and HSP level was quantified as negative control; Group2 cells were exposed to different hyperthermia treatments. The ELISA assay was used on both Group1 and Group2 cells 1, 3, 6, 12 and 24 hours after they received the hyperthermia treatment. Wells that contained only media were also included to provide a background measurement and subtracted from the wells containing both cells and media.

4.1.1 Cell seeding

When the cells reached a sufficient confluency, which was determined by viewing the culture flasks under an optical microscope, they were first detached by trypsin-EDTA solution and then counted with the aid of a hemocytometer under the microscope for cell density calculation. After removing the trypsin-EDTA and resuspending with culture media, cells were transferred to 96 well plates at a concentration between 5,000-8,000

cells per well (200 μL cell-medium suspension). Detailed cell seeding diagram in 96-well plates for both hyperthermia will be discussed below.

1) Cell seeding in 96-well plate for incubator hyperthermia

Table 2 gives a schematic diagram of cell seeding when using incubator hyperthermia. Compared to NIR laser-ICG hyperthermia where wells are treated one by one, cell seeding in incubator hyperthermia is quite simple. Basically any group of wells can be used because heat is delivered to the wells simultaneously.

	1	2	3	4	5	6	7	8	9	10	11	12
A												
B												
C	M	○	○	○	○							
D	M	○	○	○	○							
E	M	○	○	○	○							
F	M	○	○	○	○							
G												
H												

Table 2 Cell seeding diagram for incubator hyperthermia; cell density: 5000-8000 cells/well. M: wells with only media; ○: wells with cells.

2) Cell seeding in 96-well for NIR laser-ICG hyperthermia

Table 3 gives a schematic diagram of cell seeding when using laser-ICG hyperthermia. Since wells are treated one by one in this circumstance, it is important to maintain other wells at normal temperature while one well is under laser exposure. Therefore, cells were seeded differently compared to the incubator hyperthermia. A schematic cell seeding diagram is shown in Table 3. In order to eliminate any potential for laser-light cross talk,

the neighboring 8 wells of any single well are left blank if that well is going to receive laser treatment.

	1	2	3	4	5	6	7	8	9	10	11	12
A	Δ	Δ	Δ	Δ	Δ	Δ	Δ	Δ	Δ	Δ	Δ	Δ
B	Δ										Δ	Δ
C	M		○		○		○		○		Δ	Δ
D	M										Δ	Δ
E	M		○		○		○		○		Δ	Δ
F	M										Δ	Δ
G	Δ		○		○		○		○		Δ	Δ
H	Δ										Δ	Δ

Table 3 Schematic cell seeding diagram for laser-ICG induced hyperthermia; cell density: 5000-8000 cells/well. M: wells with only media; ○: wells capable of receiving laser treatment; Δ: peripheral region which could be used for control cells.

4.1.2 Hyperthermia treatment

1) Incubator being the energy source for hyperthermia

Hyperthermia treatment was given 24 hours after cell seeding. During hyperthermia treatment, the incubator was set either at 43 °C or 50 °C. 60 minutes incubation was given to 43 °C hyperthermia treated wells while 30 minutes incubation was given to 50 °C hyperthermia treated wells.

2) NIR laser being the energy source for hyperthermia

24 hours after cell seeding, 30 µL of ICG at concentrations of 38.5µM or 77 µM was added to the wells that were originally loaded with 200 µL media to achieve 5µM or 10 µM final concentration; then the plate was returned to the standard cell culture incubator for 2 hours which allowed for the homogenous distribution of ICG in the well. Next, 3

minute laser treatment was applied to each concentration to achieve 43 °C or 50 °C hyperthermia. These concentrations of ICG were chosen because when exposed to the laser for 3 minutes, they each produced a thermal dose which is similar to 60 minutes 43 °C incubator hyperthermia or 30 minutes 50 °C incubator hyperthermia. After hyperthermia treatment, the plate was returned to the standard cell culture incubator.

4.1.3 ELISA assay

ELISA was performed to identify the HSP70 level 1, 3, 6, 12, 24 hours after hyperthermia application.

A brief description of the assay procedure is as follows: inducible HSP70 is captured by a specific mouse monoclonal antibody which has been pre-coated on the HSP70 Immunoassay plate and then detected with an HSP70 specific rabbit polyclonal antibody. A secondary antibody, horseraidish peroxidase conjugated anti-rabbit IgG, is used to bind to this rabbit polyclonal antibody. Tetramethylbenzidine (TMB) substrate then reacts with horseradish peroxidase to give a blue color in proportion to the amount of captured Hsp70. The color development is stopped with acid stop solution which converts the endpoint color to yellow. The intensity of the color is measured in a microplate reader at 450 nm and quantified with an arbitrary value. The actual concentration could be interpreted with a calibration curve.

5. The Fulfillment of Specific Aim 2

Specific Aim 2: Conduct cell culture experiments in vitro to assess the cancer cell killing/growth inhibition capability of hyperthermia delivered by incubator and NIR laser-ICG system to both non-MDR human uterine sarcoma cell line and its MDR

variant. Monitor the initiation and propagation of cell death induced by the two different hyperthermia delivery modalities.

Specific Aim 2 has 2 sub-aims, which are 1) identify the cytotoxicity induced by the two hyperthermia delivery methods; 2) investigate the necrotic/apoptotic cell death associated with the two hyperthermia delivery methods. These aspects will be discussed respectively in the following section.

5.1 Cytotoxicity Assessment to both Incubator Hyperthermia and NIR Laser-ICG Hyperthermia

Cytotoxicity assessment was based on cell proliferation after hyperthermia treatment. The procedure of the experiment is as follows: on the first day, cells were seeded, and then allowed 24 hours to attach and equilibrate; on the second day, wells were divided into 3 groups. Group1: the total number of cells was quantified as the initial value. Group2 cells was subjected to different hyperthermia treatments and returned to the 37 ºC incubator for 24 hours growth. Group3 cells served as a negative control and no treatment was given; on the third day, cell proliferation of both Group2 and Group3 cells were quantified by SRB assay, which measures the total cellular protein as an indicator of cell proliferation. Wells that contain only media was included as background and the absorbance measurement subtracted from that of the wells containing both cells and media.

5.1.1 Cell seeding

See section IV.4.1.1.

5.1.2 Hyperthermia treatment

1) Incubator being the energy source for hyperthermia

24 hours after cell seeding, the 96-well plates for studying the cytotoxicity of incubator delivery of hyperthermia was removed from the 37 ºC (standard) incubator and put into the 43 °C incubator for 60 minutes. After treatment, the plate was returned to the 37 ºC cell culture incubator for an additional 24 hours.

2) NIR laser being the energy source for hyperthermia

24 hours after cell seeding, 30 μL of ICG at concentrations of 38.5 μM was added to the wells that were originally loaded with 200 μL media to achieve 5 μM final concentration; then the plate was returned to the standard cell culture incubator for 2 hours which allowed for the homogenous distribution of ICG in the well. Next, 3 minute laser treatment was applied to elevate temperature. After hyperthermia treatment, the plate was returned to the standard cell culture incubator for 24 hours.

5.1.3 SRB assay

Cell proliferation was measured by SRB assay. In this study, SRB assay was given to group1 cells 24 hours after cell seeding and to group2 and group3 cells 24 hours after they receive hyperthermia treatment. Cells were first fixed to the bottom of 96-well plate with 10% (wt/vol) trichloroacetic acid (TCA) for 30 minutes. The plates were then washed with water for 3 times. After washing, Sulforhodamine-B (SRB) dye which binds to cellular proteins was added at a concentration of 0.4% (wt/vol) for cell staining. The staining procedure was 30 minutes followed by 3 times washing using 1% (vol/vol) acetic acid which removed the unbound SRB dye in the plate. Lastly, the protein-bound SRB was extracted by 10 mM Trizma-base and the absorbance of dissolved SRB dye was measured at 530 nm using the TECAN fluorometer (Tecan Systems Inc, San Jose, Califonia). This value was then background subtracted (from media only wells) and

compared with controls, which are the SRB values of cells without any treatment for obtaining cell growth.

5.2 Apoptotic/Necrotic Cell Death Detection to both Incubator Hyperthermia and NIR Laser-ICG Hyperthermia

The purpose is to evaluate the extent of apoptosis and necrosis associated with each hyperthermia treatment.

5.2.1 Cell seeding & hyperthermia treatment

See section IV. 4.1.1 & section IV.5.1.2.

5.2.2 Cell apoptosis/necrosis assay

24 hours after treatment, apoptosis/necrosis assay was performed to study the mode of cell death caused by the treatment. Two different assays were used to detect apoptotic and necrotic cell death.

1) apoptosis/necrosis detection based on fluorescence imaging

Apoptotic and necrotic cell death was distinguished by a method using fluorescence microscopy with Hoechst 33342 (Invitrogen Corporation, Carlsbad, California) and propidium iodide (PI) (Invitrogen Corporation, Carlsbad, California) [102, 103]. After hyperthermia treatment, cells were stained with 10 μg/ml of Hoechst 33342 and 10 μg/ml of PI for 5 min and analyzed under an Olympus IX81 fluorescent microscope at 20X and 60X magnification (Olympus America Inc. Pennsylvania). Hoechst 33342 stained all nuclei and PI stained only the nuclei of cells with a disrupted plasma membrane. Nuclei of viable, necrotic and apoptotic cells was observed under fluorescence microscopy as round blue nuclei, round pink nuclei and fragmented blue or pink nuclei, respectively.

2) Quantitative Fluorometric Assay of Caspase 3 Activity as an Indicator of Apoptosis

It has been shown that the initiation all intracellular events during apoptosis is characterized by the activation of a family of specific proteases called cysteinyl-aspartic-acid-proteases (caspases) [105]. To date, human caspase family includes twelve different caspases. Among them, caspase 3 is found responsible for the cleavage and activation of caspase 6, 7. These three effector caspases directly initiate apoptosis by cleaving specific protein substrates within the cell [106].

Since the activation of caspase 3 is a unique and universal event for the initiation of all intracellular events in cell apoptosis, cellular caspase 3 level was monitored as an indicator to support the results from the fluorescence assay.

The Caspase 3 Assay kit, Fluorimetric (Sigma-Aldrich, St. Louis, Missouri) was used for this purpose. This assay is based on the hydrolysis of the peptide substrate acetyl-Asp-Glu-Val-Asp-7-amido-4-methylcoumarin (Ac-DEVD-AMC) by caspase 3. Once Ac-DEVD-AMC is hydrolyzed by caspase 3, 7-amino-4-methylcoumarin (AMC) moiety is released, which could be detected by its fluorescence. The excitation and emission wavelengths of AMC are 360 nm and 460 nm, respectively. This assay was performed in 96-well plates and the fluorescence signal was measured by a TECAN fluorometer.

6. The Fulfillment of Specific Aim 3

Specific Aim 3: Conduct cell culture experiments in vitro to study hyperthermia chemotherapy (DOX) interaction with hyperthermia delivered by incubator as well as NIR laser-ICG system to both non-MDR human uterine sarcoma cell line and its MDR variant. A synergistic cell killing/growth inhibition effect is expected. The cytotoxicity of DOX alone was also accessed.

6.1 Synergistic Cell Killing/Growth Inhibition Measurement in DOX-Hyperthermia Combinational Treatment

To fulfill this aim, SRB assay for detecting the cytotoxicity of DOX in combination with hyperthermia treatment was carried out on DOX sensitive MES-SA cell and its MDR variant MES-SA/Dx5.

The methodology used here was the same as in detecting the cytotoxicity of hyperthermia alone. The difference is that, DOX was given together with the hyperthermia treatment 24 hours after cell seeding.

The procedure of the experiment is as follows: on the first day, cells were seeded, and then allowed 24 hours to attach and stabilize; on the second day, cells were divided into 3 groups. Group1: SRB assay performed to measure the initial cell amount. Group2 cells were treated with DOX-hyperthermia combination and allowed 24 hours of growth. Group3 cells served as a negative control and no treatment was given; on the third day, cell proliferation of both Group2 and Group3 cells was quantified by SRB assay, which measures the total viable cellular protein as an indicator of cell proliferation. SRB assay was also performed on wells that contain only media (background) and subtracted from wells containing both cells and media.

6.1.1 Cell seeding

See section IV 4.1.1.

6.1.2 DOX-hyperthermia combinational treatment

1) DOX alone without hyperthermia

24 hours after cell seeding, 30 μL of 0.77μM, 7.7 μM and 77 μM of DOX was given to the cells. Since the wells were originally loaded with 200 μL of media, the final

concentration of DOX in the well was 0.1 μM, 1 μM and 10 μM. Then the plate was returned to the standard cell culture incubator prior to SRB assay.

2) Incubator being the energy source for hyperthermia

24 hours after cell seeding, 96-well plates for studying the cytotoxicity of incubator hyperthermia was removed from the standard cell culture incubator. 30 μL of 0.77 μM, 7.7 μM and 77 μM of DOX was given to the cells. Since the wells were originally loaded with 200 μL of media, the final concentration of DOX in the well was 0.1 μM, 1 μM and 10 μM. After adding the drug, plate was placed into the 43 °C incubator for 60 minutes. After treatment, the plate was returned to the standard cell culture incubator.

3) NIR laser being the energy source for hyperthermia

ICG for heating and DOX for chemotherapy was given to the cancer cells. Then DOX was added to the wells. 1 minute laser exposure was followed to study hyperthermia-chemotherapy interaction. 24 hours after cell seeding, 30 μL of ICG at a concentration of 43.3 μM was added to the wells, and then 30 μL of 0.86 μM, 8.6 μM and 86 μM of DOX was given to the cells. The resulting final concentration of ICG in the well was 5 μM and the DOX concentration was 0.1 μM, 1 μM and 10 μM respectively. After loading DOX and ICG, the plate was returned to the standard cell culture incubator for 2 hours prior to the 1 minute laser treatment, which elevated the temperature to 43 °C. After hyperthermia treatment, the plate was returned to the standard cell culture incubator for 24 hours.

6.1.3 SRB assay

1) Cytotoxicity of DOX-hyperthermia combinational treatment

Cell proliferation was measured by SRB assay. In this study, SRB assay was given to group1 cells 24 hours after cell seeding and to group2 and group3 cells 24 hours after

they received hyperthermia-chemotherapy treatment. SRB assay was performed as described in section IV.5.1.3.

6.2 Cellular Uptake and Intracellular Distribution of DOX in 37 °C and 43 °C Achieved by Incubator or NIR laser-ICG Hyperthermia

This assay was carried out in both 37°C and 43°C to compare the kinetics of cellular uptake of DOX and its direct target site.

24 hours after cell seeding (see section IV 4.1.1), 30 µL of DOX at concentrations of 77 µM was added to the wells that were originally loaded with 200µL media to achieve a final concentration of 10 µM. Hyperthermia treatment was given immediately after the addition of DOX. Cells were observed under an Olympus IX81 fluorescent microscope (Olympus America Inc. Pennsylvania) equipped with a U-MNB2 (Olympus America Inc. Pennsylvania) filter cube which excites at 470-490 nm and collects the fluorescence signal with a 520 nm long pass filter. Images were taken 1 hour and 24 hours after hyperthermia treatment and compared with their respective controls, which were treated with DOX but not hyperthermia.

6.3 P-gp Drug Efflux Pump Activity after 43°C Hyperthermia Delivered by NIR laser-ICG or Incubator

Calcein-AM assay was used to asses P-gp function after hyperthermia. If the drug extruding capability of P-gp is impaired under heat stress, more calcein-AM can diffuse into the cell and be transformed to calcein. Therefore, intracellular calcein fluorescence intensity can be used as an indicator of P-gp function. In this study, the calcein-AM test was given to heat treated and non-treated MDR cells (MES-SA/Dx5) as well as 37°C incubated drug sensitive cells (MES-SA).

The procedure for the experiment is as follows: on the first day, cells were seeded, and then allowed 24 hours to attach and stabilize; on the second day, cells were divided into 3 groups. Group1 were DOX sensitive MES-SA cells. Calcein-AM assay was performed to group1 cells without any DOX or hyperthermia treatment. Strong fluorescence intensity is expected since there are no P-gp proteins in these cells. Group2 cells are MDR cells MES-SA/Dx5. They were first treated with NIR laser-ICG hyperthermia and then tested with the celcein-AM assay. Group3 cells were also MDR cells but they were assessed by calcein-AM assay without any DOX or hyperthermia treatment. Since MES-SA/Dx5 cells are P-gp abundant, a low level of fluorescence intensity is expected.

6.3.1 Cell seeding

See section IV.4.1.1.

6.3.2 NIR laser-ICG hyperthermia treatment to MDR cells

See section IV.5.1.2.

6.3.3 Calcein-AM assay

Calcein-AM assay was given to Group1 and Group3 cells 24 hours after cell seeding. For group2 cells, calcein-AM assay was given immediately after NIR irradiation.

7. Data Analysis

In this section, data processing methods associated with each assay will be described. Differences and significance among each treatment was tested by statistical analysis.

7.1 Cytotoxicity and Synergistic/Additive Effect Determination

SRB assay was used to measure cell proliferation. Cytotoxicity was obtained in the following treatment groups:

Incubator hyperthermia;

ICG alone;

Laser alone;

NIR laser-ICG hyperthermia;

DOX alone;

DOX + incubator hyperthermia;

DOX + ICG;

DOX + Laser;

DOX + NIR laser-ICG;

Percentage of cell killing/growth inhibition for each treatment group was calculated according to the method described by Monks et al. [107]. Denoting initial SRB value as T_0, control SRB value as C and treatment SRB value as T:

$$\text{cell survival } S = (T - T_0)/(C - T_0) * 100, \ if\ T > T_0 \quad \text{(Equation 3)}$$

$$\text{cell killing } K = (T - T_0)/(C - T_0) * 100, \ if\ T < T_0 \quad \text{(Equation 4)}$$

Note that two equations have been used [107]. If $T > T_0$, the treatment could be considered as growth inhibition; if $T < T_0$, there is no net growth after the treatment, its effect could be considered as cell killing.

Synergistic effect was determined with the assumption that both DOX and hyperthermia treatment have exponential dose-response curves in cancer cells [108] and calculated by a method described by Berenbaum [109]. Denoting the cytotoxicity of DOX alone as E(D), hyperthermia alone as E(H) and the combinational treatment as E(D,H), synergistic effect could be assumed if:

$$E(D,H) > E(D) + E(H) - E(D) \times E(H), \text{ (Equation 5)}$$

where E = 1 - S when $T > T_0$, and E = K when $T < T_0$. The data was then analyzed by ANOVA test with bonferroni post-hoc correction when the comparisons were made between more than two samples. When comparison was between two samples, the *t*-test was used. The combinational treatment is considered synergistic at a significance level of $\alpha = 0.05$ for both ANOVA and *t*-test.

7.2 Caspase 3 & HSP70 Activity

Caspase 3 assay was used to quantify apoptosis. The extent of apoptosis in incubator hyperthermia or NIR laser-ICG hyperthermia was compared to non-treated cells as described in section IV.5.2.2. If denoting caspase 3 quantity in control cells as C, hyperthermia treated as T, apoptosis could be calculated as follows:

$$(T - C)/C * 100, \quad \text{(Equation 6)}$$

Percentage increase of HSP expression treated with incubator hyperthermia or NIR laser-ICG hyperthermia was also calculated according to Equation 6. Calculated percentage increase in cell apoptosis/HSP expression was then analyzed by ANOVA test with bonferroni post-hoc correction when the comparisons were made between more than two samples. When comparison was between two samples, the *t*-test was used. Differences were considered significant when $p<0.05$ for both tests.

V. RESULTS

1. Selection of Isoeffect Dose

1.1 Temperature Profile during Laser-ICG Hyperthermia

As shown in Figure 3, the heat production of ICG was highly concentration dependant. More ICG generated more heat. Heat rapidly accumulated during the first 30 seconds of

laser application and reached maximum at about 3 minutes, then the temperature dropped slowly probably due to photo bleaching.

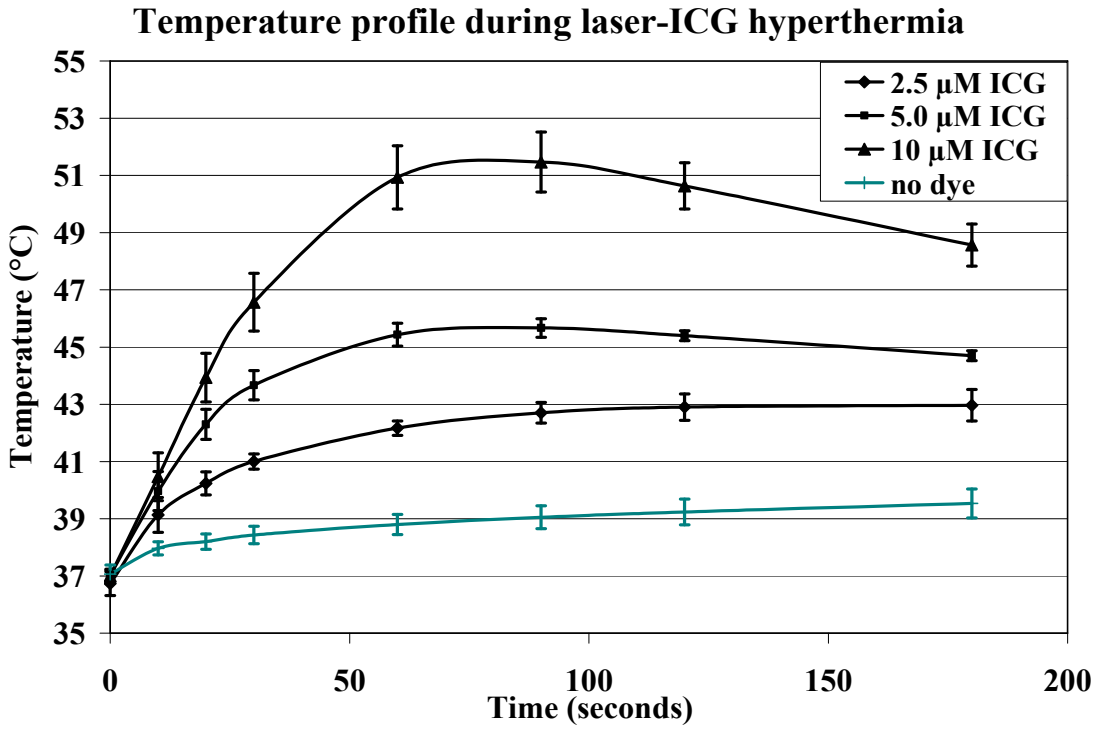

Figure 3 Heat generation as a function of ICG concentration (n=3).

Without ICG, about 2 °C increase was observed with the current laser setting, which is due to the thermocouple absorbing laser energy. This temperature increase was subtracted from the actual temperature profile of laser-ICG hyperthermia when calculating the thermal dose. The cytotoxicity assay indicated that the laser exposure itself with ICG did not affect cancer cell proliferation (shown in Figure 6). During the 3 minutes, 2.5 µM, 5 µM and 10 µM ICG produced peak temperatures of about 40 °C, 43 °C and 50 °C respectively, after subtracting the temperature increase due to the thermocouple.

1.2 Temperature Profile during Incubator Hyperthermia

As shown in Figure 4, the temperature increase rate in the incubator hyperthermia is much slower than the temperature increase rate observed during ICG/laser exposure. The reason could be that, in incubator hyperthermia, heat has to be first absorbed by the tissue culture flask and then diffuse into the wells. The plastic well plate apparently acts as a huge heat sink. It absorbed heat energy and transferred the energy gradually to the media; whereas in laser ICG hyperthermia, heat was produced directly from the ICG solution.

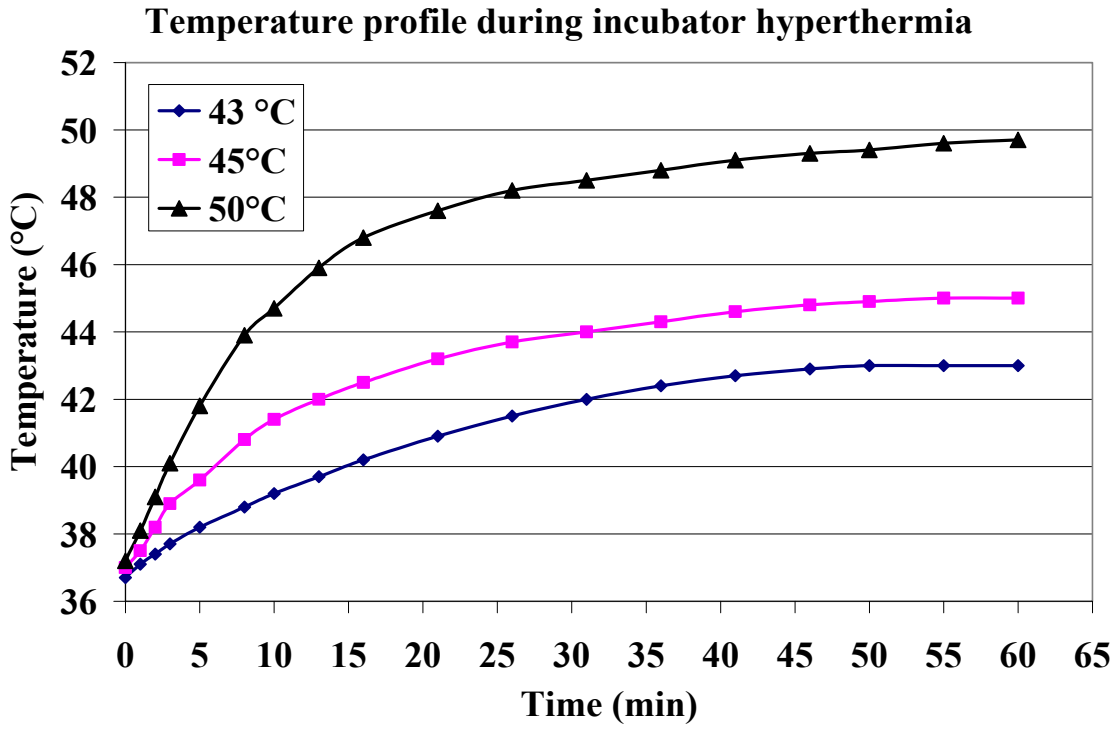

Figure 4 Heat generation as a function of ICG concentration (n=1).

1.3 Thermal Dose Calculation

Table 4 lists calculated CEM_{43} for several different hyperthermia treatments. In this study, the effect of "5 μM ICG + 3 min laser" was compared to "43°C incubator 1h", while "10 μM ICG + 3 min laser" was compared to "50°C incubator 30 min" because the two

treatment pairs have similar temperature and total thermal dose. Thus, any difference produced by these two pairs will be because of the rate of heating.

Treatment type	CEM_{43} (min)
5 μM ICG + 3 min laser	6.2
10 μM ICG + 3 min laser	331.0
43°C incubator 1h	23.5
45°C incubator 1h	116.4
50°C incubator 1h	2706.7
50°C incubator 30 min	371.4

Table 4 Calculated CEM_{43} in different types of hyperthermia treatment, based on the temperature curves in Figure 3&4 and Equation 2.

2. HSP Level

HSP70 expression after different types of hyperthermia is shown in Figure 5. ELISA was repeated three times for each data point shown in the figure; each assay contains two repetitions. According to the assay protocol, the measured absorbance value at 450 nm (OD 450) represents the amount of HSP70. Since the cell growth was inhibited after hyperthermia treatment, which may affect the total cellular HSP, the obtained HSP70 absorption values were corrected using the SRB toxicity absorption value to account for changes in cellular protein for a particular treatment. Briefly, after obtaining cell SRB value, the HSP70 values from each treatment group were normalized to the ratio of the SRB value from that treatment to the SRB value from the control, that is, from cells that did not receive any treatment. We observed that the baseline HSP70 level in the MDR positive MES-SA/Dx5 cells is about two times higher than in the non-MDR MES-SA cells when both cells were cultured in normal temperature (37 ºC). Since the two cells

were seeded at the same density and given that they have similar doubling time, this increased baseline HSP70 expression in the MES-SA/Dx5 cell suggests a correlation between MDR and heat resistant.

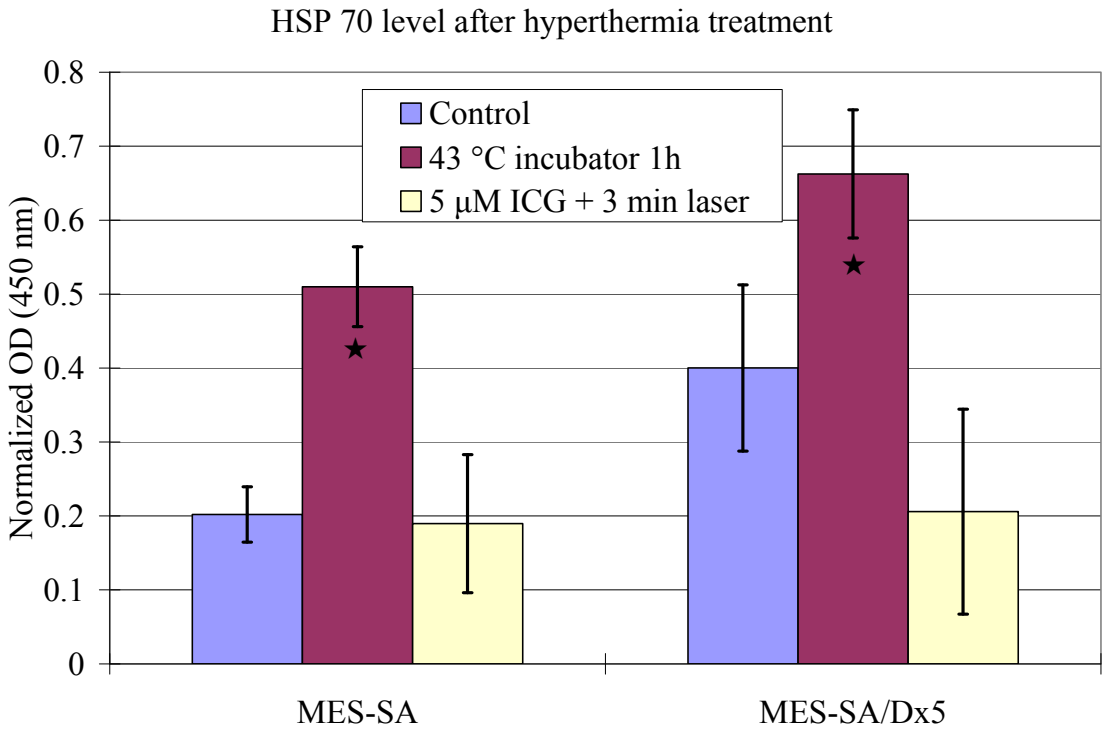

Figure 5 HSP70 expression after different types of hyperthermia treatment (n=3). Data were normalized as described above. "★" Significantly higher cellular HSP70 level among the three groups by ANOVA test with bonferroni post-hoc correction.

When comparing different hyperthermia treatments, increased HSP70 expression was observed in 1 hour 43 ºC incubator hyperthermia treatment. The treatment promoted HSP70 expression in both MDR and non-MDR MES-SA cells. After the treatment, the HSP70 level in MES-SA/Dx5 cell was still higher than in MES-SA cell; however the percentage increase is higher in MES-SA cell than in MES-SA/Dx5 cell. About a 70%

increase was observed in MES-SA/Dx5 cell, whereas the HSP70 level in MES-SA cell was more than doubled.

3. Cytotoxicity of Incubator Hyperthermia and NIR Laser-ICG Hyperthermia

3.1 Cytotoxicity of NIR Laser-ICG Hyperthermia

ICG is considered safe and has been approved by the FDA for some clinical uses for over 50 years. Our data suggested ICG did not affect cell growth at a wide range of concentrations as shown in Figure 6. ICG was slightly toxic only at high concentrations. As shown in the figure, "*" indicates statistical significance. Statistical analysis was performed by comparing each treatment value with the control value, which did not receive any treatment. Cell growth was inhibited at 100 μM ICG concentration in both MES-SA and MES-SA/Dx5 even without exposure to NIR irradiation. Although MES-SA cell growth was inhibited at 50 μM ICG concentration, considering that the inhibition is only 15% we can conclude that 5 μM or 10 μM ICG itself should be safe to the cells.

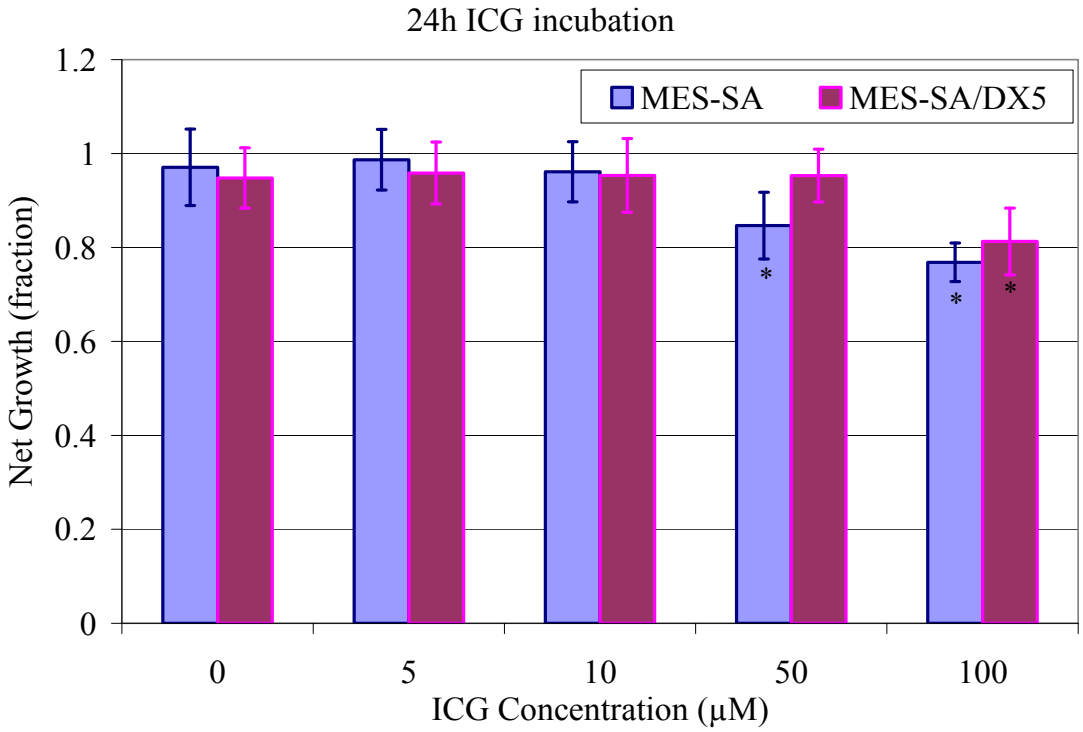

Figure 6 ICG cytotoxicity in MES-SA and MES-SA/Dx5 cells without laser exposure (n=4). * P < 0.05 (by paired t-test) between samples and control (cells without any treatment), indicating significant difference due to high concentration of ICG.

Figure 7 shows the cytotoxicity of NIR laser-ICG hyperthermia alone without DOX. "0" ICG concentration means 30 μL of DPBS without ICG was added to the wells. No differences could be detected when ICG was not present in the wells, indicating that the laser radiation itself did not affect cell growth. Cell proliferation was significantly lower when ICG was present. In contrast, ICG alone at 5μM was not toxic. The data clearly indicates the cytotoxicty effect of ICG when excited with NIR radiation. Note that no difference could be detected between treated MES-SA and MES-SA/Dx5 cells suggesting that these two cell lines have similar sensitivity toward 3 minute laser-ICG hyperthermia treatment aside from the fact that MES-SA/Dx5 is a MDR cell line while MES-SA is not.

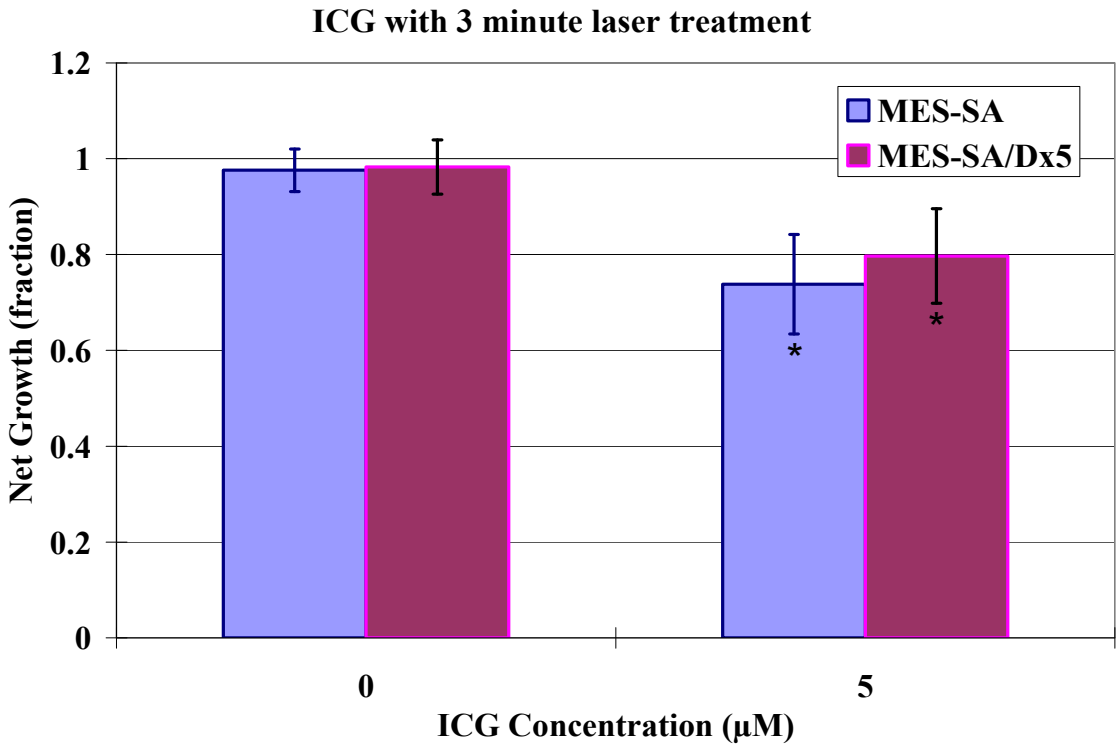

Figure 7 Cytotoxicity of NIR laser-ICG hyperthermia (n=4). "*" symbol indicates statistical significance. Statistical analysis was performed by comparing each treatment to control (0 ICG concentration), with paired t-test (α = 0.05).

3.2 Cytotoxicity of Incubator Hyperthermia

The cytotoxicity of 1 hour 43 °C incubator hyperthermia is shown in Figure 8. In order to be able to compare with DOX treatment, in which DOX was dissolved in 30 μL of DPBS, 30 μL of DPBS was added to the cells prior to treatment as the "0" concentration. Compared to control cells, the addition of 30 μL of DPBS did not affect cell growth at normal temperature (37 °C). The 1 hour 43 °C incubator hyperthermia treatment caused about 25% cell growth inhibition in MES-SA cell and 15% in MES-SA/Dx5 cells. However, no statistical significance could be detected between the two cells.

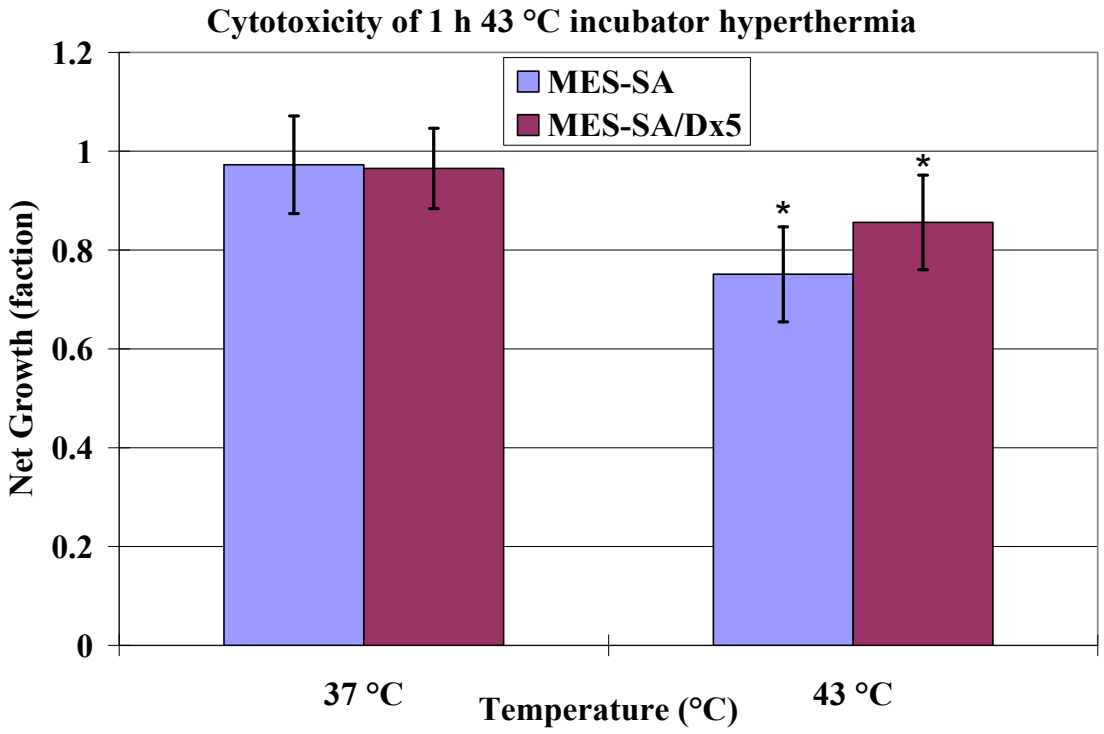

Figure 8 Cytotoxicity of 1hour 43 °C hyperthermia (n=4). "*" symbol indicates statistical significance. Statistical analysis was performed by comparing each treatment to control (37 °C), with paired t-test (α = 0.05).

4. Cytotoxicity of the Combinational Treatment

In order to determine whether there is a synergistic effect when combining DOX and hyperthermia, the predicted additive effect was calculated by subtracting the effect of each "hyperthermia alone" (no DOX) treatment from the "DOX only" (no hyperthermia) group. Specifically, for incubator hyperthermia, the predicted additive effect of combining incubator hyperthermia with DOX was calculated by subtracting the cytotoxcity of "incubator hyperthermia alone" from "DOX alone"; for laser-ICG hyperthermia, the predicted additive effect of combining laser-ICG hyperthermia with

DOX was calculated by subtracting the cytotoxcity of "laser-ICG hyperthermia alone" from "DOX + 5 μM ICG" group.

4.1 Cytotoxicity of DOX Chemotherapy with 1 hour 43 °C Incubator Hyperthermia

The effect of combining DOX chemotherapy and 1 hour 43 °C incubator hyperthermia on MES-SA and MES-SA/Dx5 cells is shown in Figures 9-10 respectively.

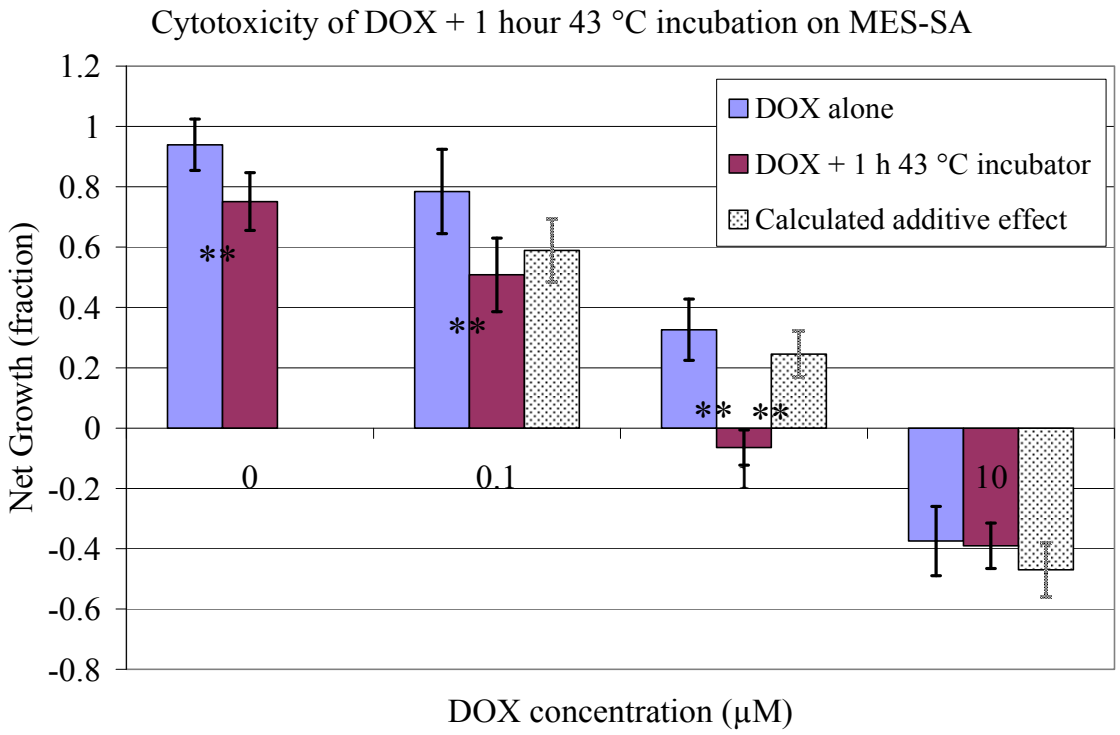

Figure 9 Cytotoxicity of DOX alone and DOX in combination with incubator hyperthermia on MES-SA cells (n=4). "**": statistical significance between "DOX alone" group and "DOX + 1 h 43 °C incubator" group or between "DOX + 1 h 43 °C incubator" group and the calculated additive effect by parried t-test (α = 0.05).

As shown in Figure 9, the MES-SA cell proliferation in the DOX + incubator hyperthermia group and DOX alone group decreased with increasing DOX concentration. When comparing the two treatment groups, DOX in combination with incubator

hyperthermia is more toxic than DOX itself at all DOX concentrations except at 10 μM. The reason is probably due to the fact that MES-SA cells are DOX sensitive and 10 μM DOX itself is so toxic to the cells that the addition of hyperthermia did not magnify the cytotoxic effect. Synergistic effect was observed at 1 μM DOX concentration only.

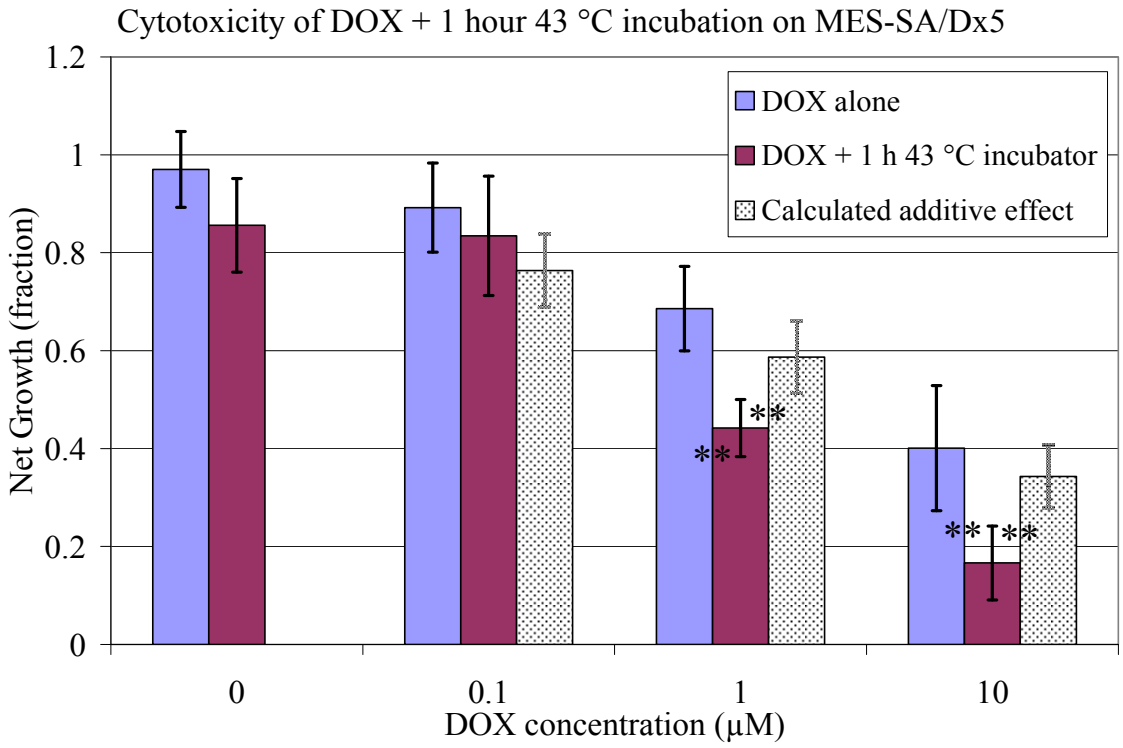

Figure 10 Cytotoxicity of DOX alone and DOX in combination with incubator hyperthermia on MES-SA/Dx5 cells (n=4). "**": statistical significance between "DOX alone" group and "DOX + 1 h 43 °C incubator" group or between "DOX + 1 h 43 °C incubator" group and the calculated additive effect by parried t-test (α = 0.05).

Figure 10 shows the cytotoxcity of DOX + incubator hyperthermia group and DOX alone group to MES-SA/Dx5 cells. Again, decreased cell number with increasing DOX concentration was observed. When comparing the two treatment groups, unlike in MES-SA cells, in MES-SA/Dx5 cells, DOX in combination with incubator hyperthermia is

more toxic than DOX itself at all DOX concentrations except at 0.1 μM. When comparing the actual cytotoxicity produced by the combinational treatment with the predicted additive effect value, we observed synergistic cell killing with increasing DOX concentration at both 1 μM and 10 μM, while at 0.1 μM DOX concentration, the interaction between incubator hyperthermia and DOX was additive.

4.2 Cytotoxcity of DOX Chemotherapy with Laser (3 minutes) - ICG (5 μM) Hyperthermia

Figures 11-12 show the cytotoxcity of DOX + laser-ICG hyperthermia compared to DOX alone. For both MES-SA and MES-SA/Dx5 cells, decreased cell number with increasing DOX concentration was observed. Greater cell growth inhibition was achieved by simultaneous administration of DOX and NIR laser hyperthermia. Cytotoxcity of the combined treatment modality is larger than DOX alone or hyperthermia alone. When comparing the actual cytotoxicity produced by the combinational treatment with the predicted additive effect value, synergistic cell killing/growth inhibition was observed at 1 μM DOX concentrations in DOX sensitive MES-SA cells and at all DOX concentrations in MDR MES-SA/Dx5 cells.

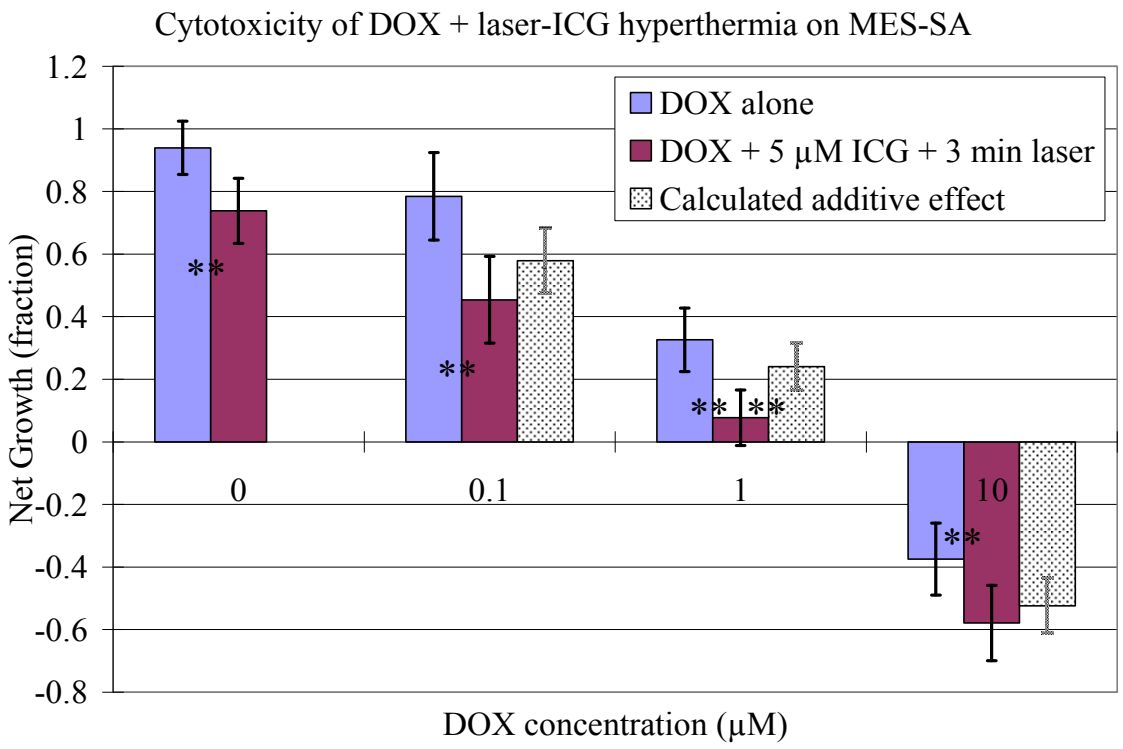

Figure 11 Cytotoxicity of DOX alone and DOX in combination with laser-ICG hyperthermia on MES-SA cells (n=4). "**": statistical significance between "DOX alone" group and "DOX + 5 µM ICG + 3 min laser" group or between "DOX + 5 µM ICG + 3 min laser" group and the calculated additive effect by parried t-test (α = 0.05).

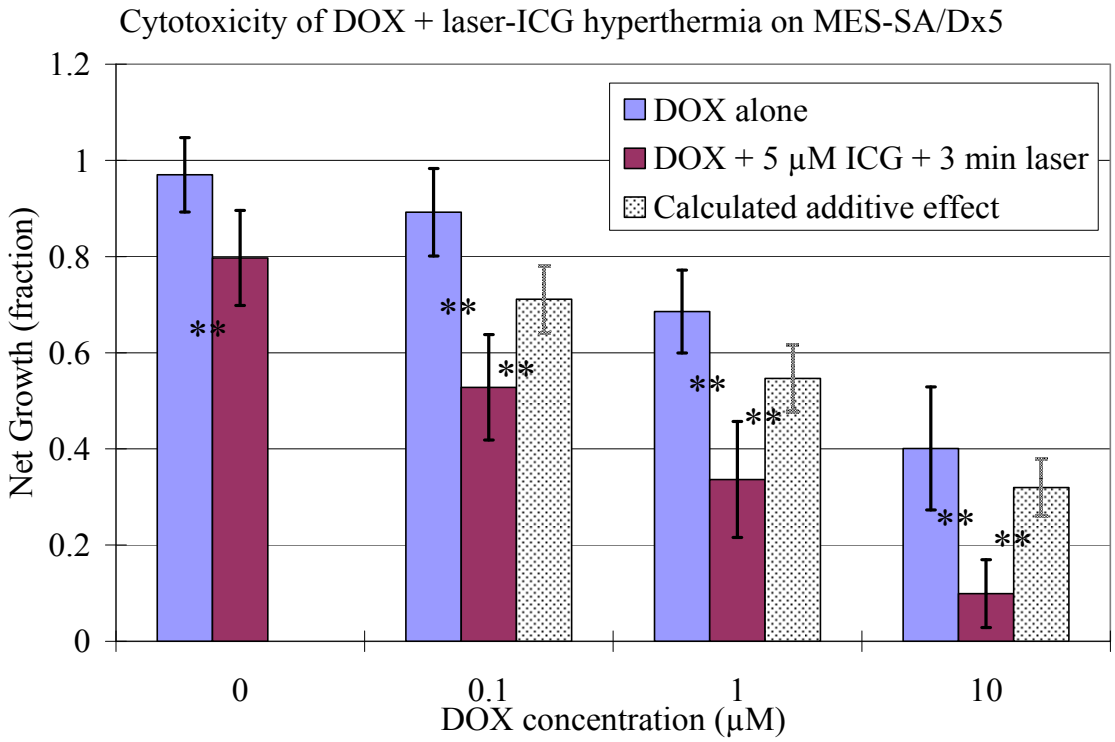

Figure 12 Cytotoxicity of DOX alone and DOX in combination with laser-ICG hyperthermia on MES-SA/Dx5 cells (n=4). "**": statistical significance between "DOX alone" group and "DOX + 5 µM ICG + 3 min laser" group or between "DOX + 5 µM ICG + 3 min laser" group and the calculated additive effect by parried t-test (α = 0.05).

Figures 13-14 summarize the cytotoxicity of different treatments on MES-SA and MES-SA/Dx5 cells respectively. An ANOVA test with bonferroni post-hoc correction suggested that there is no difference among DOX alone group, DOX with ICG but without laser group and DOX with laser but without ICG group in either cell line, which is expected because ICG alone should not change DOX activity and laser itself without ICG does not produce hyperthermia. When comparing the two hyperthermia treatments by paired *t*-test, laser-ICG hyperthermia achieved better chemotherapy-hyperthermia interaction at 10 µM DOX concentration in MES-SA cells. However, this difference fails

to reach statistical significance when ANOVA was applied to all the five treatment groups with bonferroni post-hoc correction. At other concentrations, no difference could be detected between cells treated by the two hyperthermia delivery methods.

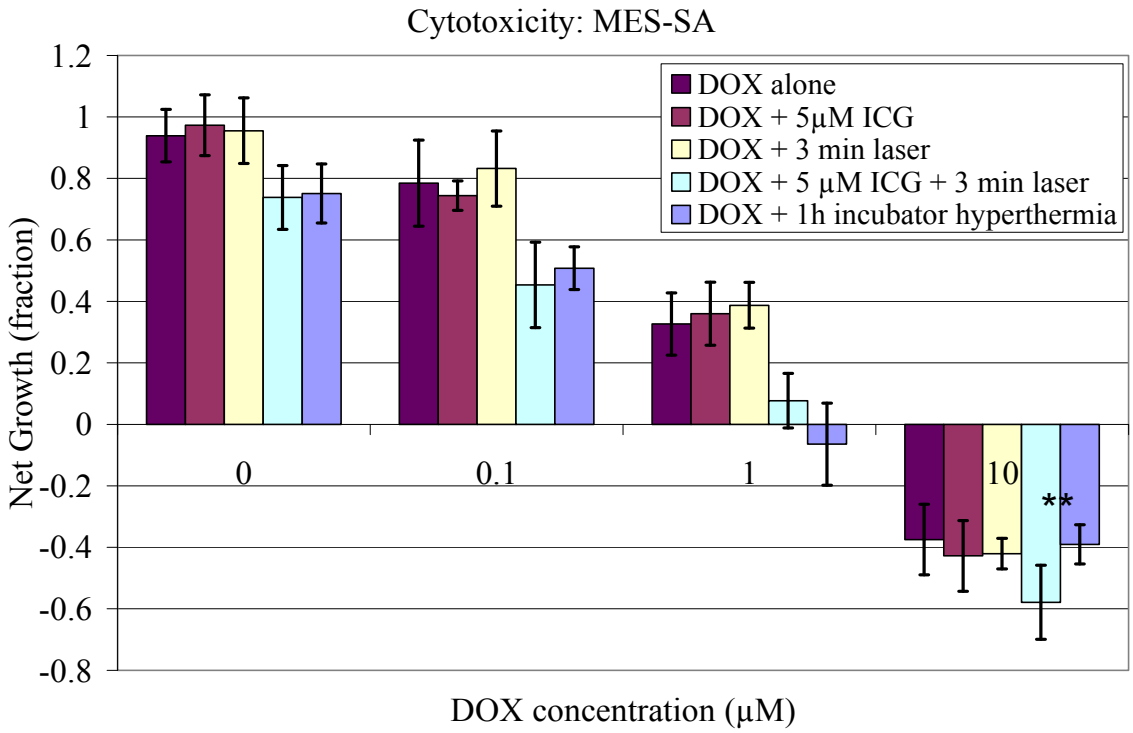

Figure 13 Cytotoxicity of different treatments on MES-SA cells (n=4). "**": statistical significance by comparing "DOX + 5 μM ICG + 3 min laser" group to "DOX + 1 h incubator hyperthermia" group by parried t-test (α = 0.05); this difference fails to reach statistical significance when ANOVA is applied to all the five treatment groups.

As to the MES-SA/Dx5 cell (Figure 14), laser-ICG hyperthermia achieved better chemotherapy-hyperthermia interaction than did incubator hyperthermia at 0.1 μM DOX concentration in MES-SA/Dx5 cells both by paired *t*-test and ANOVA. At all the other concentrations, laser-ICG hyperthermia showed no statistically significant difference compared to incubator hyperthermia.

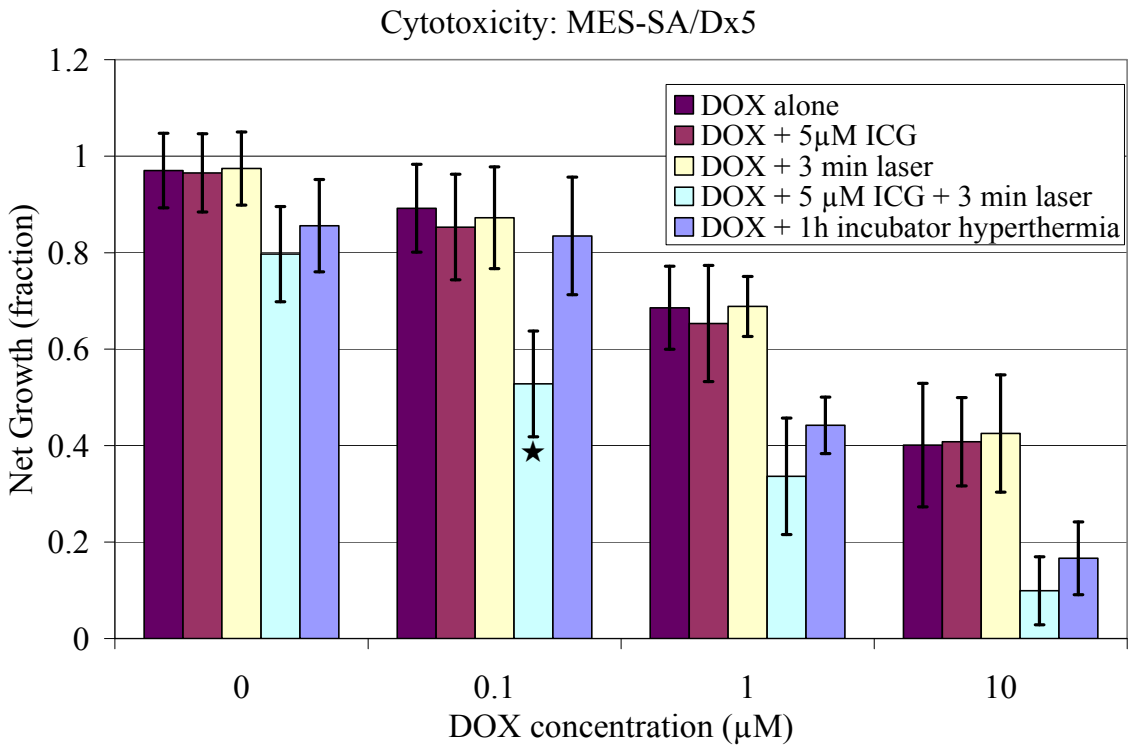

Figure 14 Cytotoxicity of different treatments on MES-SA/Dx5 cells (n=4). "★": statistical significance among the groups by ANOVA with bonferroni post-hoc correction (α = 0.05).

5. Cell Death Pathway: Apoptosis/Necrosis

5.1 DOX Induced Apoptosis

In this experiment, MES-SA and MES-SA/Dx5 cells were treated with 1 μM or 5 μM DOX for up to 24 hours. Caspase 3 levels were quantified at 1, 3, 6, 9, 12, 18 and 24 hours post DOX treatment. Results from the caspase 3 activity assay (Figure 15) suggested that there is apoptotic cell death occurring after DOX treatment in both MES-SA and MES-SA/Dx5 cells. In control MES-SA and MES-SA/Dx5 cells, no difference in caspase 3 expression was observed; therefore, each treatment value was presented as the percentage increase/decrease compared to control values. An ANOVA test at each time point among the treatment groups indicated that 5 μM DOX treated MES-SA cells had

higher caspase 3 than the other three treatments at 12, 18 and 24 hour time point. Meanwhile, 1 μM DOX treated MES-SA/Dx5 cells had consistently lower caspase 3 level at 12, 18 and 24 hour time point.

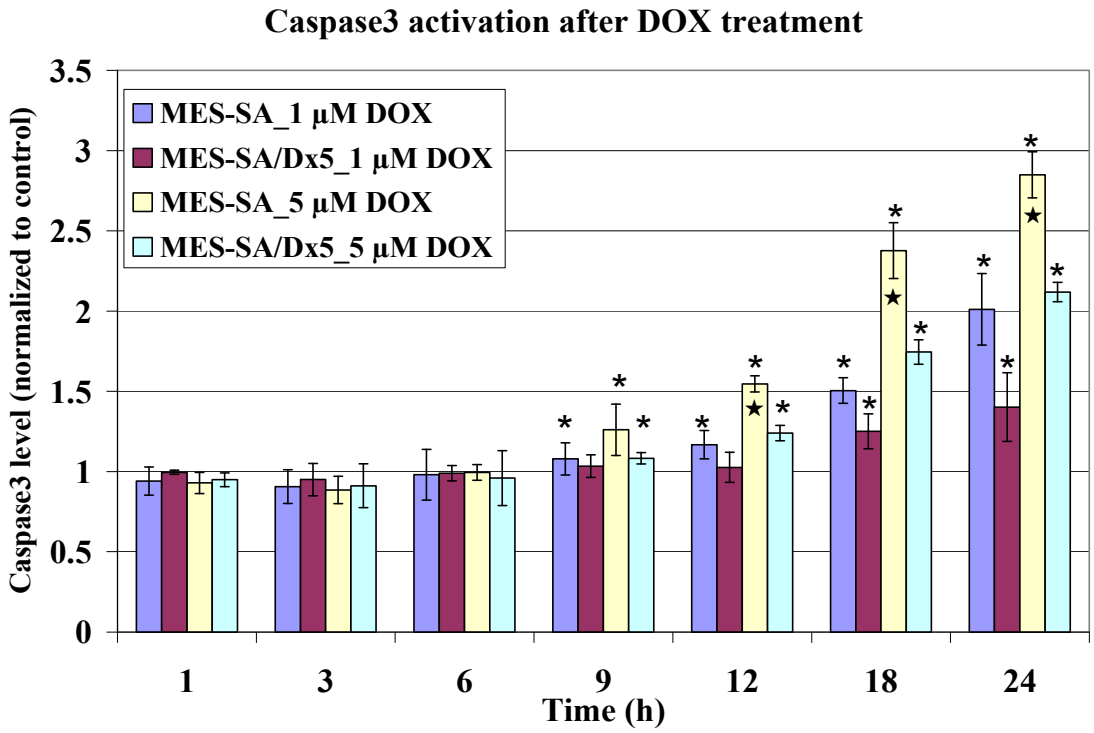

Figure 15 Caspas 3 level after DOX treatment. n =3 experiments. "*": statistical significance by comparing each treatment to control cells (cells without treatment), with one-sided Student's t-test (α = 0.05). "★": statistical significance among the groups by ANOVA with bonferroni post-hoc correction (α = 0.05).

The result indicated that the induction of apoptosis is dependent on DOX concentration; higher concentration of DOX caused more caspase 3 production. Note that due to MDR, 1 μM of DOX did not change caspase 3 expression in MES-SA/Dx5 cells, which is consistent with the cytotoxicity data. Results from the DOX uptake assay (shown below) indicated that the low caspase 3 activation and low cytotoxicity is due to MDR

decreasing DOX uptake in MES-SA/Dx5 cells Furthermore, the activation of caspase 3 depends on the DOX incubation time: longer incubation induced higher caspase 3 expression for up to 24 hours.

5.2 Slow Rate Incubator Hyperthermia

5.2.1 Hoechst/PI staining

In this set of experiments, incubator hyperthermia treated MES-SA and MES-SA/Dx5 cells were stained with Hoechst 33342 and propidium iodide either immediately after the hyperthermia treatment or 24 hours post treatment in order to distinguish normal, apoptotic and necrotic cells. Different modes of cell death were observed at the two thermal doses as shown in Figures 16 & 17, which show Hoechst/PI dual staining. For all of the MES-SA cell images, the exposure time of Hoechst was kept at 197 ms and the PI channel exposure time was 347 ms; for the MES-SA/Dx5 cell images, the exposure time for Hoechst and PI were 223 ms and 450 ms respectively.

Generally, mild apoptosis was observed 24 hours after the low thermal dose 1 hour 43 °C incubator hyperthermia; whereas the high thermal dose treatment, incubating cells for 30 minutes at 50 °C caused necrosis. As shown in Figure 16 (a) & (d), control MES-SA and MES-SA/Dx5 cells showed no PI staining indicating the integrity of cell membrane; Hoechst staining also indicted intact cell nucleus. After 1 hour 43 °C incubation, no obvious change could be observed as shown by (b) & (e), except maybe one or two dead cells. 24 hours after the treatment, cells with fragmented blue or pink nuclei could be seen in both MES-SA (Figure 16 (c)) and MES-SA/Dx5 cell images (Figure 16 (f)), indicating these cells were undergoing apoptosis. Note that although some cells were undergoing apoptosis, the majority of the cells still maintained an intact cell membrane as

evidenced by the fact that only Hoechst staining were presented in these cells. This observation, combined with the cytotoxicity data presented in Figure 8, suggests that 1 hour 43 °C incubator hyperthermia inhibited cell growth by inducing very mild apoptosis. Compared to 1 hour 43 °C incubation, 30 minutes 50 °C incubation caused more severe damage to the cells. Necrotic cell death could be seen immediately after the treatment (Figure 17 (a) & (c)). Although a lot of the cells were not stained by PI indicating they still possess an intact cell membrane at that moment, they were severely damaged by the heat stress and eventually died through necrosis as evident by the images taken 24 hours after treatment (Figure 17 (b) & (d)).

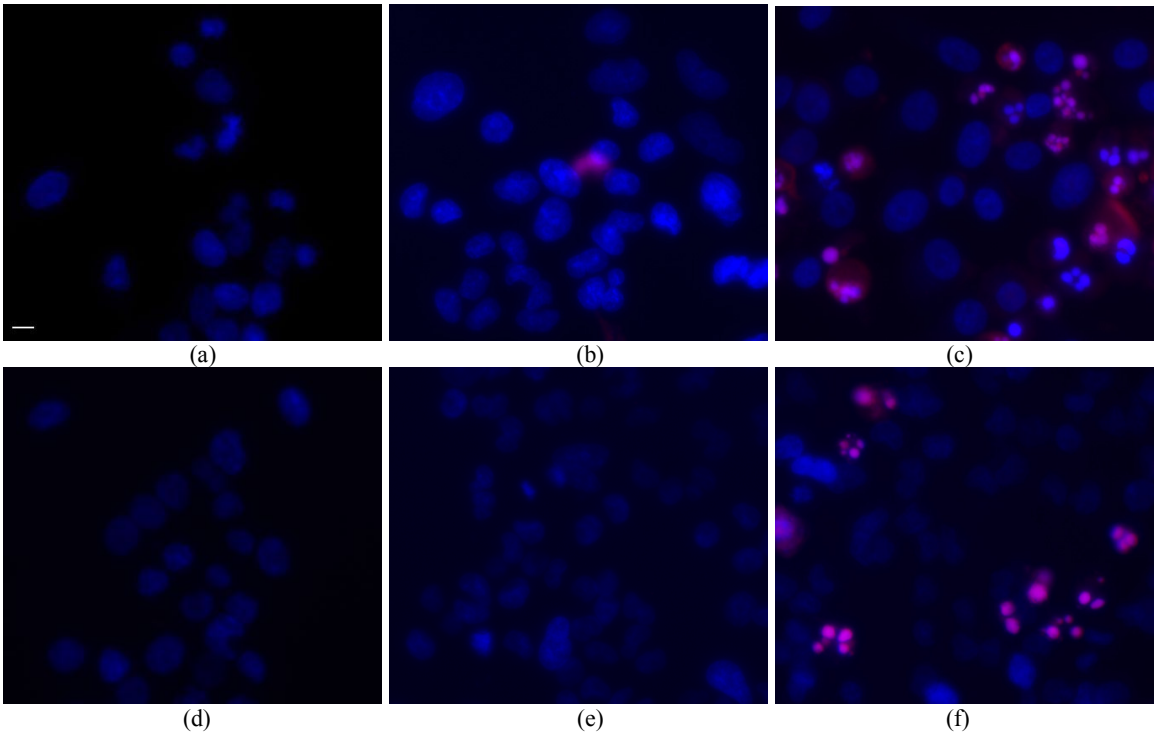

Figure 16 Hoechst/PI staining of MES-SA (upper panel) and MES-SA/Dx5 cells (lower panel) treated by 1 hour 43 °C incubation. Images were taken either immediately (b&e), or 24 hours after the treatment (c&f) and compared to the control cells (a&d). The scale bar in (a) represents 8 μm.

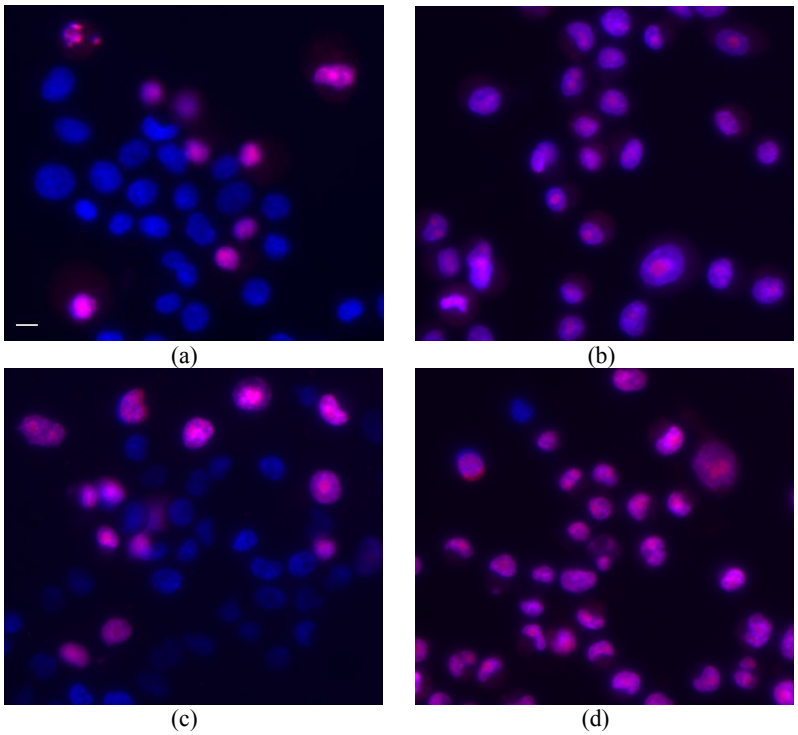

Figure 17 Hoechst/PI staining of MES-SA (upper panel) and MES-SA/Dx5 cells (lower panel) treated by 30 min 50 °C incubation. Images were taken either immediately (a&c), or 24 hours after the treatment (b&d) and compared to the control cells (Figure 16 a&d). The scale bar in (a) represents 8 µm.

5.2.2 Quantification of caspase 3

Since Hoechst/PI staining suggested mild apoptosis only in 1 hour 43 °C incubator hyperthermia treated cells and necrosis in 50 °C hyperthermia treated cells, quantitative caspase 3 assay was performed to 1 hour 43 °C incubator hyperthermia treated cells but not to 30 minutes 50 °C incubator hyperthermia treated cells. Figure 16 shows the caspase 3 expression in MES-SA and MES-SA/Dx5 cells treated with 1 hour 43 °C incubator hyperthermia. Caspase 3 levels for each cell were quantified 1, 3, 6, 12 and 24 hours after the hyperthermia treatment and then normalized to their respective control which is the caspase 3 value from cells that did not receive any treatment. Since cell

growth was known to be inhibited 24 hours after 1 hour 43 °C incubator hyperthermia, the caspase 3 fluorescence values at the 24 hour time point were normalized to the SRB value to account for changes in cell number. Briefly, caspase 3 data after the treatment were normalized to the ratio of the SRB toxicity values of the treated cells to the SRB toxicity value of the control, which did not receive treatment. Statistical significant difference could be detected at 6 hours post treatment in MES-SA/Dx5 cells and 24 hours post treatment in MES-SA cells, but the percentage increase in caspase 3 level is only about 25% - 30%, indicating the extent of apoptosis is mild, which confirmed the observation in the Hoechst/PI staining assay.

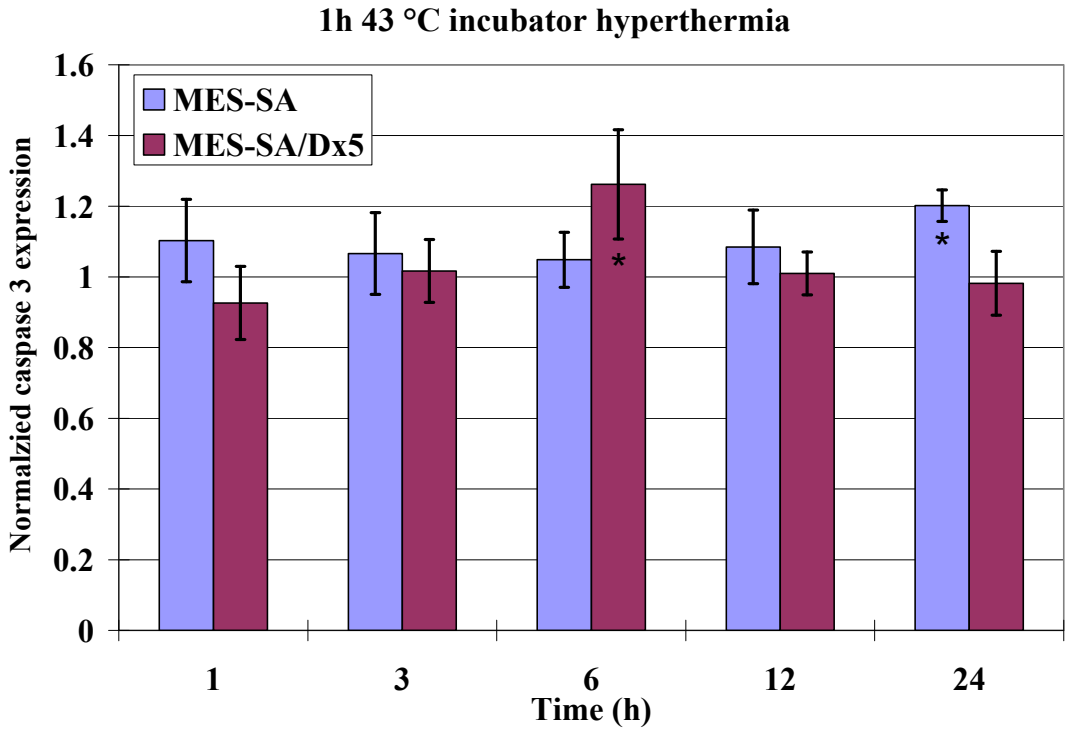

Figure 18 Caspas 3 level after 1 hour 43 °C incubation, data were normalized as described above. n =3 experiments. "*": statistical significance by comparing each treatment to control cells (cells without treatment), with one-sided Student's t-test (α = 0.05).

5. 3 Rapid Rate Laser-ICG Hyperthermia

5.3.1 Hoechst/PI staining

In both MES-SA and MES-SA/Dx5 cells, laser-ICG hyperthermia induced necrosis at both 5 μM and 10 μM ICG concentration as shown in Figures 19 & 20. Cells were treated with 5 μM or 10 μM of ICG and excited with NIR laser for 3 minutes, which produced 43 °C and 50 °C hyperthermia respectively. The images were taken either 1 or 24 hours after the NIR irradiation. This 1 hour time point was chosen because the laser irradiation was only 3 minutes, therefore images were taken 1 hour after the treatment in order to be able to compare with the 1 hour incubator hyperthermia treatment. In control cells, which did not receive any treatment, only Hoechst staining can be seen as PI cannot penetrate an intact cell membrane. With the increase of thermal dose (more ICG) the fluorescence of PI increased indicating more severe cell membrane damage. For all the MES-SA cell images the exposure time of Hoechst was kept at 143 ms and the PI channel exposure time was 332 ms; for the MES-SA/Dx5 cell images, the exposure time for Hoechst and PI were 197 ms and 450 ms respectively;

In the previous section, mild apoptosis in both MES-SA and MES-SA/Dx5 cells 24 hours after the slow rate 1 hour 43 °C incubator hyperthermia are shown. Here it is shown that, when the heating is rapid, the same thermal dose (5 μM ICG + 3 minute laser) caused cell necrosis instead of apoptosis in 24 hours, as evident by Figure 19 (c) & (f). Similar to the 1 hour 43 °C incubation treatment, there is no significant morphological change immediately after 5 μM laser-ICG hyperthermia.

When comparing the mode of cell death at the higher thermal dose, the similarity is that both slow rate (incubator) and rapid rate (3 minute laser + 10 μM ICG) hyperthermia lead

to necrosis in almost all the cells 24 hours after hyperthermia treatment (Figure 20 (b) & (d)). However, the effect of the rapid rate laser-ICG hyperthermia is also more rapid because it caused complete cell necrosis immediately after the treatment (Figure 20 (a) & (c)) whereas there are still some cells possessing intact cell membrane immediately after the 30 minutes 50 °C incubation as shown in Figure 17 (a) & (c).

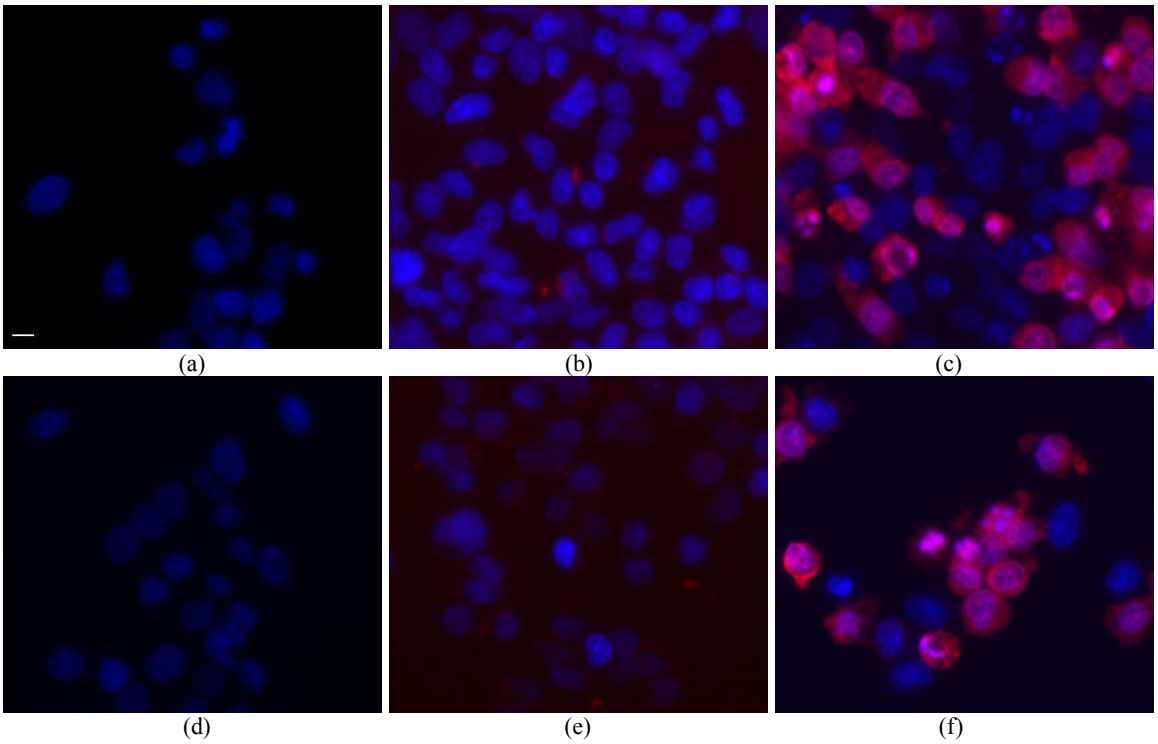

Figure 19 Hoechst/PI staining of MES-SA (upper panel) and MES-SA/Dx5 cells (lower panel) treated by laser excited (3 min) ICG (5 μM). Images were taken either immediately (b&e), or 24 hours after the treatment (c&f) and compared to the control cells (a&d). The scale bar in (a) represents 8 μm.

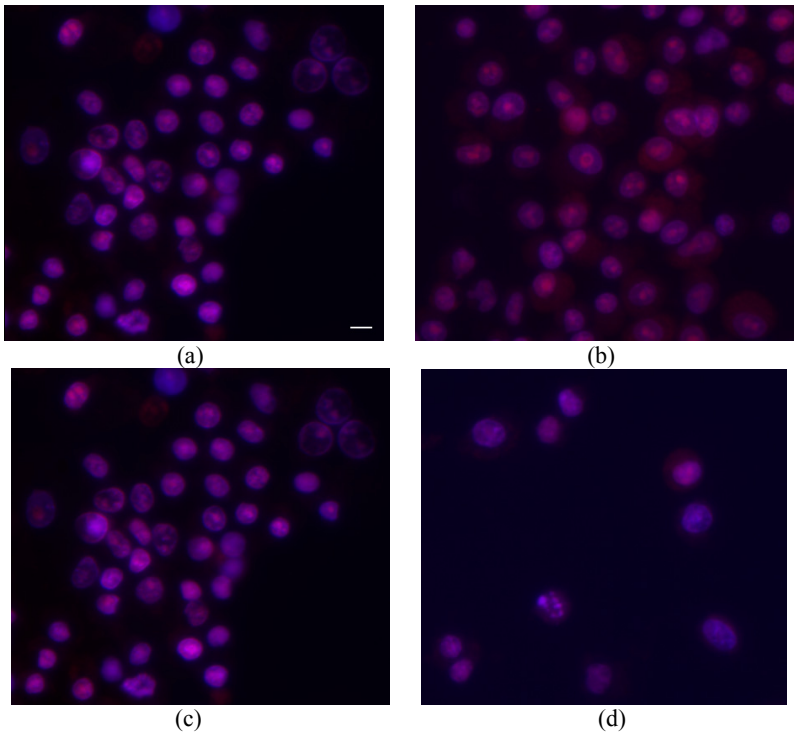

Figure 20 Hoechst/PI staining of MES-SA (upper panel) and MES-SA/Dx5 cells (lower panel) treated by laser excited (3 min) ICG (10 μM). Images were taken either immediately (a&c), or 24 hours after the treatment (b&d) and compared to the control cells (Figure 22 a&d). The scale bar in (a) represents 8 μm.

5.3.2 Quantification of caspase 3

Figure 21 shows the caspase 3 expression in MES-SA and MES-SA/Dx5 cells treated with laser-ICG hyperthermia. Cells were incubated with 5 μM of ICG and excited with NIR laser for 3 minutes to produce a 43 °C hyperthermia. Caspase 3 levels were quantified 1, 3, 6, 12 and 24 hours after the hyperthermia treatment and then normalized to their respective control, the values from cells that did not receive any treatment. Since cell growth was known to be inhibited 24 hours after the hyperthermia treatment, the caspase 3 fluorescence values at the 24 hour time point were normalized to the SRB toxicity values to account for changes in cell number. Briefly, the caspase 3 values after

the treatment were normalized to the ratio of the SRB toxicity values of treated cells to the control, which are the SRB toxicity values from cells that did not receive treatment. No significant apoptosis could be detected in both MES-SA and MES-SA/Dx5 cells after up to 24 hours post treatment.

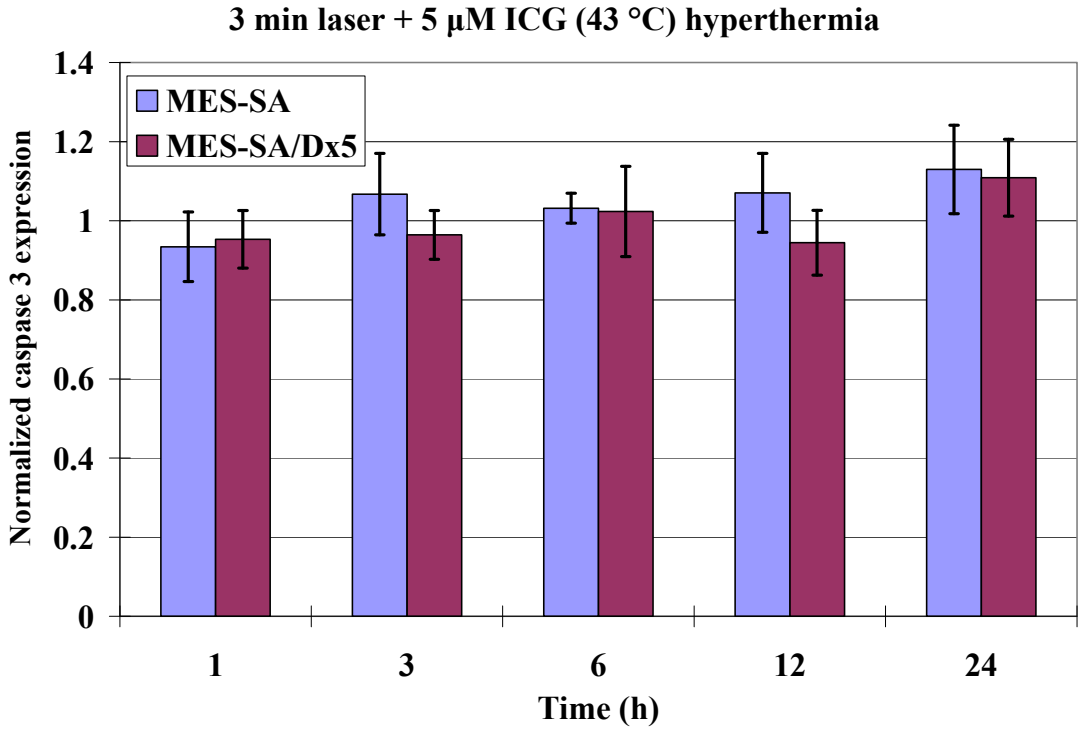

Figure 21 Caspas 3 level in MES-SA and MES-SA/Dx5 cells treated with 5 µM ICG and irradiated by laser for 3 minutes. Data were normalized as described above. The final temperature was 43 °C. n =3 experiments.

6. DOX Uptake

Figures 22-23 show the DOX fluorescence intensity and subcellular localization in incubator hyperthermia treated MES-SA and MES-SA/Dx5 cells respectively. Images were taken either immediately after the hyperthermia treatment or 24 hours post treatment. The exposure time for the DOX signal was kept at 1000 ms for all the images.

Generally, the DOX fluorescence intensity increased with increasing incubation time in both cell lines, as the images taken 24 hours after the treatment were brighter than the ones taken immediately after the treatment.

For MES-SA cell, the fluorescence intensity and subcellular localization of DOX did not change significantly after the incubator hyperthermia treatment, which is reasonable because MES-SA is DOX sensitive and DOX can diffuse freely into the cell, therefore, the facilitating effect of hyperthermia to DOX is not obvious.

Compared to MES-SA, DOX showed a different subcellular localization pattern in MES-SA/Dx5 cells. As shown in Figure 23 (b), the cell membrane was stained by the DOX fluorescence while the nucleus compartment was dark. This is because the P-gp pump was anchored in the cell membrane of MES-SA/Dx5 cells and any DOX molecule attempting to diffuse through it was captured and pumped out. Meanwhile, facilitated DOX uptake by incubator hyperthermia was obvious in MES-SA/Dx5 cells. DOX fluorescence intensity increased with the increase of thermal dose both immediately after the treatment (DOX fluorescence intensity: (e) > (c) > (a)), and 24 hours after the treatment (DOX fluorescence intensity: (f) > (d) > (b)).

Although more DOX accumulated in the MES-SA/Dx5 cell after 1 hour 43 °C incubation (Figure 23 (c) & (d)), the subcellular localization of DOX did not change compared to the DOX only treatment (Figure 23 (b)), indicating the P-gp pump activity was not compromised. The increased DOX fluorescence intensity could be due to increased cell membrane permeability or increased DOX diffusion rate under hyperthermia condition.

Different DOX subcellular localization was observed in 30 minutes 50 °C incubator hyperthermia treated cells. As shown by Figure 23 (e) & (f), most cells showed nucleus

staining. From the Hoechst/PI staining presented in Figure 17 (c), after 30 minutes 50 °C incubator hyperthermia, a large portion of the cells maintained membrane integrity as they showed only Hoechst fluorescence, thus, the cell nucleus staining shown in Figure 23 (f) suggests that P-gp pump activity was compromised immediately after the treatment.

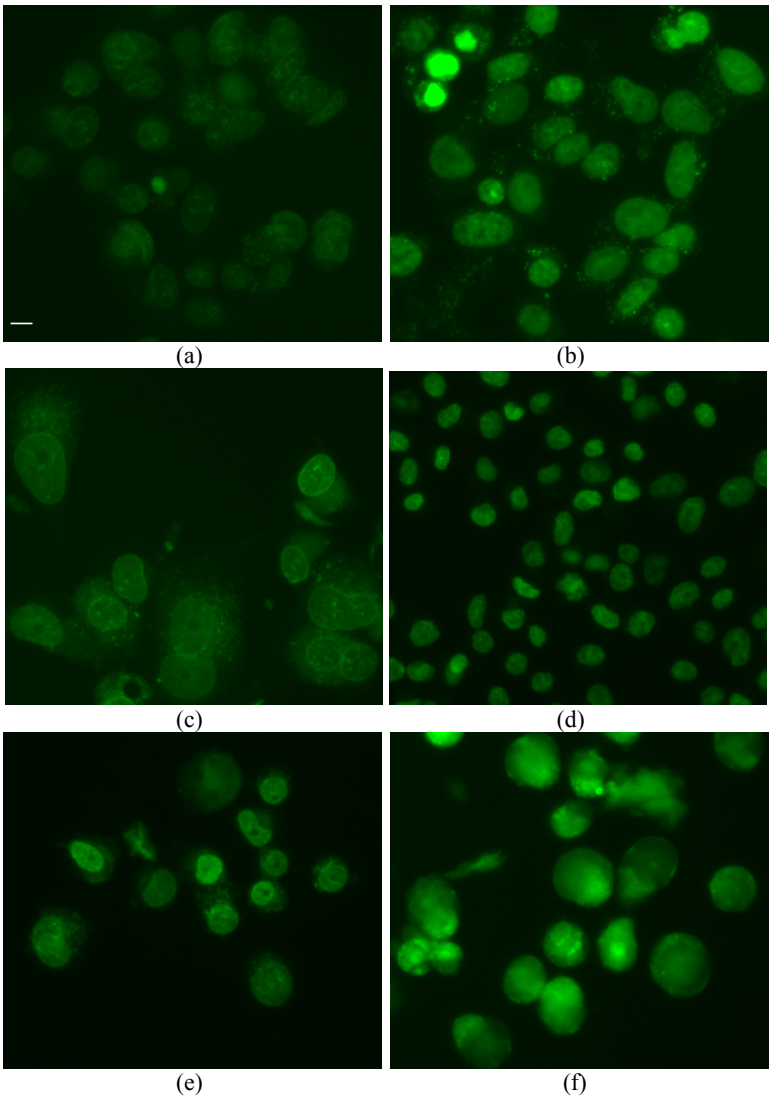

Figure 22 DOX fluorescence in MES-SA cell treated by only DOX (a&b), DOX + 1 hour 43 °C incubation (c&d), and DOX + 30 minutes 50 °C incubation (e&f). Images were taken either immediately (a, c & e), or 24 hours after the treatment (b, d & f). The scale bar in (a) represents 8 μm.

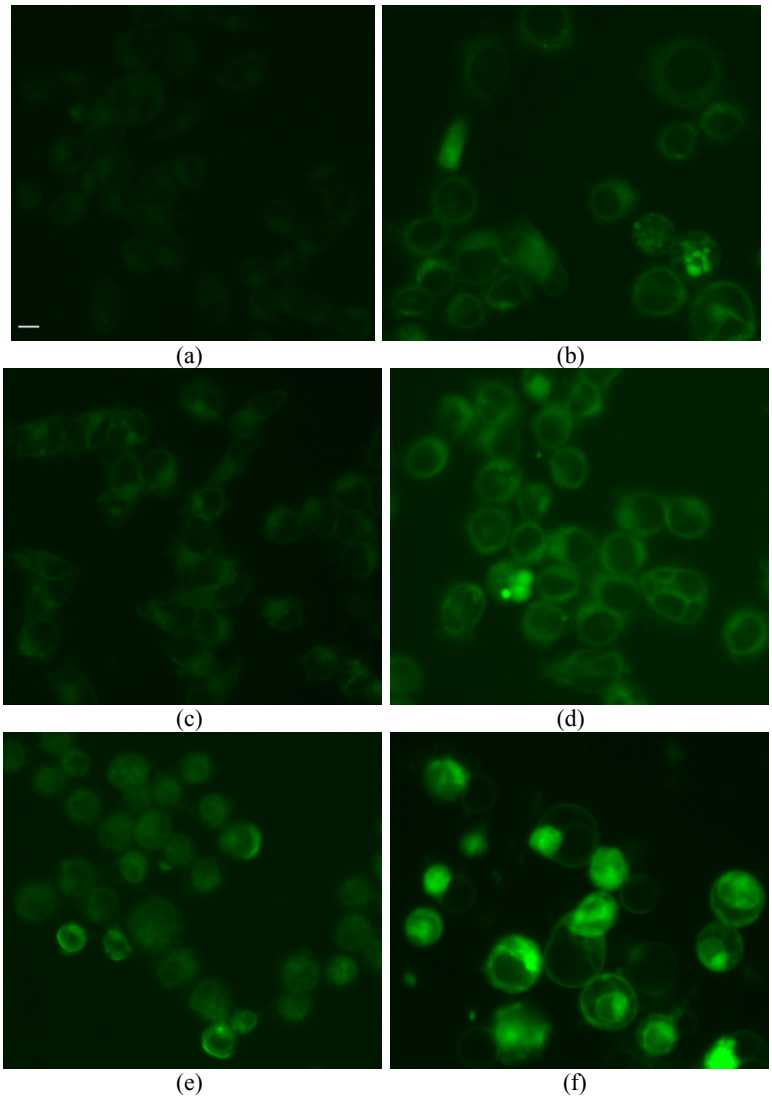

Figure 23 DOX fluorescence in MES-SA/Dx5 cell treated by only DOX (a&b), DOX + 1 hour 43 °C incubation (c&d), and DOX + 30 minutes 50 °C incubation (c&d). Images were taken either immediately (a, c & e), or 24 hours after the treatment (b, d & f). The scale bar in (a) represents 8 μm.

Figures 24-25 show the DOX fluorescence intensity and subcellular localization in laser-ICG hyperthermia treated MES-SA and MES-SA/Dx5 cells respectively. Images were taken either 1 hour after the hyperthermia treatment (in order to compare with incubator

hyperthermia) or 24 hours post treatment. The exposure time for the DOX signal was kept at 1000 ms for all the images.

Generally, the DOX fluorescence intensity increased with increasing incubation time in both cell lines, as the images taken 24 hours later were brighter than the ones taken immediately after the treatment.

For MES-SA cell, the subcellular localization of DOX did not change because they are DOX sensitive and DOX mainly binds to the DNA, thus the cell nucleus brightness was enhanced. Previously, we have shown that incubator hyperthermia treatment did not increase DOX uptake significantly in MES-SA cell. Here increased DOX fluorescence intensity indicating increased DOX retention after the laser-ICG hyperthermia was observed, probably because laser-ICG hyperthermia caused more severe cell membrane damage than the incubator hyperthermia as evident by the Hoechst/PI staining.

Similar to the incubator hyperthermia treated MES-SA/Dx5 cell, facilitated DOX uptake was obvious also by the laser excited ICG (5 μM) hyperthermia. DOX fluorescence intensity increased with the increase of thermal dose both immediately after the treatment (DOX fluorescence intensity: (e) > (c) > (a)), and 24 hours after the treatment (DOX fluorescence intensity: (f) > (d) > (b)).

We have shown that 1 hour 43 °C hyperthermia did not change P-gp pump activity in MES-SA/Dx5 cells. However, at the same thermal dose, the rapid rate laser-ICG hyperthermia caused DOX accumulation in the cell nucleus. As shown in Figure 25 (d), only a few cells showed dark cell nucleus probably due to severe cell membrane damage as evident by the Hoechst/PI assay shown in Figure 20 (c). At higher thermal dose (10

μM ICG), DOX fluorescence was present in almost all the cells, which is similar to the incubator hyperthermia at the same dose.

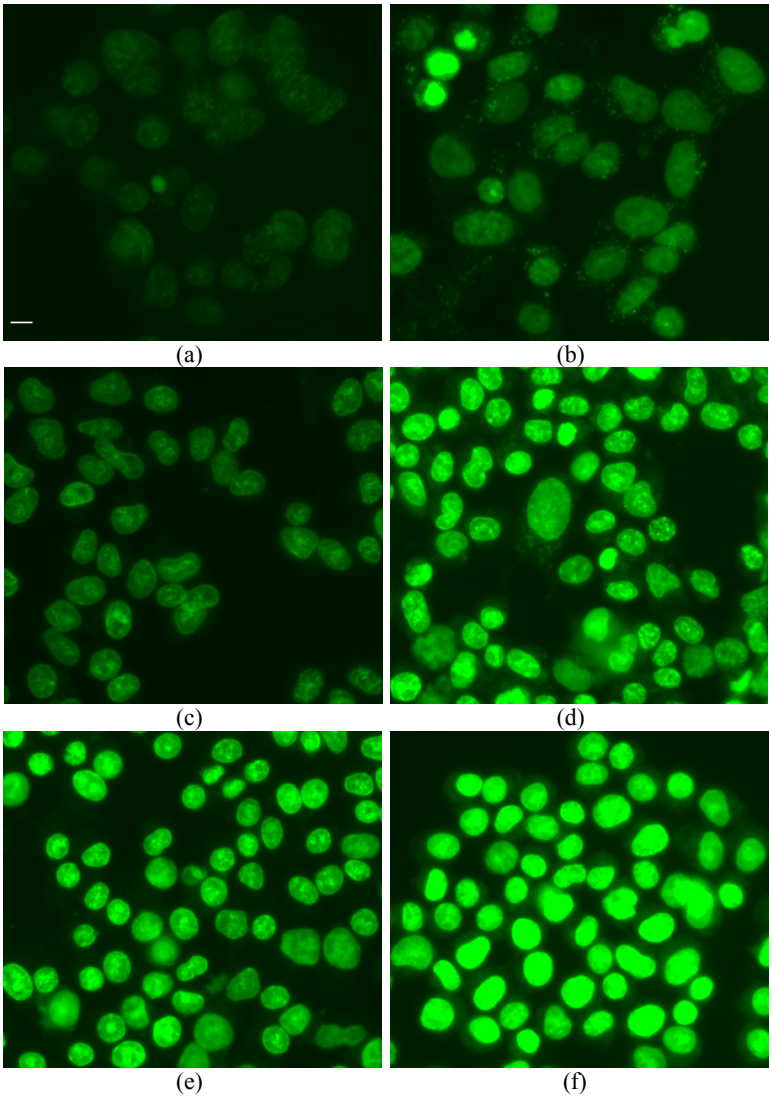

Figure 24 DOX fluorescence in MES-SA cell treated by only DOX (a&b), DOX + 3 min laser/5 μM ICG (c&d), and DOX + 3 min laser/5 μM ICG incubation (e&f). Images were taken either immediately (a, c & e), or 24 hours after the treatment (b, d & f). The scale bar in (a) represents 8 μm.

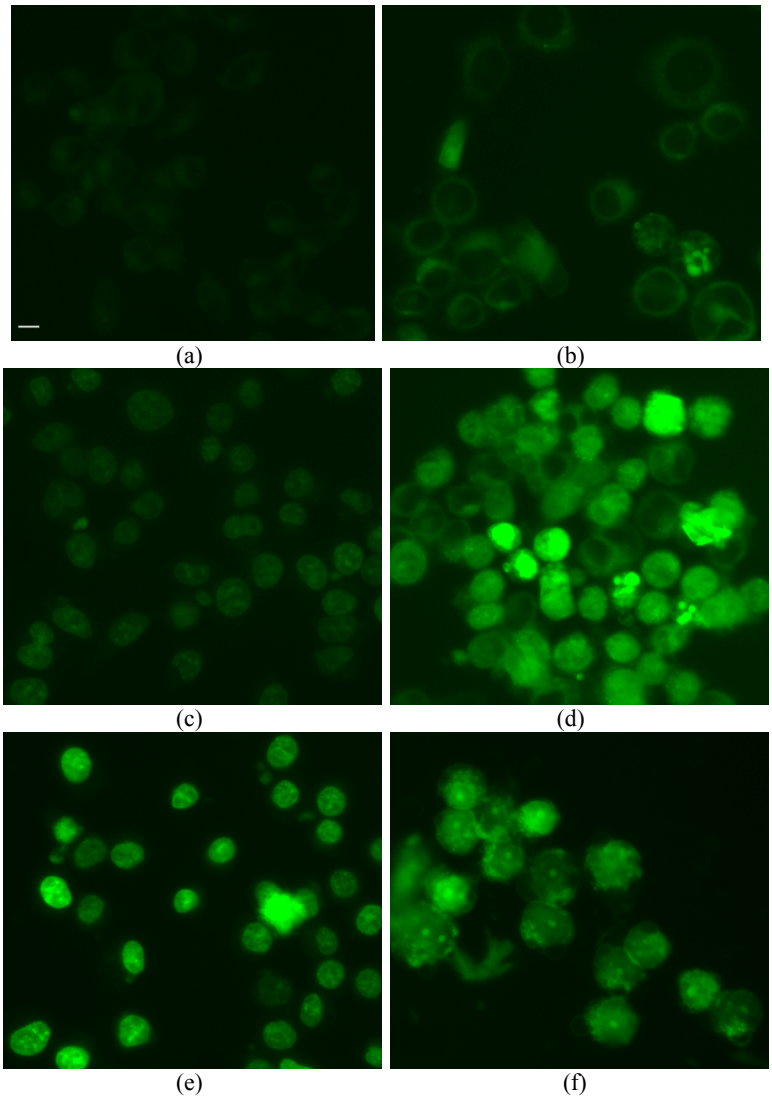

Figure 25 DOX fluorescence in MES-SA/Dx5 cells treated by only DOX (a&b), DOX + 3 min laser/5 μM ICG (c&d), and DOX + 3 min laser/5 μM ICG incubation (e&f). Images were taken either immediately (a, c & e), or 24 hours after the treatment (b, d & f). The scale bar in (a) represents 8 μm.

When comparing the rapid rate laser-ICG hyperthermia to the slow rate incubator hyperthermia, they both exhibited the ability to overcome P-gp at high thermal dose; however, at low thermal dose, the laser-ICG hyperthermia showed its superiority in helping DOX bypass P-gp mediated MDR as more DOX were presented in cell nucleus.

7. P-gp Activity

From the results of pervious experiments, we can see an increased DOX fluorescence indicating facilitated uptake during hyperthermia condition in both MES-SA and MES-SA/Dx5 cells. However, the reason for this increase in DOX uptake is not clear. We performed P-gp activity assay to find out whether this increase is due to the inhibition of p-gp drug efflux pump activity in the MES-SA/Dx5 cell. The calcein-AM assay was used to determine if the increased permeability can help drugs bypass the P-gp MDR system.

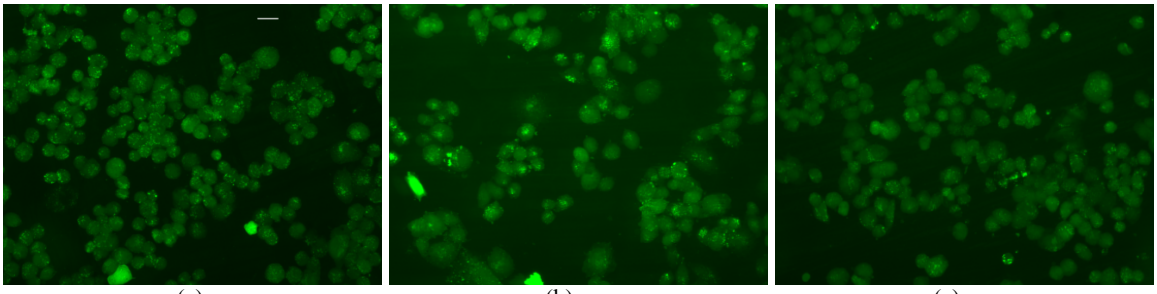

(a) (b) (c)

Figure 26 Calcein fluorescence after hyperthermia treatment. (a) MES-SA without any treatment; (b) MES-SA treated by 1 hour 43ºC incubator hyperthermia; (c) MES-SA treated with verapamil. Exposure time 1000 ms. The scale bar in (a) represents 24 µm.

MES-SA cells do not overexpress P-gp, thus, calcein-AM can diffuse freely into the cell and be cleaved to form bright green fluorescence. As shown in Figure 26 (c), the induction of P-gp inhibitor verapamil does not increase calcein fluorescence compared to the control. Meanwhile, 1hour 43 ºC incubator hyperthermia did not change P-gp activity as well, as evident by Figure 26 (b).

For the MES-SA/Dx5 cells, since it highly overexpresses P-gp, calcein-AM does not remain intracellular, as evident by the low fluorescence in Figure 27 (a). In Figure 27 (d), MES-SA/Dx5 cells were treated with the P-gp inhibitor verapamil; therefore, calcein-AM entered the cell and was cleaved to form fluorescent calcein. Figure 27 (b) showed that 1

hour 43 ºC incubator hyperthermia did not reduce P-gp activity as fluorescence signal was weak and similar to the control cell which did not receive any treatment. The laser exposure to 5 μM ICG for 3 minutes, on the other hand, caused a slight increase in calcein-AM fluorescence which is consistent with what was seen in the DOX uptake study. This assay indicated that the rapid rate laser-ICG hyperthermia can achieve better P-gp inhibition than the slow rate incubator hyperthermia.

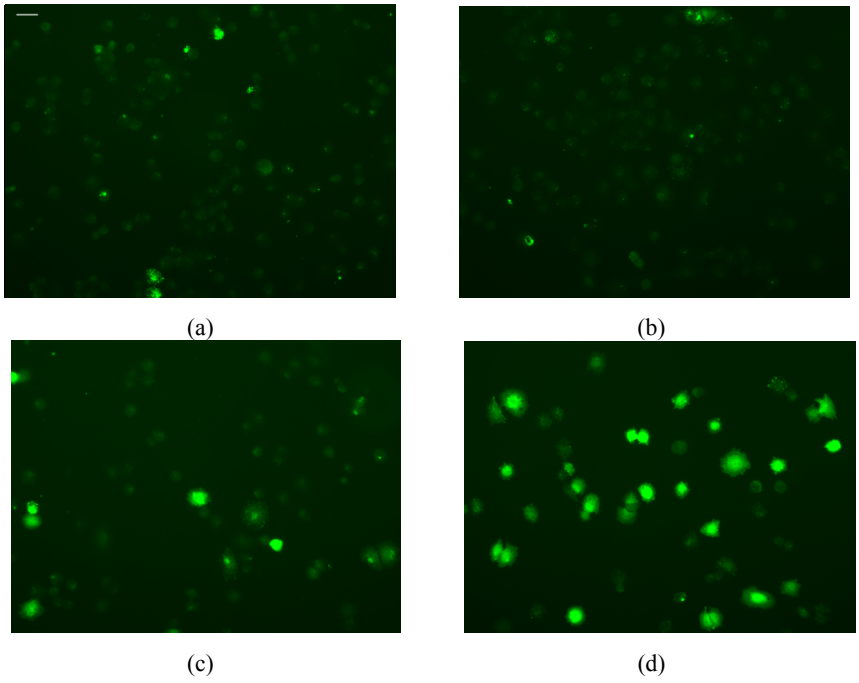

Figure 27 Calcein fluorescence after hyperthermia treatment. (a) Dx5 cell without any treatment; (b) Dx5 cell treated by 1h 43ºC incubator hyperthermia; (c) Dx5 cell treated by 5 μM ICG + 3 min laser; (d) Dx5 treated with verapamil. All the images were taken under 20X magnification and the exposure time was 1000 ms. The scale bar in (a) represents 24 μm.

VI. DISCUSSION

1. The Induction of Thermotolerance

In specific aim 1, it is hypothesized that the rate of heating is a determinant factor in cells acquiring thermal tolerance, which is more likely to occur in low dose hyperthermia with

longer exposure time. Therefore, it was proposed that the rapid rate NIR laser-ICG hyperthermia could avoid the induction of thermal tolerance because the duration of treatment is short while the slow rate incubator hyperthermia could cause thermal tolerance induction. This hypothesis is supported by the results from the HSP70 ELISA assay where the HSP70 level after 1 hour 43 ºC hyperthermia was significantly higher than the non-treated control cells while at the same thermal dose, the rapid rate 3 minute laser + 5 μM ICG hyperthermia did not cause any increase compared to the controls. This difference suggested the importance of the rate of heating because thermotolerance obviously developed to a greater degree during slow heating rates when the temperature of hyperthermia was near the breakpoint. A breakpoint temperature (usually around 43 ºC) is where cytotoxicity of hyperthermia starts to occur. Below the breakpoint, cells can survive under even extended hyperthermia through overexpressing HSPs.

It has been discovered by both *in vitro* and *in vivo* studies that a rapid rate of heat accumulation can reduce cell survival or increase thermal injury [110-112]. In this regard, some researchers have already tried to correlate cellular HSP70 level as the biomarker of thermotolerance with different heating rates but none of them had achieved positive results.

In 1995, Flanagan et al. [110] found that HSP70 level was significantly higher after a rapid rate hyperthermia but not increased after a slow one, a result opposite to ours. The reason for this difference could be that their heating is too slow, even in the rapid rate heating. In their study, the rapid rate was chosen at 0.166 ºC/min, a rate that is similar to the slow rate (0.1 ºC/min) used in this study. As a comparison, the rapid rate heating

employed in this study was about 4 ºC/min. From this point of view, their result supported our conclusion.

In early research conducted by Burns et al. [111] gradually heated L1210 leukemia cells did not overexperss HSP70, while increased HSP70 synthesis was observed in rapidly heated cells. However, their experiment had a similar problem to Flanagan's, that is, the thermal dose in the slow rate heating was much higher than in the rapid rate heating.

Since thermal tolerance is dependent on thermal dose, it is crucial to keep thermal dose constant when studying the effect of heating rates on the induction of thermal tolerance. My study showed for the first time that slow rate heating is more likely to induce thermal tolerance than a rapid rate heating when the thermal dose is similar.

2. Thermal Resistance and Drug Resistance

The HSPs are a family of highly conserved stress proteins present in the cells of all living organisms [113]. It could be found to be expressed at very low levels in healthy cells to help newly synthesized proteins to fold to an appropriate special conformation. Its expression can increase not only when cells are under heat stress but also due to other stresses such as infection, inflammation, or toxins exposure [114]. Our observation that the baseline HSP70 level in MES-SA/Dx5 cells was two times higher than in MES-SA cells suggests that the induction of MDR might induce HSP70 overexpression. MES-SA/Dx5 cells are developed by incubating DOX sensitive MES-SA cells with stepwise increased concentration of DOX, which is a serious stress condition to the cells. It has long been discovered that the induction of thermal tolerance can simultaneously increase drug resistant. Tumor cells sequentially exposed to nonlethal hyperthermia and then chemotherapy showed higher cell survival than when the two were given simultaneously

[115, 116]. Pirity et al. [117] conducted research with rat hepatoma and observed that cells which were induced to overexpress P-gp did not overexpress HSPs, whereas cells which were induced to overexpress HSPs showed increased level of P-gp. These results suggested that hyperthermia should not be given prior to chemotherapy in order to avoid heat induced MDR, however, none of these findings can explain the increased baseline HSP70 expression in MDR positive MES-SA/Dx5 cells. Recently, Tchénio et al. [118] successfully isolated heat shock factor 1 (HSF1) transcription factor, which regulates the expression of the HSPs, in cultured human U2-OS osteosarcoma cells that confer DOX resistance. Their results indirectly supported our observation in MES-SA/Dx5 cells that drug resistance might increase cell's thermal tolerance.

3. Apoptosis in DOX Chemotherapy

DOX can cause apoptotic cell death through several distinct mechanisms [93]. DOX induced apoptosis had been reported in various cell lines and with a wide range of concentrations [119-123]. In a study conducted by Angelini et al. [124], 5 μM and 10 μM DOX concentration induced apoptosis in MES-SA/Dx5 cells. Moreover, they observed increasing apoptosis with increasing DOX intracellular accumulation, which to some extent supports the data presented in this study. In the current study, 1 μM DOX induced apoptosis in DOX sensitive MES-SA cells but not in DOX resistant MES-SA/Dx5 cells probably because the intracellular DOX concentration in MES-SA cells is much higher than in MES-SA/Dx5 cells due to the P-gp pump in the MES-SA/Dx5 cells.

4. Mode of Cell Death by Hyperthermia

As has been mentioned previously, hyperthermia is capable of inducing apoptosis or necrosis depending on the temperature/thermal dose [125]. Generally, above the

"breakpoint" temperature, cancer cells start to die because of heat stress. With the increase of temperature, the percentage of apoptotic cells decreases with a concomitant increase in necrotic cells [29, 126]. Some other factors can slightly affect this response process, such as cell type, stage of cell cycle and prior exposure to heat [1, 29, 127].

In specific aim 2, we have hypothesized that other than temperature/thermal dose, differences in heating rates can lead to different modes of cell death. More specifically, moderate slow rate hyperthermia at 43 °C induced by the incubator is not enough to exert necrosis; indirect cellular damage is most likely and apoptotic cell death results from this indirect process; while in the rapid rate 43 °C NIR laser-ICG hyperthermia, necrotic cell death is expected through protein denaturing caused by rapid heat accumulation at the ICG bound cellular proteins. Meanwhile, at 50 °C, both slow rate incubator hyperthermia and rapid rate laser-ICG hyperthermia should lead to necrotic cell death.

The results of the Hoechst/PI assay on the 50 °C treated cells support the hypothesis made in specific aim 2 since the two hyperthermia treatments caused complete necrosis both immediately or 24 hours after treatment, which is consistent with what was reported in the literature. The result of the Hoechst/PI assay on the 43 °C treated cells suggest that, at the same temperature and thermal dose, rapid rate laser-ICG hyperthermia results in necrosis while slow rate incubator hyperthermia results in apoptosis, which also support the hypothesis made in specific aim 2. Moreover, it indicates for the first time that necrotic cell death could be induced at a temperature that typically would cause apoptosis as long as the rate of heating is rapid. Since a variety of cancer cells have an impaired apoptosis pathway, the ability to induce necrosis by the rapid rate heating at 43 °C provide us more opportunity to treat cancers that are resistant to apoptosis.

An inconsistence in the apoptosis assay results was also observed. In the 50 °C hyperthermia, cellular caspase 3 levels were found to be decreased after both rapid rate and slow rate hyperthermia treatment, probably because the number of cells decreased significantly due to the extremely high thermal dose. The assay could be more accurate if it were coupled with a cell viability assay.

5. DOX-hyperthermia Synergism and Clinical Prospect

Although DOX is considered one of the most effective anticancer agents [128], its clinical use is restricted due to its side effect of inducing cardiomyopathy and congestive heart failure, which is cumulative and irreversible [129]. In order to increase its therapeutic effect as well as minimize its cardiotoxicity to cancer, considerable research has been conducted. Second-generation DOX analogs like epirubicin or idarubicin showed improved therapeutic index over DOX, but the side effect of cardiotoxicity still exists [130]. Besides its side effect, MDR induction in tumor is another major obstacle to DOX chemotherapy. In order to overcome MDR, drug carriers such as liposomes have been used. Pegylated liposomal DOX has been clinically used to treat advanced ovarian cancer [94]. However, its improvement in response rate was not satisfying (the response rate was less than 30%) [94].

In specific aim 3 it was hypothesized that a synergistic effect may exist when combining DOX chemotherapy with the rapid rate hyperthermia, especially in the MDR MES-SA/Dx5 cells. Results from the cytotoxicity assay generally support this hypothesis; furthermore, this synergistic effect is due to increased uptake of DOX and the reversal of MDR as evident by the DOX fluorescence imaging. Therefore, by applying rapid rate hyperthermia to DOX chemotherapy, a significant reduction in the overall patient dose

could be achieved in order to reach the same therapeutic effect compared to when using DOX alone, thus the side effect of DOX could be minimized. More importantly, rapid rate hyperthermia could be a safe approach to help DOX overcome MDR.

VII. CONCLUSION

It has been recognized for years that synergetic cancer cell killing can be achieved by simultaneously deliver of chemotherapy and hyperthermia. This *in vitro* study in cultured cancer cells shows that the potentiating effect of hyperthermia to chemotherapy can be maximized by increasing the rate of heating as evident by the results from the cytotoxicity assay. When delivered at the same thermal dose, rapidly increasing temperature from 37 °C to 43 °C caused more cell membrane damage than gradually heating the cells from 37 °C to 43 °C and thus allowed for more intracellular accumulation of the chemotherapeutic agents DOX. Different modes of cell death were observed under low thermal dose hyperthermia by the two hyperthermia delivery methods. The rapid rate laser-ICG hyperthermia @ 43 °C caused cell necrosis whereas the slow rate incubator hyperthermia @ 43 °C induced very mild apoptosis. At 43 °C a positive correlation between thermal tolerance and the length of hyperthermia exposure was identified. More importantly, this study shows that by increasing the rate of heating, less thermal dose is needed in order to overcome P-gp mediated MDR.

LIST OF REFERENCES

[1] Hildebrandt B, Wust P, Ahlers O, Dieing A, Sreenivasa G, Kerner T, et al. The cellular and molecular basis of hyperthermia. Critical reviews in oncology/hematology. 2002 Jul;43(1):33-56.

[2] van der Zee J. Heating the patient: a promising approach? Annals of oncology : official journal of the European Society for Medical Oncology / ESMO. 2002 Aug;13(8):1173-84.

[3] Hokland SL, Pedersen M, Salomir R, Quesson B, St²dkilde-J²rgensen H, Moonen CT. MRI-guided focused ultrasound: methodology and applications. IEEE transactions on medical imaging. 2006 Jun;25(6):723-31.

[4] Vertree RA, Leeth A, Girouard M, Roach JD, Zwischenberger JB. Whole-body hyperthermia: a review of theory, design and application. Perfusion. 2002 Jul;17(4):279-90.

[5] Urano M, Kuroda M, Nishimura Y. For the clinical application of themochemotherapy given at mild temperatures. nternational journal of hyperthermia : the official journal of European Society for Hyperthermic Oncology, North American Hyperthermia Group. 1999;15:79–107.

[6] Dewey WC. Arrhenius relationships from the molecule and cell to the clinic. International journal of hyperthermia : the official journal of European Society for Hyperthermic Oncology, North American Hyperthermia Group. 1994 Jul-Aug;10(4):457-83.

[7] Dewhirst MW, Prosnitz L, Thrall D, al. e. Hyperthermic treatment of malignant disease: current status and a view toward the future. Seminars in Oncology. 1997;24(6):616-25.

[8] Hahn GM, Braun J, Har-Kedar I. Thermochemotherapy: synergism between hyperthermia (42-43 degrees) and adriamycin (of bleomycin) in mammalian cell inactivation. Proceedings of the National Academy of Sciences of the United States of America. 1975 Mar;72(3):937-40.

[9] Jones EL, Oleson JR, Prosnitz LR, Samulski TV, Vujaskovic Z, Yu D, et al. Randomized trial of hyperthermia and radiation for superficial tumors. Journal of clinical oncology : official journal of the American Society of Clinical Oncology. 2005 May 1;23(13):3079-85.

[10] Coffey DS, Getzenberg RH, DeWeese TL. Hyperthermic biology and cancer therapies: a hypothesis for the "Lance Armstrong effect". JAMA : the journal of the American Medical Association. 2006 Jul 26;296(4):445-8.

[11] Cavaliere R, Ciocatto EC, Giovanella BC, Heidelberger C, Johnson RO, Margottini M, et al. Selective heat sensitivity of cancer cells. Biochemical and clinical studies. Cancer. 1967 Sep;20(9):1351-81.

[12] Day ES, Morton JG, West JL. Nanoparticles for thermal cancer therapy. Journal of biomechanical engineering. 2009 Jul;131(7):074001.

[13] Lepock JR. Cellular effects of hyperthermia: relevance to the minimum dose for thermal damage. International journal of hyperthermia : the official journal of European Society for Hyperthermic Oncology, North American Hyperthermia Group. 2003 May-Jun;19(3):252-66.

[14] Streffer C. Strahleneffekte nach Exposition wèahrend der prèanatalen Entwicklung. Der Radiologe. 1995 Mar;35(3):141-7.

[15] Dickson JA, Shah DM. The effects of hyperthermia (42 degrees C) on the biochemistry and growth of a malignant cell line. European journal of cancer. 1972 Oct;8(5):561-71.

[16] Christophi C, Winkworth A, Muralihdaran V, Evans P. The treatment of malignancy by hyperthermia. Surgical oncology. 1998 Jul-Aug;7(1-2):83-90.

[17] Coss RA, Dewey WC, Bamburg JR. Effects of hyperthermia on dividing Chinese hamster ovary cells and on microtubules in vitro. Cancer research. 1982 Mar;42(3):1059-71.

[18] Coss RA, Linnemans WA. The effects of hyperthermia on the cytoskeleton: a review. International journal of hyperthermia : the official journal of European Society for Hyperthermic Oncology, North American Hyperthermia Group. 1996 Mar-Apr;12(2):173-96.

[19] Gabai VL, Kabakov AE. Tumor cell resistance to energy deprivation and hyperthermia can be determined by the actin skeleton stability. Cancer letters. 1993 Jun 15;70(1-2):25-31.

[20] Urano M. Kinetics of thermotolerance in normal and tumor tissues: a review. Cancer research. 1986 Feb;46(2):474-82.

[21] Henle KJ, Dethlefsen LA. Heat fractionation and thermotolerance: a review. Cancer research. 1978 Jul;38(7):1843-51.

[22] Majima H, Gerweck LE. Kinetics of thermotolerance decay in Chinese hamster ovary cells. Cancer research. 1983 Jun;43(6):2673-7.

[23] Li GC, Mivechi NF, Weitzel G. Heat shock proteins, thermotolerance, and their relevance to clinical hyperthermia. International journal of hyperthermia : the official

journal of European Society for Hyperthermic Oncology, North American Hyperthermia Group. 1995 Jul-Aug;11(4):459-88.

[24] Ellis RJ, van der Vies SM. Molecular chaperones. Annual review of biochemistry. 1991;60:321-47.

[25] Mizzen LA, Welch WJ. Characterization of the thermotolerant cell. I. Effects on protein synthesis activity and the regulation of heat-shock protein 70 expression. The Journal of cell biology. 1988 Apr;106(4):1105-16.

[26] Sciandra JJ, Subjeck JR. Heat shock proteins and protection of proliferation and translation in mammalian cells. Cancer research. 1984 Nov;44(11):5188-94.

[27] Buchner J. Supervising the fold: functional principles of molecular chaperones. The FASEB journal : official publication of the Federation of American Societies for Experimental Biology. 1996 Jan;10(1):10-9.

[28] Jèaèattelèa M. Heat shock proteins as cellular lifeguards. Annals of medicine. 1999 Aug;31(4):261-71.

[29] Samali A, Holmberg CI, Sistonen L, Orrenius S. Thermotolerance and cell death are distinct cellular responses to stress: dependence on heat shock proteins. FEBS letters. 1999 Nov 19;461(3):306-10.

[30] Ciocca DR, Oesterreich S, Chamness GC, McGuire WL, Fuqua SA. Biological and clinical implications of heat shock protein 27,000 (Hsp27): a review. Journal of the National Cancer Institute. 1993 Oct 6;85(19):1558-70.

[31] Kerr JF, Wyllie AH, Currie AR. Apoptosis: a basic biological phenomenon with wide-ranging implications in tissue kinetics. British journal of cancer. 1972 Aug;26(4):239-57.

[32] Webb SJ, Harrison DJ, Wyllie AH. Apoptosis: an overview of the process and its relevance in disease. Advances in pharmacology (San Diego, Calif). 1997;41:1-34.

[33] Lowe SW, Ruley HE, Jacks T, Housman DE. p53-dependent apoptosis modulates the cytotoxicity of anticancer agents. Cell. 1993 Sep 24;74(6):957-67.

[34] Lowe SW, Bodis S, McClatchey A, Remington L, Ruley HE, Fisher DE, et al. p53 status and the efficacy of cancer therapy in vivo. Science (New York, NY. 1994 Nov 4;266(5186):807-10.

[35] Bottini A, Berruti A, Bersiga A, Brizzi MP, Brunelli A, Gorzegno G, et al. p53 but not bcl-2 immunostaining is predictive of poor clinical complete response to primary chemotherapy in breast cancer patients. Clin Cancer Res. 2000 Jul;6(7):2751-8.

[36] Harmon BV, Corder AM, Collins RJ, Gobâe GC, Allen J, Allan DJ, et al. Cell death induced in a murine mastocytoma by 42-47 degrees C heating in vitro: evidence that the form of death changes from apoptosis to necrosis above a critical heat load. International journal of radiation biology. 1990 Nov;58(5):845-58.

[37] Yonezawa M, Otsuka T, Matsui N, Tsuji H, Kato KH, Moriyama A, et al. Hyperthermia induces apoptosis in malignant fibrous histiocytoma cells in vitro. International journal of cancer Journal international du cancer. 1996 May 3;66(3):347-51.

[38] Roizin-Towle L, Pirro JP. The response of human and rodent cells to hyperthermia. International journal of radiation oncology, biology, physics. 1991 Apr;20(4):751-6.

[39] Dewhirst MW, Viglianti BL, Lora-Michiels M, Hanson M, Hoopes PJ. Basic principles of thermal dosimetry and thermal thresholds for tissue damage from hyperthermia. International journal of hyperthermia : the official journal of European Society for Hyperthermic Oncology, North American Hyperthermia Group. 2003 May-Jun;19(3):267-94.

[40] Morris CC, Myers R, Field SB. The response of the rat tail to hyperthermia. The British journal of radiology. 1977 Aug;50(596):576-80.

[41] Sapareto SA, Dewey WC. Thermal dose determination in cancer therapy. International journal of radiation oncology, biology, physics. 1984 Jun;10(6):787-800.

[42] Herman TS, Teicher BA, Jochelson M, Clark J, Svensson G, Coleman CN. Rationale for use of local hyperthermia with radiation therapy and selected anticancer drugs in locally advanced human malignancies. International journal of hyperthermia : the official journal of European Society for Hyperthermic Oncology, North American Hyperthermia Group. 1988 Mar-Apr;4(2):143-58.

[43] Hamazoe R, Maeta M, Kaibara N. Intraperitoneal thermochemotherapy for prevention of peritoneal recurrence of gastric cancer. Final results of a randomized controlled study. Cancer. 1994 Apr 15;73(8):2048-52.

[44] Ghussen F, Kru¨ger I, Smalley R, Groth W. Hyperthermic perfusion with chemotherapy for melanoma of the extremeties. World Journal of Surgery 1989;13:598–602.

[45] Hafstrom L, Rudenstam M, Blomquist E, al. e. Regional hyperthermic perfusion with melphalan after surgery for recurrent melanoma of the exremities. Swedish Melanoma Study Group. Journal of Clinical Oncology. 1991;9(12):2085–7.

[46] Koops HS, Vaglini M, Suciu S, al. e. Prophylactic isolated limb perfusion for localized, high-risk limb melanomas: results of a multicenter randomized phase III trial. Journal of Clinical Oncology. 1998;16:2906–12.

[47] Gottesman MM. How cancer cells evade chemotherapy: sixteenth Richard and Hinda Rosenthal Foundation Award Lecture. Cancer research. 1993 Feb 15;53(4):747-54.

[48] Riordan JR, Deuchars K, Kartner N, Alon N, Trent J, Ling V. Amplification of P-glycoprotein genes in multidrug-resistant mammalian cell lines. Nature. 1985 Aug 29-Sep 4;316(6031):817-9.

[49] Liu Y, Cho CW, Yan X, Henthorn TK, Lillehei KO, Cobb WN, et al. Ultrasound-Induced hyperthermia increases cellular uptake and cytotoxicity of P-glycoprotein substrates in multi-drug resistant cells. Pharmaceutical research. 2001 Sep;18(9):1255-61.

[50] Moriyama-Gonda N, Igawa M, Shiina H, Wada Y. Heat-induced membrane damage combined with adriamycin on prostate carcinoma PC-3 cells: correlation of cytotoxicity, permeability and P-glycoprotein or metallothionein expression. British journal of urology. 1998 Oct;82(4):552-9.

[51] Kampinga HH. Hyperthermia, thermotolerance and topoisomerase II inhibitors. British journal of cancer. 1995 Aug;72(2):333-8.

[52] Oh HJ, Chen X, Subjeck JR. Hsp110 protects heat-denatured proteins and confers cellular thermoresistance. The Journal of biological chemistry. 1997 Dec 12;272(50):31636-40.

[53] Fisher B, Kraft P, Hahn GM, Anderson RL. Thermotolerance in the absence of induced heat shock proteins in a murine lymphoma. Cancer research. 1992 May 15;52(10):2854-61.

[54] Fajardo LF. Pathological effects of hyperthermia in normal tissues. Cancer research. 1984 Oct;44(10):4826s-35s.

[55] Sminia P, van der Zee J, Wondergem J, Haveman J. Effect of hyperthermia on the central nervous system: a review. International journal of hyperthermia : the official journal of European Society for Hyperthermic Oncology, North American Hyperthermia Group. 1994 Jan-Feb;10(1):1-30.

[56] Wondergem J, Haveman J, Rusman V, Sminia P, Van Dijk JD. Effects of local hyperthermia on the motor function of the rat sciatic nerve. International journal of radiation biology and related studies in physics, chemistry, and medicine. 1988 Mar;53(3):429-38.

[57] Habash RW, Bansal R, Krewski D, Alhafid HT. Thermal therapy, part 2: hyperthermia techniques. Critical reviews in biomedical engineering. 2006;34(6):491-542.

[58] Chou CK. APPLICATION OF ELECTROMAGNETIC ENERGY IN CANCER-TREATMENT. IEEE Trans Instrum Meas. 1988 Dec;37(4):547-51.

[59] Narayan P, Crocker I, Elder E, Olson JJ. Safety and efficacy of concurrent interstitial radiation and hyperthermia in the treatment of progressive malignant brain tumors. Oncology reports. 2004 Jan;11(1):97-103.

[60] Hiraoka M, Mitsumori M, Hiroi N, Ohno S, Tanaka Y, Kotsuka Y, et al. Development of RF and microwave heating equipment and clinical applications to cancer treatment in Japan. IEEE Trans Microw Theory Tech. 2000 Nov;48(11):1789-99.

[61] Sullivan D. MATHEMATICAL-METHODS FOR TREATMENT PLANNING IN DEEP REGIONAL HYPERTHERMIA. IEEE Trans Microw Theory Tech. 1991 May;39(5):864-72.

[62] Xi L, Tekin D, Bhargava P, Kukreja RC. Whole body hyperthermia and preconditioning of the heart: basic concepts, complexity, and potential mechanisms. International journal of hyperthermia : the official journal of European Society for Hyperthermic Oncology, North American Hyperthermia Group. 2001 Sep-Oct;17(5):439-55.

[63] Pettigrew RT, Galt JM, Ludgate CM, Horn DB, Smith AN. Circulatory and biochemical effects of whole body hyperthermia. The British journal of surgery. 1974 Sep;61(9):727-30.

[64] Bull JM, Lees D, Schuette W, Whang-Peng J, Smith R, Bynum G, et al. Whole body hyperthermia: a phase-I trial of a potential adjuvant to chemotherapy. Annals of internal medicine. 1979 Mar;90(3):317-23.

[65] Milligan AJ. Whole-body hyperthermia induction techniques. Cancer research. 1984 Oct;44(10):4869s-72s.

[66] Wust P, Hildebrandt B, Sreenivasa G, Rau B, Gellermann J, Riess H, et al. Hyperthermia in combined treatment of cancer. The lancet oncology. 2002 Aug;3(8):487-97.

[67] Latorre M, Rinaldi C. Applications of magnetic nanoparticles in medicine: magnetic fluid hyperthermia. Puerto Rico health sciences journal. 2009 Sep;28(3):227-38.

[68] Diederich CJ, Hynynen K. The feasibility of using electrically focused ultrasound arrays to induce deep hyperthermia via body cavities. IEEE transactions on ultrasonics, ferroelectrics, and frequency control. 1991;38(3):207-19.

[69] Salomir R, Rata M, Cadis D, Petrusca L, Auboiroux V, Cotton F. Endocavitary thermal therapy by MRI-guided phased-array contact ultrasound: experimental and numerical studies on the multi-input single-output PID temperature controller's convergence and stability. Medical physics. 2009 Oct;36(10):4726-41.

[70] D'Andrea JA, Ziriax JM, Adair ER. Radio frequency electromagnetic fields: mild hyperthermia and safety standards. Progress in brain research. 2007;162:107-35.

[71] Brace CL. Radiofrequency and microwave ablation of the liver, lung, kidney, and bone: what are the differences? Current problems in diagnostic radiology. 2009 May-Jun;38(3):135-43.

[72] Habash RW, Bansal R, Krewski D, Alhafid HT. Thermal therapy, Part III: ablation techniques. Critical reviews in biomedical engineering. 2007;35(1-2):37-121.

[73] Chen WR, Adams RL, Heaton S, Dickey DT, Bartels KE, Nordquist RE. Chromophore-enhanced laser-tumor tissue photothermal interaction using an 808-nm diode laser. Cancer letters. 1995 Jan 6;88(1):15-9.

[74] Huang X, Jain PK, El-Sayed IH, El-Sayed MA. Plasmonic photothermal therapy (PPTT) using gold nanoparticles. Lasers in medical science. 2008 Jul;23(3):217-28.

[75] Shao N, Lu S, Wickstrom E, Panchapakesan B. Integrated molecular targeting of IGF1R and HER2 surface receptors and destruction of breast cancer cells using single wall carbon nanotubes. Nanotechnology. 2007 Aug;18(31):9.

[76] Kam NW, O'Connell M, Wisdom JA, Dai H. Carbon nanotubes as multifunctional biological transporters and near-infrared agents for selective cancer cell destruction. Proceedings of the National Academy of Sciences of the United States of America. 2005 Aug 16;102(33):11600-5.

[77] Xiao Y, Gao X, Taratula O, Treado S, Urbas A, Holbrook RD, et al. Anti-HER2 IgY antibody-functionalized single-walled carbon nanotubes for detection and selective destruction of breast cancer cells. BMC cancer. 2009;9:351.

[78] Moon HK, Lee SH, Choi HC. In vivo near-infrared mediated tumor destruction by photothermal effect of carbon nanotubes. ACS nano. 2009 Nov 24;3(11):3707-13.

[79] Burke A, Ding X, Singh R, Kraft RA, Levi-Polyachenko N, Rylander MN, et al. Long-term survival following a single treatment of kidney tumors with multiwalled carbon nanotubes and near-infrared radiation. Proceedings of the National Academy of Sciences of the United States of America. 2009 Aug 4;106(31):12897-902.

[80] Ann-Ann D, Ying-Yi C, Wang CC, Pai-Chi L, Dar-Bin S. HER-2 Antibody Conjugated Gold Nano Rod for in Vivo Photothermal Therapy. Nanotechnology, 2008 NANO '08 8th IEEE Conference on; 2008 18-21 Aug. 2008; 2008. p. 882-5.

[81] O'Neal DP, Hirsch LR, Halas NJ, Payne JD, West JL. Photo-thermal tumor ablation in mice using near infrared-absorbing nanoparticles. Cancer letters. 2004 Jun 25;209(2):171-6.

[82] Hirsch LR, Stafford RJ, Bankson JA, Sershen SR, Rivera B, Price RE, et al. Nanoshell-mediated near-infrared thermal therapy of tumors under magnetic resonance guidance. Proceedings of the National Academy of Sciences of the United States of America. 2003 Nov 11;100(23):13549-54.

[83] Li Z, Huang P, Zhang X, Lin J, Yang S, Liu B, et al. RGD-conjugated dendrimer-modified gold nanorods for in vivo tumor targeting and photothermal therapy. Molecular pharmaceutics. Feb 1;7(1):94-104.

[84] James WD, Hirsch LR, West JL, O'Neal PD, Payne JD. Application of INAA to the build-up and clearance of gold nanoshells in clinical studies in mice. J Radioanal Nucl Chem. 2007 Feb;271(2):455-9.

[85] Gannon CJ, Patra CR, Bhattacharya R, Mukherjee P, Curley SA. Intracellular gold nanoparticles enhance non-invasive radiofrequency thermal destruction of human gastrointestinal cancer cells. Journal of nanobiotechnology. 2008;6:2.

[86] Cardinal J, Klune JR, Chory E, Jeyabalan G, Kanzius JS, Nalesnik M, et al. Noninvasive radiofrequency ablation of cancer targeted by gold nanoparticles. Surgery. 2008 Aug;144(2):125-32.

[87] Gannon CJ, Cherukuri P, Yakobson BI, Cognet L, Kanzius JS, Kittrell C, et al. Carbon nanotube-enhanced thermal destruction of cancer cells in a noninvasive radiofrequency field. Cancer. 2007 Dec 15;110(12):2654-65.

[88] Hergt R, Andra W, d'Ambly CG, Hilger I, Kaiser WA, Richter U, et al. Physical limits of hyperthermia using magnetite fine particles. IEEE Trans Magn. 1998 Sep;34(5):3745-54.

[89] Wang XM, Gu HC, Yang ZQ. The heating effect of magnetic fluids in an alternating magnetic field. J Magn Magn Mater. 2005 May;293(1):334-40.

[90] Kalambur VS, Longmire EK, Bischof JC. Cellular level loading and heating of superparamagnetic iron oxide nanoparticles. Langmuir : the ACS journal of surfaces and colloids. 2007 Nov 20;23(24):12329-36.

[91] Lin R, Shi Ng L, Wang CH. In vitro study of anticancer drug doxorubicin in PLGA-based microparticles. Biomaterials. 2005 Jul;26(21):4476-85.

[92] Bodley A, Liu LF, Israel M, Seshadri R, Koseki Y, Giuliani FC, et al. DNA topoisomerase II-mediated interaction of doxorubicin and daunorubicin congeners with DNA. Cancer research. 1989 Nov 1;49(21):5969-78.

[93] Thorburn A, Frankel AE. Apoptosis and anthracycline cardiotoxicity. Molecular cancer therapeutics. 2006 Feb;5(2):197-9.

[94] Rose PG. Pegylated liposomal doxorubicin: optimizing the dosing schedule in ovarian cancer. The oncologist. 2005 Mar;10(3):205-14.

[95] Zhu XD, Wei S, Guo XW. Imaging objects in tissuelike media with optical tagging and the diffuse photon differential transmittance. Journal of the Optical Society of America. 1997 Jan;14(1):300-5.

[96] Maarek JM, Holschneider DP, Harimoto J. Fluorescence of indocyanine green in blood: intensity dependence on concentration and stabilization with sodium polyaspartate. Journal of photochemistry and photobiology. 2001 Dec 31;65(2-3):157-64.

[97] Joie ENL, Barofsky AD, Gregory KW, Prahl SA. Welding Artificial Biomaterial with a Pulsed Diode Laser and Indocyanine Green Dye. Lasers in Surgery: Advanced Characterization, Therapeutics, and Systems, Proc SPIE. 1995;2395:508-16.

[98] Abels C, Fickweiler S, Weiderer P, Bäumler W, Hofstädter F, Landthaler M, et al. Indocyanine green (ICG) and laser irradiation induce photooxidation. Archives of Dermatological Research 2000;292 404–11

[99] Skrivanovâa K, Skorpâikovâa J, Svihâalek J, Mornstein V, Janisch R. Photochemical properties of a potential photosensitiser indocyanine green in vitro. Journal of photochemistry and photobiology B, Biology. 2006 Nov 1;85(2):150-4.

[100] Tang Y, McGoron AJ. Combined effects of laser-ICG photothermotherapy and doxorubicin chemotherapy on ovarian cancer cells. Journal of photochemistry and photobiology B, Biology. 2009 Dec 2;97(3):138-44.

[101] Fickweiler S, Szeimies RM, Bèaumler W, Steinbach P, Karrer S, Goetz AE, et al. Indocyanine green: intracellular uptake and phototherapeutic effects in vitro. Journal of photochemistry and photobiology B, Biology. 1997 Apr;38(2-3):178-83.

[102] Eguchi Y, Shimizu S, Tsujimoto Y. Intracellular ATP levels determine cell death fate by apoptosis or necrosis. Cancer research. 1997 May 15;57(10):1835-40.

[103] Shacter E, Williams JA, Hinson RM, Sentèurker S, Lee YJ. Oxidative stress interferes with cancer chemotherapy: inhibition of lymphoma cell apoptosis and phagocytosis. Blood. 2000 Jul 1;96(1):307-13.

[104] Minchin RF, Johnston MR, Aiken MA, Boyd MR. Pharmacokinetics of doxorubicin in isolated lung of dogs and humans perfused in vivo. The Journal of pharmacology and experimental therapeutics. 1984 Apr;229(1):193-8.

[105] Alnemri ES, Livingston DJ, Nicholson DW, Salvesen G, Thornberry NA, Wong WW, et al. Human ICE/CED-3 Protease Nomenclature. Cell. 1996;87(2):171-.

[106] Emad SA. Mammalian cell death proteases: A family of highly conserved aspartate specific cysteine proteases. Journal of Cellular Biochemistry. 1997;64(1):33-42.

[107] Monks A, Scudiero D, Skehan P, Shoemaker R, Paull K, Vistica D, et al. Feasibility of a high-flux anticancer drug screen using a diverse panel of cultured human tumor cell lines. Journal of the National Cancer Institute. 1991 Jun 5;83(11):757-66.

[108] Park H, Yang J, Lee J, Haam S, Choi IH, Yoo KH. Multifunctional nanoparticles for combined doxorubicin and photothermal treatments. ACS Nano. 2009 Oct 27;3(10):2919-26.

[109] Berenbaum MC. What is synergy? Pharmacological reviews. 1989 Jun;41(2):93-141.

[110] Flanagan SW, Ryan AJ, Gisolfi CV, Moseley PL. TISSUE-SPECIFIC HSP70 RESPONSE IN ANIMALS UNDERGOING HEAT-STRESS. Am J Physiol-Regulat Integr Compar Physiol. 1995 Jan;268(1):R28-R32.

[111] Burns CP, Lambert BJ, Haugstad BN, Guffy MM. INFLUENCE OF RATE OF HEATING ON THERMOSENSITIVITY OF L1210 LEUKEMIA - MEMBRANE-LIPIDS AND MR 70,000 HEAT-SHOCK PROTEIN. Cancer Research. 1986 Apr;46(4):1882-7.

[112] Herman TS, Gerner EW, Magun BE, Stickney D, Sweets CC, White DM. RATE OF HEATING AS A DETERMINANT OF HYPERTHERMIC CYTO-TOXICITY. Cancer Research. 1981;41(9):3519-23.

[113] Amorim FT, Yamada PM, Robergs RA, Schneider SM, Moseley PL. The effect of the rate of heat storage on serum heat shock protein 72 in humans. European journal of applied physiology. 2008 Dec;104(6):965-72.

[114] De Maio A. Heat shock proteins: facts, thoughts, and dreams. Shock. 1999;11(1):1-12.

[115] Donaldson SS, Gordon LF, Hahn GM. Protective effect of hyperthermia against the cytotoxicity of actinomycin D on Chinese hamster cells. Cancer Treatment Reports. 1978;62(10):1489-95.

[116] Wallner K, Li GC. Adriamycin resistance, heat resistance and radiation response in Chinese hamster fibroblasts. International Journal of Radiation Oncology, Biology, Physics. 1986;12(5):829-33.

[117] Pirity M, Hevâer-Szabâo A, Venetianer A. Overexpression of P-glycoprotein in heat- and/or drug-resistant hepatoma variants. Cytotechnology. 1996;19(3):207-14.

[118] Tchâenio T, Havard M, Martinez LA, Dautry F. Heat shock-independent induction of multidrug resistance by heat shock factor 1. Molecular and cellular biology. 2006 Jan;26(2):580-91.

[119] Ling YH, Priebe W, Perez-Soler R. Apoptosis induced by anthracycline antibiotics in P388 parent and multidrug-resistant cells. Cancer research. 1993 Apr 15;53(8):1845-52.

[120] Skladanowski A, Konopa J. Adriamycin and daunomycin induce programmed cell death (apoptosis) in tumour cells. Biochemical pharmacology. 1993 Aug 3;46(3):375-82.

[121] Zaleskis G, Berleth E, Verstovsek S, Ehrke MJ, Mihich E. Doxorubicin-induced DNA degradation in murine thymocytes. Molecular pharmacology. 1994 Nov;46(5):901-8.

[122] Bose R, Verheij M, Haimovitz-Friedman A, Scotto K, Fuks Z, Kolesnick R. Ceramide synthase mediates daunorubicin-induced apoptosis: an alternative mechanism for generating death signals. Cell. 1995 Aug 11;82(3):405-14.

[123] Jaffrâezou JP, Levade T, Bettaèieb A, Andrieu N, Bezombes C, Maestre N, et al. Daunorubicin-induced apoptosis: triggering of ceramide generation through sphingomyelin hydrolysis. The EMBO journal. 1996 May 15;15(10):2417-24.

[124] Angelini A, Iezzi M, Di Febbo C, Di Ilio C, Cuccurullo F, Porreca E. Reversal of P-glycoprotein-mediated multidrug resistance in human sarcoma MES-SA/Dx-5 cells by nonsteroidal anti-inflammatory drugs. Oncology reports. 2008 Oct;20(4):731-5.

[125] Kampinga HH. Cell biological effects of hyperthermia alone or combined with radiation or drugs: a short introduction to newcomers in the field. International journal of hyperthermia : the official journal of European Society for Hyperthermic Oncology, North American Hyperthermia Group. 2006 May;22(3):191-6.

[126] Milleron RS, Bratton SB. 'Heated' debates in apoptosis. Cellular and molecular life sciences : CMLS. 2007 Sep;64(18):2329-33.

[127] Bettaieb A, Averill-Bates DA. Thermotolerance induced at a mild temperature of 40 degrees C protects cells against heat shock-induced apoptosis. Journal of cellular physiology. 2005 Oct;205(1):47-57.

[128] Weiss RB. The anthracyclines: will we ever find a better doxorubicin? Seminars in oncology. 1992 Dec;19(6):670-86.

[129] Singal PK, Li T, Kumar D, Danelisen I, Iliskovic N. Adriamycin-induced heart failure: mechanism and modulation. Molecular and cellular biochemistry. 2000 Apr;207(1-2):77-86.

[130] Minotti G, Menna P, Salvatorelli E, Cairo G, Gianni L. Anthracyclines: molecular advances and pharmacologic developments in antitumor activity and cardiotoxicity. Pharmacological reviews. 2004 Jun;56(2):185-229.

APPENDICES

General Protocol for Preparing and Filtering Medium

Preparing medium

1) Start the hot water bath and set its temperature to 37°C.

2) Take the Penicillin and FBS (fetal bovine serum) from the freezer and the required Medium brand from the refrigerator. Insert them in the hot water bath at 37°C. (Note: to avoid repeated freezing and thawing, penicillin and FBS aliquots of predetermined volume must be made and stored in the freezer)

3) When the penicillin, FBS and medium are sufficiently warm, take them out and spray them with alcohol. Let it air dry and place them in the Laminar Flow Hood.

4) Insert a Medium Filter bottle in the Laminar Flow Hood after spraying with alcohol.

5) Add 5mL of Penicillin + 50mL of FBS + 445mL of Medium, to the filter bottle. (Note: these volumes are dependant on the Complete Growth Medium requirement of the cell lines used which may vary)

Filtering the medium

1) Connect the filter bottle to a vacuum. Make sure the vacuum "switch" is off when connecting.

2) Upon opening the vacuum switch, the liquid from the bottle is filtered and transferred to an adjoined container. Separate the adjoined container and cap it.

3) Label the container "filtered medium + penicillin, FBS, name, date". Store container in the refrigerator.

4) Any remaining penicillin and FBS can be store in the freezer.

General Protocol for Cell Culturing

Day n

1) Place the medium in a water bath to bring up its temperature to 37°C.

2) When the medium is ready, spray it with alcohol and place it in the laminar flow hood. Make sure that the sterile flaks and all necessary accessories are already in the hood.

3) Add 12mL or 4.5mL of medium to the 250mL or 50mL culture flask respectively.

4) Obtain a cryo-vial with the appropriate cell line from the liquid nitrogen freezer.

5) Wrap the mouth of the vial with a paraffin film. These vials should then be quickly thawed by immersing the bottom half of the vial in the 37°C water bath and gently stirring it.

6) When the vial is thawed, take it to the laminar flow hood; gently pipette the contents of the vial up and down once. Then add all of the vial contents (~1.8mL) to the 250mL culture flask already containing the media. If using the 50mL culture flask, add ~1mL of the content of the vial to culture flask and repeat with another 50mL flask for the remainder of the vial contents. (Note: it is preferable to culture cancer cell lines in the 250mL flasks as they become confluent sooner than normal cell lines; also if the cancer cell density of the cryo-vial is high then the vial contents can be split equally in two 250mL culture flasks; for cell lines such as the HUVEC, add all the contents of the vial to the 50mL flask as the HUVECs grow slower compared to the cancer cell lines.)

7) Label the flask (Medium+Cell line, Name, Date).

8) Put this flask in the incubator for 4 hours. (Note: for cell lines like the HUVEC, 24 hours should be used instead for this step.)

9) After 4 hours, change the medium in the cell culture flask, by removing the old medium and adding 12mL or 4.5mL of new medium depending on the flask size.

Day n+3

1) Put the medium and trypsin in hot water bath. Make a beaker labeled waste, spray with alcohol and put them in the laminar flow hood.

2) In the Laminar flow hood, take out the spent medium from the 250mL culture flask labeled “medium + cells” via pipette, and dispose in the beaker labeled “waste”.

3) Pipette 4mL of trypsin and add it to the 250mL culture flask, gently shake it. (Note: for the 50mL culture flask add 2mL of trypsin.)

4) Remove the trypsin, dispose it in the beaker labeled “Waste”.

5) Repeat steps 3, but leave flask with the trypsin in the incubator for 5-10 minutes, keep monitoring the culture flask in the microscope to make sure cells are detaching.

6) In the meantime prepare a new 250mL culture flask with 12mL of fresh medium. (Note: use 4.5mL of medium for the 50mL flask.)

7) When the cells seem to detach, take out 10uL of the trypsin + cell solution (from the trypsinized flask), and use it in the hemocytometer to get an average count of cell density per mL. (Note: depending on the cell density, one can choose to reduce the cell concentration in the trypsinized culture flask by adding fresh medium.)

8) Take 1mL of the cell solution (cell+trypsin) from the trypsinized flask and pipette them in a new flask consisting of 12mL or 4.5mL of fresh medium depending on the Flask size. Label and incubate them for future use. The rest of the cell solution can be used for seeding in 96-well plates.

General Protocol for Seeding Culture Cells

1) After the cells have been counted in the hemocytometer, calculate the required concentration of the cell solution for seeding in the 96-well plates. (Note: this can be between 5000-10000 cells per well depending on the experimental design.)

2) Depending on the above calculation mix the cell solution with the appropriate volume of fresh medium in a pipette basin.

3) Take three 96-well plates and label them A, B and C.

4) Use a multipipetter and mix the cell solution + fresh medium mixture in the basin by pipetting in and out into the basin a few times. (Note: From this point onwards the cells can be seeded using a multipipetter in any number of combinations in different well plates depending upon the experimental design)

5) After this use the multipipetter to pipette 200uL of the basin solution into 8 wells (8 rows of column 2) in plate A simultaneously. Then repeat this for plate B and C. Make sure to leave column 1 empty for the time being.

6) Then repeat step 5 in column 3 for plates A, B and C.

7) Keep on repeating until column 6 (depending on the experimental design) of plates A, B and C is filled with the basin solution.

8) Use the multipipetter to add fresh medium in column 1 for all the three plates.

9) Incubate the 96-well plates at 37°C.

General Protocol for SRB Assay

1) When the cells in the 96 well plates are ready for the assay, put TCA in the refrigerator for 40 min.

2) When the TCA is ice cold, add 50μL of TCA to each well.

3) Wrap the plate in foil paper and put the well plate in the fridge for 1 hour.

4) After 1 hour, rinse the plate with De-ionized water and let it air dry.

5) Add 100μL of SulfoRhodamine B solution (SRB Dye-purple dye) and let it stain for 20-30 minutes.

6) Rinse the plate 3 times with 1% Acetic Acid (you might need to dilute the Acetic Acid in distilled water). Let it air dry.

7) Add 200μL of Tris Base solution into the wells; let it sit for 5 minutes. Make sure that the SRB is thoroughly dissolved in the Tris Base. (Note: allow more than 5 minutes to dissolve if the need arises so)

8) Put the plate in the Tecan machine.

9) On the Computer, follow: Tecan--RdrOle4--Instrument--Connect.

Tecan--Magellan--Insert--Measurement Parameter: select part of the plate where cells are (ex. A1:D5), Measurement 530:690 Kinetics N., Shaking (check) 60 sec.

Instrument--Start measurement.

VITA

YUAN TANG

2002 B.S. Biomedical Engineering
Shanghai Second Medical University
Shanghai, China.

2010 Doctoral Candidate in Biomedical Engineering
Florida International University
Miami, FL, USA.

PUBLICATIONS AND PRESENTATIONS

Tang Y, Lei T, Manchanda R, Nagesetti A, Fernandez-Fernandez A, Srinivasan S, et al. Simultaneous Delivery of Chemotherapeutic and Thermal-Optical Agents to Cancer Cells by a Polymeric (PLGA) Nanocarrier: An In Vitro Study. Pharm Res. Aug 6. DOI 10.1007/s11095-010-0231-6

Tang Y, McGoron AJ. Combined effects of laser-ICG photothermotherapy and doxorubicin chemotherapy on ovarian cancer cells. Journal of photochemistry and photobiology B, Biology. 2009 Dec 2;97(3):138-44.

Tang Y, McGoron AJ. The Role of Temperature Increase Rate in Combinational Hyperthermia Chemotherapy Treatment. Proc. SPIE, Vol. 7565, 75650C (2010)

Tang Y, McGoron AJ. Interaction of dye-enhanced photothermotherapy and chemotherapy in the treatment of cancer: an in vitro study Proc. SPIE Vol. 7164, 71640X-1 (2009)

Manchanda R, Lei T, Tang Y, Fernandez-Fernandez A, McGoron AJ. Cellular uptake and cytotoxicity of a novel ICG-DOX-PLGA dual agent polymer nanoparticles delivery system. Southern Biomedical Engineering Conference Proceedings 2010; In press.

W. Haider, N. Munroe, Y. Tang, A. J. McGoron, C. Pulletikurthi, P. K. S. Gill, Endothelialization of Ternary Nitinol Alloys Materials and Processes for medical devices-Conference and Exhibition, August 10-12, 2009, Minneapolis, Minnesota.

W. Haider, N. Munroe, V. Tek, P. K. S. Gill, Y. Tang, A. J. McGoron, An Assessment of Metal Ions Release from Ternary Nitinol Alloys under Static and Dynamic Conditions-Part I